1968

Semiempirical determination of the differential fast flux spectrum for U-235 fission with water moderator

Henry Anthony Till

SEMIEMPIRICAL DETERMINATION OF THE DIFFERENTIAL FAST FLUX SPECTRUM FOR U-235 FISSION WITH WATER MODERATOR

by

Henry Anthony Till, 1933

A

THESIS

submitted to the faculty of the

UNIVERSITY OF MISSOURI AT ROLLA

in partial fulfillment of the requirements for the

Degree of

Master of Science in Nuclear Engineering

Rolla, Missouri

1968

Approved by

D R Edwards (Advisor) Albert E. Bolon

Fred C. Glandthe

ABSTRACT

The differential fast flux spectrum of the UMR Pool Research and Training Reactor core was determined by simultaneous activations of threshold foil detectors by neutron-nucleon reactions. This represents one phase of the composite neutron environment at two sample irradiation locations and the center of a fuel element during a power operation of 200 Kw (th). To accomplish this measurement a semiempirical least-squares approximation fitting activation data to a theoretical Cranberg U-235 fission spectrum was applied. This is a technique designed specifically for water moderated systems and takes into consideration both virgin and down-scatter neutrons.

Gamma decay photopeaks were reduced using computer code PPA (Photopeak Analysis), and the differential fast neutron spectrum was resolved by computer code RUFF. The results of the method used in this work were compared with spectrum results of a previously applied weighted orthonormal method. A parameter variational study was made for determination of spectrum effects.

Use was made of the following reactions: In-115(n,n')In-115m; Ni-58(n,p)Co-58; Fe-54(n,p)Mn-54; Al-27(n,p)Mg-27; Fe-56(n,p)Mn-56; Mg-24(n,p)Na-24; Al-27(n,α)Na-24; Fe-54(n,α)Cr-51; and In-115(n,2n)In-114. Tables of neutron-nucleon cross-sections for these reactions are included.

ACKNOWLEDGEMENT

The author wishes to express his sincere appreciation to Dr. D. R. Edwards, Director of the UMR Nuclear Reactor Facility, for the suggestion of this thesis topic and for his assistance throughout its preparation.

He also wishes to extend his gratitude to the Nuclear Reactor Staff, Alva Elliott, Reactor Supervisor, Murvel Little, and Ervin Wenz for their assistance in obtaining the necessary data.

TABLE OF CONTENTS

TABLE OF CONTENTS (Continued)

LIST OF FIGURES

LIST OF FIGURES (Continued)

LIST OF FIGURES (Concluded)

LIST OF TABLES

LIST OF TABLES (Concluded)

I. INTRODUCTION

A knowledge of the differential spectrum of the neutron flux is essential, especially when the reactor is to be used for research purposes. The more common reasons why this information is important are: instrument calibration, reactor experiment monitoring, shielding purposes, and in a field that is gaining more prominence, radiation effects in materials.

Although there are various means available for measuring neutron fluxes and spectra, the activation of metal foils is one of the best. Foils are small, simple to use, insensitive to gamma radiation, and affect the environment very little. For the thermal and epithermal regions this is accomplished by inducing activity through neutron capture, but for the fast region, which is what this thesis deals with specifically, neutron threshold reactions must transpire. By using a number of suitably chosen foils a simultaneous measurement can be accomplished.

A semiempirical method for determining the unknown spectra was used. This approach was designed specifically for an hydrogenous system and assumes that the differential form of the fast flux could be described by Cranberg's theoretical fission spectra. Taken into consideration are both the virgin and down-scattered neutrons. A least-squares expansion method, using the foil activation information, was employed for the evaluation.

The technique described is a method for determining the neutron energy distribution as well as the flux in a water moderated reactor.

II. PRELIMINARY RESEARCH

The activity obtained in a threshold foil can be expressed by the following:

$$A = \int_0^\infty \sigma(E)\, \phi(E)\, dE$$

where A is the foil activity, σ (E) is the absorption cross-section as a function of energy, and ϕ (E) is the differential neutron flux as a function of energy. The foil activity is corrected for foil weight, irradiation time, counting time, decay time, material concentration, counting detector efficiency, and path of decay.

It is important to establish the energy distribution and absolute flux because certain nuclear properties of the core depend upon the fast flux, and it is important in determining radiation effects in materials. The problem is not simply the determination of this spectrum but the determination of it rapidly and conveniently with as few detectors as possible.

A. Fission Spectrum

The neutron spectrum may be broken up into three sections, the thermal portion, the epithermal portion and the fast portion.

The fast flux determination is what this dissertation will deal with specifically, and the fast flux may be considered to be all neutrons with energies above 0.1 Mev.

In actual practice it is difficult to determine the fast spectrum accurately because foil detectors in general do not have the ideal step function property and often deviate significantly from this ideal situation. As a result, the spectral shape is usually assumed to be a fission spectrum (1,2). There have been numerous investigations of the total neutron fission spectrum from thermal neutron fission of U-235 (3,4,5,6,7). The earlier work has been summarized by B. E. Watt with a convenient formula covering the energy spectrum from 0.075 to 17 Mev (5).

$$N(E) = \sqrt{2/\pi e}\ \sinh \sqrt{2E}\ e^{-E}$$

where N (E) is the fraction of neutrons per unit energy emitted per fission and E is the neutron energy in Mev. This is called the Watt Spectrum.

L. Cranberg et al. has proposed a similar equation extending from 0.18 to 12 Mev that gives a better fit to all data in this region (7).

$$N(E) = 0.453\, e^{-E/0.965} \sinh \sqrt{2.29E}$$

There is little difference between the two formulas except for energies above 6 Mev, but for all practical purposes they are the same. This is called the Cranberg Spectrum and is illustrated in Figure 2.1. A simpler approximation has also been developed by Cranberg which has enjoyed wide acceptance (7). Normalized to one neutron per second, the representation is

$$N(E) = 0.776\, E^{1/2}\, e^{-0.776E}$$

This representation is a straight line over the greater part of the energy range where 0.776 is the parameter that gives the best slope. This spectrum is the one used in this work and is illustrated in Figure 2.2. The major drawback to this approximation is the prediction of too many neutrons above 9 Mev.

B. Threshold Detectors

Threshold detectors were used to determine the spectral characteristics of the fast region of the neutron flux. They are materials which undergo neutron-nucleon interaction above a given energy. These reactions may be of the (n,p); (n,2n); (n,n'); (n, α); or (n,fission) type which lead to the production of radioactive isotopes. In most cases threshold reactions are characterized by low sensitivity; hence, spectral measurements are usually limited to high intensity neutron flux fields. Self-shadowing of neutrons and flux perturbations, which are very serious problems with the lower energy neutron detectors, are unimportant in the use of threshold detectors (11).

The essential requirement for the use of threshold detectors is that the cross-sections versus energy curve be known with sufficient accuracy. Currently there are discrepancies in these values (9,30,31). Some of the cross-sections safest for use are: Al-27(n,p)Mg-27; Fe-56(n,p)Mn-56; Al-27(n, α)Na-24; and In-115(n,n')In-115m. The lower and higher end of the fast flux range is adequately covered by the inclusion of the last reaction.

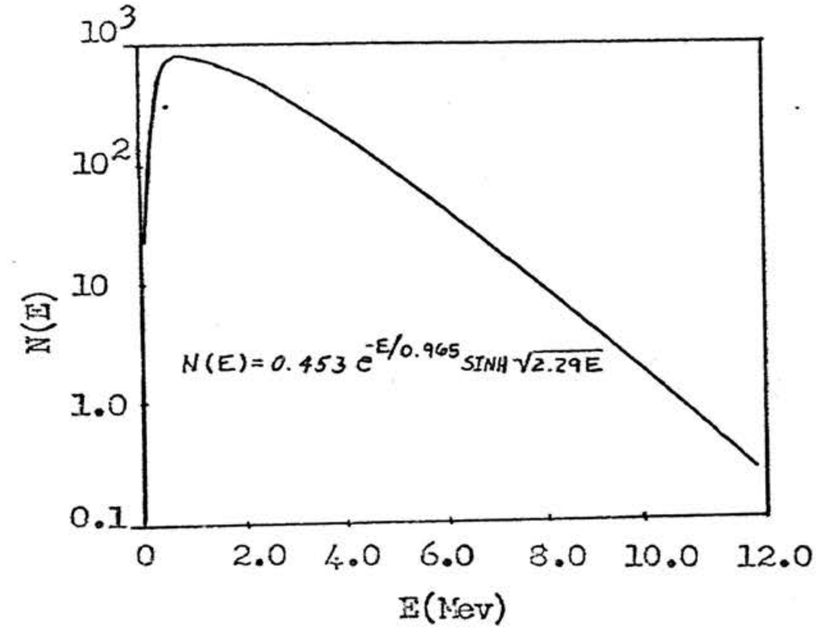

Fig. 2.1 Cranberg Spectrum of U-235 Fission Neutrons on a Logarithmic Scale Over the Energy Range of 0.18 to 12 Mev.

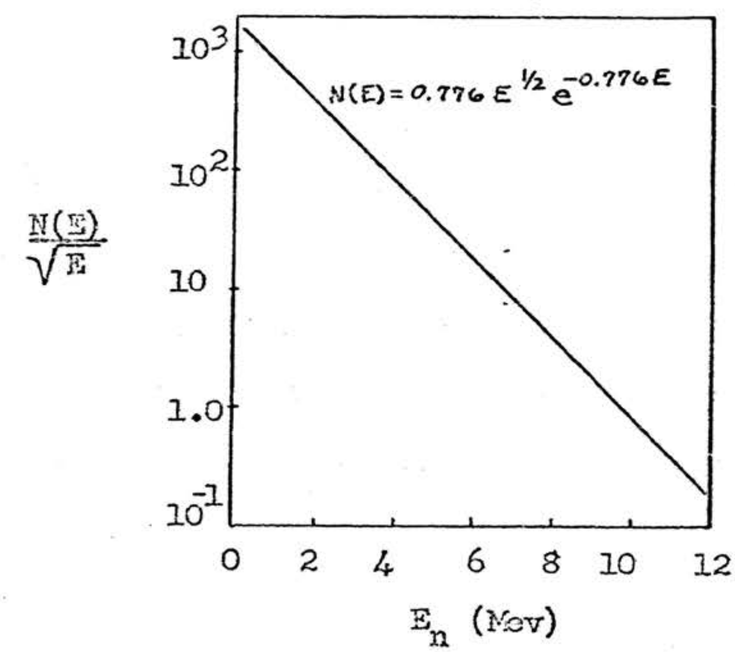

Fig. 2.2 Straight-Line Representation of Cranberg Fission Neutron Spectrum of U-235

The advantages of this method of neutron detection are: convenience of insertion in irradiation position, the slight perturbation of the system by the presence of the foil, insensitive to the accompanying gamma radiation, and generally inexpensive. The major disadvantage is the unavailability of completely accurate cross-section data. The criteria that must be met for validity of this technique are: the purity of the metal must be high, the emitted radiation identifiable and countable, the chosen thresholds must be spaced as evenly as possible and cover as much of the desired spectrum as possible, the activity formed must be of sufficient quantity, the gamma peaks of interest distinguishable from nuisance peaks, and the reaction cross-section curve as a function of energy must be known within reasonable accuracy.

B.1 Effective Threshold Energy

The concept of "effective threshold energy" was introduced by D. J. Hughes (8). The activation cross-section of an ideal threshold detector should have the following kind of step-function behavior, namely, it should be zero below the threshold value E_o and equal to the plateau cross-section σ_o above this value. The activation would then be proportional to the integrated flux above the threshold value. The actual cross-sections exhibit this step function only in a very rough approximation in the vast majority of cases. This is compensated for by defining a value called the effective threshold energy, E_o^{eff} (9,10,11,12). Then

$$\int_0^{\infty} \sigma_{act}(E)\, \phi(E)\, dE = \sigma_0 \int_{E_0^{eff}}^{\infty} \phi(E)\, dE$$

or the true reaction rate comes from the plateau cross-section.

In this work five types of foil material were used, the choice of which was based on the aforementioned criteria. These are listed in Table 2.1 along with other described pertinent information. The latest tabulated values were used whenever available.

B.2 Flux Effects on Reaction Products

The foils grouped together during irradiation were surrounded by the thermal neutron absorbent material cadmium. Reasons for this were to prevent burn-up of the product isotopes, and to prevent unnecessary irradiation. This burn-up is especially prominent in the Ni-58(n,p)Co-58 reaction (1,13). Hogg, Weber, and Yeats have shown that the isomeric state of Co-58 has an extremely large thermal cross-section, 178,000 barns, and therefore must be guarded against or corrected for (14). This is especially important in facilities where the thermal neutron flux is 10^{13} or greater. In spite of what may be considered a drawback for the use of Ni-58 foils, according to Passell and Heath, Ni-58 has good practical advantages as a fast flux monitor (15). Very little information is available on the other reaction products. No fast neutron-nucleon reactions were found for any of the product isotopes. It was impossible to prevent

Table 2.1

Threshold Reactions Employed in This Work

Target Reaction and Product	Thresh. Energy E_o (Mev)	Effect. Cross-Section σ_o^{eff}(mb)	Effect. Thresh. Energy E_o^{eff} (Mev)	Ave. Cross-Section $\bar{\sigma}$ (mb)	Gamma Photo-Peak (Mev)	Half-life T 1/2 (min)	Contaminant Products (Threshold and Half-life)	References
In-115(n,n')In-115m	.335	350	1.65	171	.335	270	In-116m(Resonance,54.1 min) In-114m (12 mev, 49 day)	9,16,24,30
Ni-58(n,p)Co-58	1.10	550	3.10	100	.805	102,672	Ni-57 (12.0, 36 hr)	9,16,24
Fe-54(n,p)Mn-54 (5.82%)	2.3	525	3.75	53	.840	419,040	Cr-51 (2.0, 27.8 day) Mn-56 (5.00, 154 - 8 min)	9
Al-27(n,p)Mg-27	2.70	80	5.30	3.5	.83 1.015	9.39	Na-24 (3.26, 14.97 hr)	9.16,24
Fe-56(n,p)Mn-56 (93.6%)	5.00	115	7.70	.97	.845	154.8	Cr-51 (2.0, 27.8 day) Mn-54 (2.3, 291 day)	9,24,30
Mg-24(n,p)Na-24	6.00	201	8.00	1.2	1.368 2.754	900		9,16,24
Al-27(n, α)Na-24	6.80	132	8.15	.61	1.368 2.754	900	Mg-27 (2.7, 9.39 min)	9,16,24
Fe-54(n, α)Cr-51	2.0	110	9.00	.37	.320	38,880	Mn-56 (5.0, 154.8 min) Mn-54 (2.3, 291 day)	9
In-115(n,2n)In-114m	12.0	1375	13.00	-	.191	72,000	In-116m(Resonance,54.1 min) In-115m (.335, 4.5 hrs)	9

fast reactions with the reaction products, therefore, this remains an uncorrectable source of error.

C. Methods of Spectral Measurements with Threshold Detectors

There are three different approsches in determining spectral information by threshold measurements. There are mathematical methods, semiempirical methods, and there are cases in which the neutron spectrum is already known and threshold detectors serve to verify the spectral distribution.

C.1 Mathematical Methods

Mathematical methods are highly theoretical and assume nothing about the shape or form of the spectrum. They usually use an expansion technique in terms of the differential cross-section and the radioactivity obtained from the foils. Three techniques in this category are: Multigroup Method, Hartmann's Method, and the Weighted Orthonormal Method.

In the Multigroup Method the foil activation is divided into a series of energy groups using an average value for the cross-sections in each energy group. If there are M threshold detectors then a system of M linear equations is developed and solved for the unknown flux. Good accuracy is attainable only by using a large number of detectors.

Hartmann's Method is very similar to the previous method except that it is designed for work with only a few detectors, and the auxiliary function is fitted in a least-squares sense.

It has been shown that this method can sometimes give negative values in places.

The Weighted Orthonormal Method assumes the flux is given by a weighting function times an expansion of unknown functions of energy which are required to form an orthonormal set (11,16,17,18). As many coefficients are used in the expansion as there are foils and thus the coefficients can be uniquely determined from the foil activation data. The orthonormal requirements add m additional constraints to the problem with m additional pieces of information. The advantage of the method is that the expansion coefficients are determined by a best-fit. This method was used by K. L. Cage to analyze the fast flux spectrum of the UMRR (18). While the integral spectrum was a reasonably smooth curve, the differential spectrum had large periodic dips that resembled oscillation. A method similar to this is the Weighted Orthonormal Polynomial Method. It is essentially a combination of this method and the polynomial method, and expands the flux in a series of polynomials which are defined to be orthonormal (16). The advantage of this system is the polynomials are smoother functions of energy, and the tendency to oscillate is reduced.

C.2 Semiempirical Methods

Semiempirical methods assume that something is already known about the basic form of the spectrum and without exception are more accurate than the purely mathematical methods. In this approach the problem is attacked in the following manner: an appropriate form of the spectral shape is assumed, which has unspecified coefficients; the foil activation cross-section curves are numerically integrated over an energy interval with respect to the assumed spectral shape; and the experimentally measured activations are used to specify the appropriate coefficients of the assumed shape and hence specify the measured spectrum. Examples of this method are: Polynomial Method, Uthe's Method, Dietrich's Method, Dierckx's Method, and the Italian Iterative Method.

In the Polynomial Method the spectral shape is assumed to be composed of an arbitrary weighting function times a polynomial in energy (16,19). As many terms n of the polynomial are taken as there are different values from foils. The resulting set of linear equations is poorly conditioned which causes small oscillations of the flux (20).

In Uthe's Method the neutron spectrum is written so that the activation results from the threshold detectors are best approximated in the least-squares sense (19). If the results are fitted to an existing expression of the fission neutron spectrum, this method should give good results if enough detectors are used. This is similar to Hartmann's Method, only here data is fitted to an existing shape.

Dietrich's Method was developed specifically for water-moderated reactors where it could be assumed that each neutron produced in fission loses the majority of its energy in one collision. Therefore, after one collision its energy will be reduced so much that it can no longer contribute to the activation of the threshold detector (16,21).

The Dierckx Method assumes the following: the spectral shape is a decreasing exponential function of energy, the total energy range can be divided into discrete energy bands with a spectral shape assumed in each band, the initial part of the cross-section curve for each detector contributes essentially all of the activation, and if there are n foils there will be n-1 bands (16,22).

The Italian Iterative Method is essentially a combination of the Dierckx and Effective Threshold Methods and offers a solution to the problem of curve fitting in the former (20). Values are obtained for the coefficients and then resubstituted to find the next case at which point the coefficients are redetermined. This recursion process is repeated until the spectrum is obtained. This method is restricted to reactor type spectra just as the Dierckx Method is.

III. THEORETICAL ANALYSIS

This is a semiempirical approach for the determination of the flux spectrum and assumes the form to fit a Cranberg Spectrum. Detailed derivations of results presented here are given in Appendix A.

The method applied was a least-squares expansion for determining the differential flux by foil activations (2). It is an approximation designed specifically for water moderated systems and takes into consideration not only virgin neutrons but all down-scatter neutrons. Neutrons can lose all their energy in a single collision with hydrogen, and this fact considerably simplifies the analytical problem by reducing the number of neutrons in the resonance region. Due to the proximity and position of the foils to the fuel, the hydrogenous medium was considered to have uniformly distributed sources emitting neutrons at a constant rate. Following emission, these neutrons lose energy mostly by elastic collisions. It was assumed that the medium did not absorb neutrons, an assumption which is essentially true except for neutrons of very low energy.

The collision density F(E) for hydrogen was determined by considering the scattering of neutrons into and out of an energy interval. The neutrons arrive in this interval directly from the source and from scattering collisions at higher energies. Since a scattering occurance with a hydrogen nuclei can reduce the neutron energy to any value, it is uncertain how many collisions the neutron has before it arrives at the interval, but this information is of little interest. In steady state, the number of neutrons scattered into an interval must be equal to the number scattered out. The number of neutrons arriving in an energy interval dE from all energies above is described by the transport of neutrons in energy for an infinite hydrogenous medium (34).

$$F(E)=\frac{S(E)}{E_o}+\int_E^\infty \frac{F(E')(1-B(E))}{E'}\,dE'$$

where E_o is the source energy and E' is an energy level above E. The solution of this equation as used in this dissertation is derived in Appendix A. The second term is equivalent to the scattered neutrons, and the first term represents the neutrons coming from the source. The (1-b(E)) multiplier of the second term indicates the number of neutrons which survived their first collision. The B(E) term is the absorption of neutrons in water and is generally small so that neglecting this multiplier is a reasonably accurate first approximation. Development of the transport equation yields the following form.

$$F(E)=-a\int_E^{E_o} E^{-1/2}e^{-bE}\,dE$$

The similarity of this equation to Cranberg's equation of the fission spectrum

$$I=-\int_E^{E_o} E^{1/2}\,e^{-bE}\,dE$$

suggests using Cranberg's form as the desired spectrum shape. The following equation was then obtained to describe the flux

$$\phi(E) = \frac{\phi_o a}{E^k}\left[(bE)^{3/2} e^{-bE} + \sqrt{bE}\; e^{-bE} + \frac{\sqrt{\pi}}{2}\left(1 - erf\sqrt{bE}\right)\right]$$

The data was collected by foil irradiations

$$A_i = \int_{E_i}^{\infty} \sigma_i(E)\,\phi(E)\,dE = \int_{E_i}^{\infty} \sigma_i(E)\,\frac{\phi_o}{E^k} f(E)\,dE$$

where f(E) is the term in the parenthesis above. This was fit as well as possible by least-squares with parameters k and ϕ_o.

$$\sum_i \left[A_i - \int_{E_i}^{\infty} \sigma_i(E)\,\phi_o\,\frac{f(E)}{E^k}\,dE\right]^2 \leq q$$

For q to be a minimum the partial derivatives of q with respect to k and ϕ_o must be equal to zero. The derivative with respect to ϕ_o produces the term

$$\sum_i A_i I_i(k) = \phi_o \sum_i I_i^2(k)$$

where

$$I_i(k) = \int_{E_i}^{\infty} \sigma_i \,\frac{f(E)}{E^k}\,dE$$

The derivative with respect to k produces the term

$$\sum_i A_i I_i'(k) = \phi_o \sum I_i(k)\, I'(k)$$

where

$$I_i'(k) = \int_{E_i}^{\infty} \frac{\sigma_i(E)\, f(E)\, \ln E}{E^k}\,dE$$

The flux normalization constant is the same for both terms, therefore,

$$X(k) = \frac{\sum_i A_i I_i(k)}{\sum_i I_i^2(k)}$$

and

$$Y(k) = \frac{\sum_i A_i I_i'(k)}{\sum_i I_i(k) I_i'(k)}$$

The condition sought is

$$\left| X(k) - Y(k) \right| \leqslant \epsilon$$

If convergence did not occur with the original choices of k, new values were extrapolated by fitting X(k) and Y(k) to parabolic curves. The point of intercept of these two curves being the best value of k for substitution back into the spectrum approximation. The problem of solving these sets of quadratic equations was accomplished conveniently by setting them up in matrix form. The value of the radical produced by the solution of the quadratic equations was not less than zero. This produced only one value for the exponent. For two values of k the one closest to k_3 would have been used.

This approach for determining the differential flux was developed into a computer code called RUFF by Dr. D. R. Edwards. The code derives its name because it is a rough spectral approximation. This code is described in more detail, with a flow diagram and listing, in Appendix B.

IV. EXPERIMENTAL PROCEDURE

A. Requirements for Threshold Detector Materials

There were a number of qualities required in the detectors used for this experiment (11,23). These requirements were divided into two categories, those pertaining to the detector material and those pertaining to the products formed from the detector material.

A.1 Detector Materials

The magnitude of the cross-sections chosen were moderate (50 to 500 mb) in most cases. Enough activity to count was necessary, but too much could cause counting and handling problems. Both of these situations did occur.

The cross-sections for the threshold detectors were chosen to approximate a step function in most cases and was the latest information available (24,25,26). These cross-sections were chosen so that the effectiveness of the approximated step functions fell at selected energy locations of the spectrum.

The contribution to the measured activity from the activation of impurities was kept as low as possible. Cadmium was used to shield the thermal neutrons, but resonance neutrons were a nuisance in the case of In-115 and precluded the use of Au-197 as a detector.

The size of the foils was also a factor in the choice because it was desirable that the encapsulated group of foils be thin enough to make them accessible to narrow channels. Also smaller foils detect a spatially more uniform flux spectrum.

A.2 Activation Products

The half-life of the radioactive products was a factor taken into consideration. The half-life had to be long enough so that counting could be performed accurately. This was not a major problem because of the proximity of the counting device to the reactor pool. The shortest half-life was 9.39 minutes. For weak reactions long half-life products were sought so that all the nuisance peaks could decay away leaving the peak of interest uncluttered. But in cases where the half-life was too long the specific activity was small and the count rate too low to make a significant photopeak. This was partially the case in the Al-27(n,2n)Al-26 reaction. Al-26 is metastable with an extremely short half-life (6.7 seconds) and an extremely long half-life (8×10^5 years). Otherwise this reaction would have been a good one for the 16 Mev range. Half-lives of hours to days are most convenient.

It was necessary that the reaction products have gamma emission as part of its decay because of the detecting device used. Gamma is more reliable and accurate to use and has less self-absorption in the foils (11).

The reaction product cross-sections had to be as low as possible so that they would not burn out as they were being produced. A case in point is the Ni-58(n,p)Co-58 reaction, which was discussed previously. The difficulty in using the Ni-58(n,2n)Ni-57 reaction was the main photopeak fell under the sum peak for Co-58, another reaction product of Ni-58.

B. Foil Preparation and Activation

The foil dimensions were one-half inch in diameter and approximately 0.005 inches thick, with weights ranging from 0.03 to 0.28 grams per foil. The purity of the metals, as stated by the manufacturer, Reactor Experiments, Inc., were all above 99.9%. The foils were cleaned and placed inside cadmium containers in the same sequence for each irradiation. The order being: nickel, aluminum, magnesium, and iron. The indium foil was separated from the rest so that it could be left in the pool for the In-116 activity to decay. Otherwise the experimenter would be exposed to excessive amounts of radiation.

In order to make as much use of the foils as possible, two or more reactions were utilized in all except magnesium and nickel, and three reactions were used with the iron foil. Nine reactions were extracted from the five foils and the energy range tested went from 0.335 to 13 Mev. Other reactions such as Al-27(n,2n)Al-26, Ni-58(n,2n)Ni-57, Vi-51(n, α)Sc-48, Au-197(n,2n)Au-196, and Au-197(n,p)Pt-197 were tested to give a detector for the region above 13 Mev but for various reasons they were not acceptable.

Attention must be given to the thermal flux depression when measuring the magnitude of the flux spectrum, especially when the sampled point is in a fuel element or at the center of the core. A reduction in the thermal flux will create a corresponding reduction of the fast flux in the immediate volume.

C. Counting Technique

The foil induced activity was determined by counting the gamma emission with dual right angle cylindrical 3" x 3" sodium-iodide thallium-activated crystals in conjunction with a 400 channel analyzer. The crystals were adjustable so that they could be closed tightly on the foil and essentially gave 4π counting geometry. The crystals were located in a lead shielded counting chamber.

The foils were individually counted by placing each in a small plastic bag and placing it between the crystals in the vertical position and bringing the crystals up tightly against it. The major factor determining the order of counting was the half-life of the reaction product, but also considered was the induced activity created by considering the cross-sections. The following counting order was used: Mg-27, Mn-56, two Na-24, In-115m, Cr-51, Co-58, In-114m, Mn-54. Background subtraction was performed on each spectrum. Foils were never used more than once, so residual activity remaining in the foils was never a problem.

The spectrum of each foil was transferred to punch tape from the pulse height analyzer, from which it was converted to IBM cards for use in the photopeak analysis code (PPA) (27). A flow diagram and listing of this computer code is presented in Appendix B. PPA fits a biased Gaussian function to form one to five photopeaks in a spectrum and gives the following information about each fit: the exact channel location of each peak, the full width at half maximum of the photopeak (FWHM), the peak count rate, the integrated count rate in the photopeak, and the integrated count rate in the photopeak corrected for radioactive decay to "zero-time".

The foil activity determinations by PPA were fed into the computer program RUFF which is a computer program to estimate the differential fast flux spectrum from a limited number of foil measurements (2). The material as presented in Appendix A.1 and A.2 is what composes RUFF, and a flow diagram, listing, and further information on this code are presented in Appendix B. Graphs of the differential spectrum are given in the results.

The multi-channel analyzer was calibrated qualitatively for associating the correct reaction product photopeaks. The qualitative calibration was performed by using known standards, Cs-137, Na-22 and standardizing the energy increment per channel. These standards produce photopeaks at 0.662 and 1.28 Mev respectively. The photopeaks from the foils were then located by channel. Accurate quantitative concentrations were obtained by the computer codes and were printed as part of the output.

Computed efficiencies were used to approach, as close as possible, absolute disintegration rates from the observed area under the photopeak (28). The following corrections were considered: geometry Ω, incident intrinsic efficiency ϵ, and source intrinsic efficiency $\Omega\epsilon$. The geometry is the fraction of the total radiation from the source which is incident on the crystal face. This term was taken to be unity because of the normal incidence and the 4π contact condition. The incident intrinsic efficiency is the fraction of the monochromatic isotropic radiation impinging on the crystal face which interacts to produce a measurable scintillation. The source intrinsic efficiency is the fraction of the total monochromatic isotropic radiation of a source incident on the crystal face, which interacts to produce a measurable scintillation. Because of the geometry term these factors are equal. Source intrinsic efficiencies have been calculated for the dual right cylindrical sodium iodide crystals with the source in contact and are tabulated in Table 4.1. (28).

Table 4.1

Source Intrinsic Efficiencies for Dual Right Cylinder Sodium Iodide (thallium activated) Crystals

Gamma-Ray Energies (Mev)	Source Intrinsic Efficiencies
0.0089	1.000
0.0237	1.000
0.0295	1.000
0.0484	1.000
0.0622	1.000
0.081	1.000
0.105	1.000
0.129	1.000
0.152	1.000
0.212	0.900
0.332	0.970
0.545	0.895
1.10	0.774
1.89	0.688
3.75	0.625
5.25	0.516

V. RESULTS

The experiment concerned the following: determination of the fast flux spectrum, estimation of parameters for best fit of program code RUFF to Cranberg Spectrum, and choice of threshold foils for greatest spectrum range and ease of use at power levels of 200 Kw (th).

A. Differential Fast Spectrum

Differential fast flux determinations, by threshold foils, were conducted at three locations in the UMRR core at power levels of 200 Kw, and activation time lengths of 30 minutes. Core loading 31T was used for all three tests, and is illustrated in Figure D.1. The three positions used were: C-3, a popular sample activation location; F-7, the cadmium covered pneumatic irradiation facility; and D-7, between two plates of fuel element F-18.

A.1 Flux Determination

The activation between the fuel element plates gave the greatest flux values and position C-3 gave the lowest values. This was due to the proximity of each position to the neutron production. The same slope parameter and closeness of fit were used for all spectral determinations. Figures 5.1, 5.2, and 5.3 are the differential fast flux determinations for locations C-3, F-7, and D-7 respectively. Respective energy incremental flux tabulations are given in Appendix E, Tables E.1, E.2, and E.3.

A comparison of these results to those obtained by

K. L. Cage in a previous similar experiment using orthonormal methods is illustrated in Figure 5.4. The point stressed by this comparison is the similarity of the slopes of the two methods. The difference in magnitude can be adjusted by the flux normalization parameter. It is seen that the semiempirical approach gives a much smoother distribution. One bad feature in the RUFF approximation is the increased values at energies below 1 Mev. This is discussed later in the results.

A.2 Parameter Effects

There were three parameters to consider, b, k, and ϕ_o. The parameter b was introduced in the Cranberg expression of the spectrum as a term that determined the slope of the straight line portion of the fission spectrum. The value that gave the best results was k = 0.77. This was acceptable only out to 9 Mev. Beyond this it proved inaccurate because of the drop-off in the spectrum.

The parameter k determines the slope of the experimental spectrum. Values giving the best results were the minimum k value of 0.600 and the maximum k value of 0.770. This value of k was to be expected because it plays the same role in the empirical sense as b does in the theoretical. The maximum value of k is the one that had the ultimate effect on the spectrum. The minimum value of k only became effective when an iteration was necessary for the determination of k. The best maximum value was obtained by adjusting the experimental curve to the Cranberg curve. Figures 5.5 through 5.8 illustrate the effect of this parameter on the slope of the experimental curve. Brief tabulated results of these plots are given in Appendix E, Tables E.4 through E.7. Table 5.1 represents the change in calculated activities, as a function of the exponential parameter. To obtain this optimum k, values were varied from 0.20 to 0.90. A value of k of 0.77 gives a good fit for all energies above 1 Mev, but gives an upswing in the spectrum for energies lower than this. This is contrary to the form of the Cranberg Spectrum. The lower values of k gave a better form to the spectrum in the region below 1 Mev, but predicted a thermal neutron flux that was too low.

The parameter ϕ_o establishes the magnitude of the spectrum. It is a product of the foil activations multiplied by the concentration composing the foil. The values determined were in the area of what might be considered a good approximation, but in view of the results below 1 Mev, they are a little low. The thermal flux of the UMRR is approximately 1.5 x 10^{12}; therefore, a fast flux ranging from 10^{10} down to 10^{2} maintains the spectrum continuity considering the gap between the two filled by the epithermal and resonance region. For the best overall results for all regions the normalization parameter should be changed to produce a spectrum of greater magnitude and the slope parameter should be lowered to a value between 0.1 and 0.2.

The parameter describing the degree of experimental deviation was the delta term. This value deviated significantly for the second of the three determinations. For the first run a value of 9 percent was the best achievable, for the second 51 percent, and for the third 7.5 percent. Three sets of data were too few to establish the reason for this deviation or how to correct it.

B. Activation Measurements

There are two sets of activation measurements presented, measured ones and ones calculated by computer code RUFF. The code utilized the effective threshold, the foil material concentration, and the integral of the theoretical spectrum from the effective threshold energy to the maximum neutron energy, to determine a calculated foil activation. The ideal case would occur when the related measured values and calculated values were equal. Reaction results in decreasing order of closeness were: In-115(n,n')In-115m; Ni-58(n,p)Co-58; Al-27(n,p)Mg-27; Fe-56(n,p)Mn-56; Mg-24(n,p)Na-24; Al-27(n, α)Na-24; Fe-54(n, α)Cr-51; Fe-54(n,p)Mn-54; and In-115(n,2n)In-114m. The chi-square value is a measure of the discrepancy existing between the empirical and calculated values. For an exact agreement this term would be equal to zero, and the larger this value the greater is the discrepancy. The degree of freedom in all cases was seven. The results obtained for the three measurements are presented in Tables 5.2, 5.3, and 5.4.

Included with the original criteria for choosing threshold reactions should be the degree of similarity between empirical and calculated values. Reactions having great dissimilarities should be discarded. Of course, this information will not be known until after the data is taken and reduced. Of the lower accuracy reactions the Fe-54(n,p)Mn-54 could be removed because the effective area in which it falls could partially be covered by the Ni-58(n,p)Co-58 and Al-27(n,p)Mg-27 reactions. The Fe-54(n, α)Cr-51 and In-115(n,2n)In-114m are also poorly matched, but they are effective in the higher energy areas and cannot be removed without altering the spectrum.

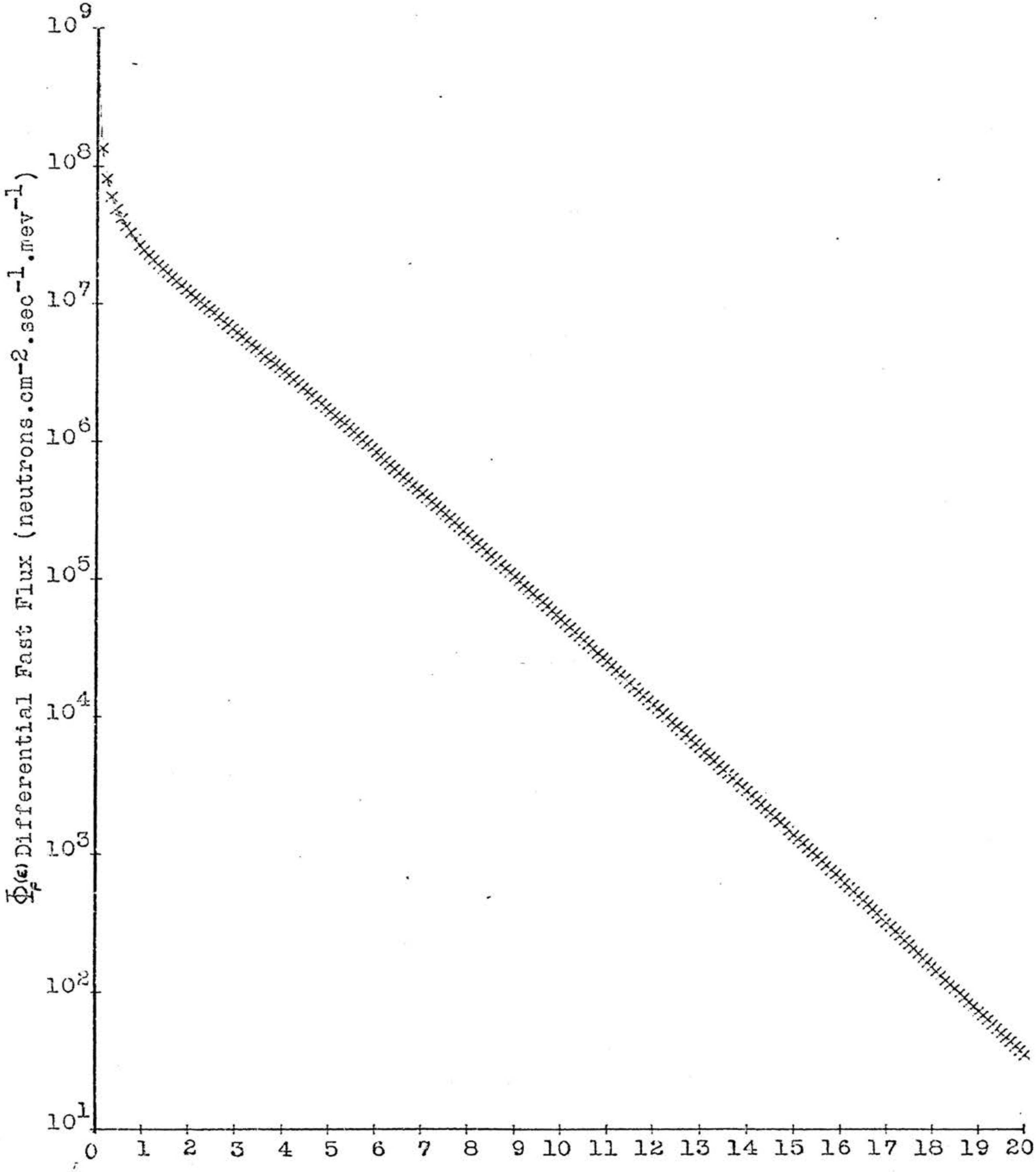

Figure 5.1 Differential Flux Spectrum at C.3

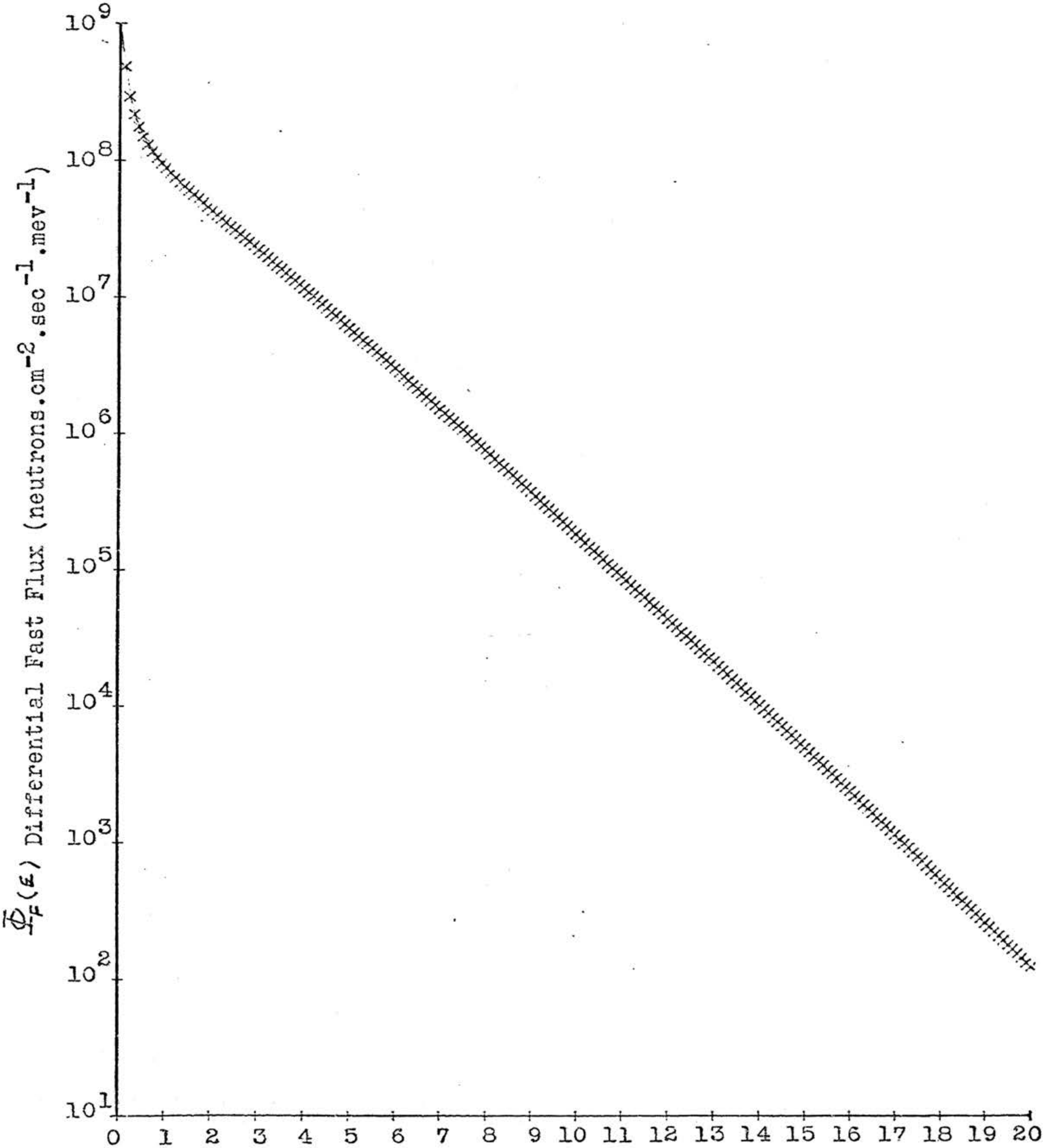

Figure 5.2 Differential Flux Spectrum at F.7

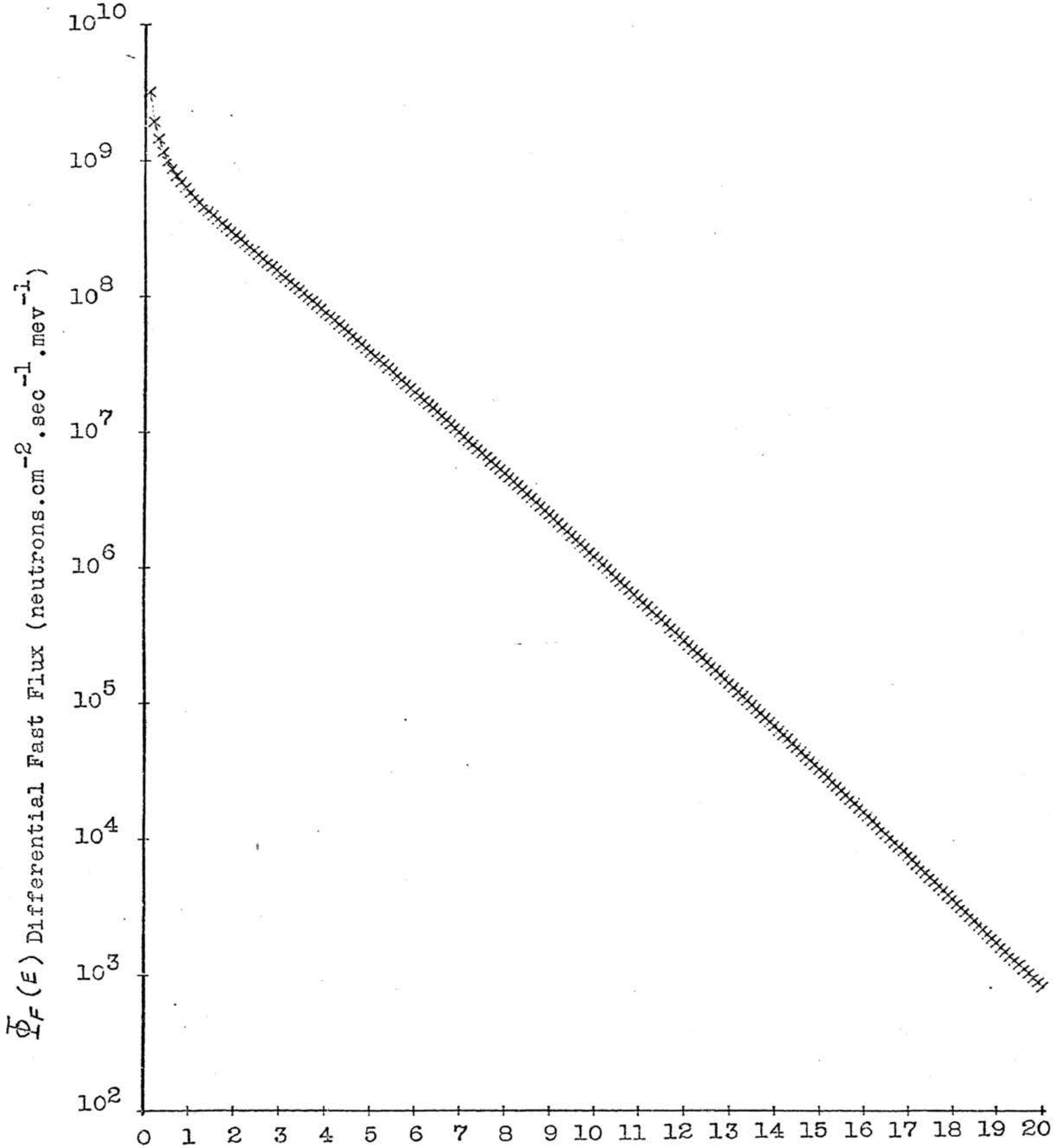

Figure 5.3 Differential Flux Spectrum at D.7

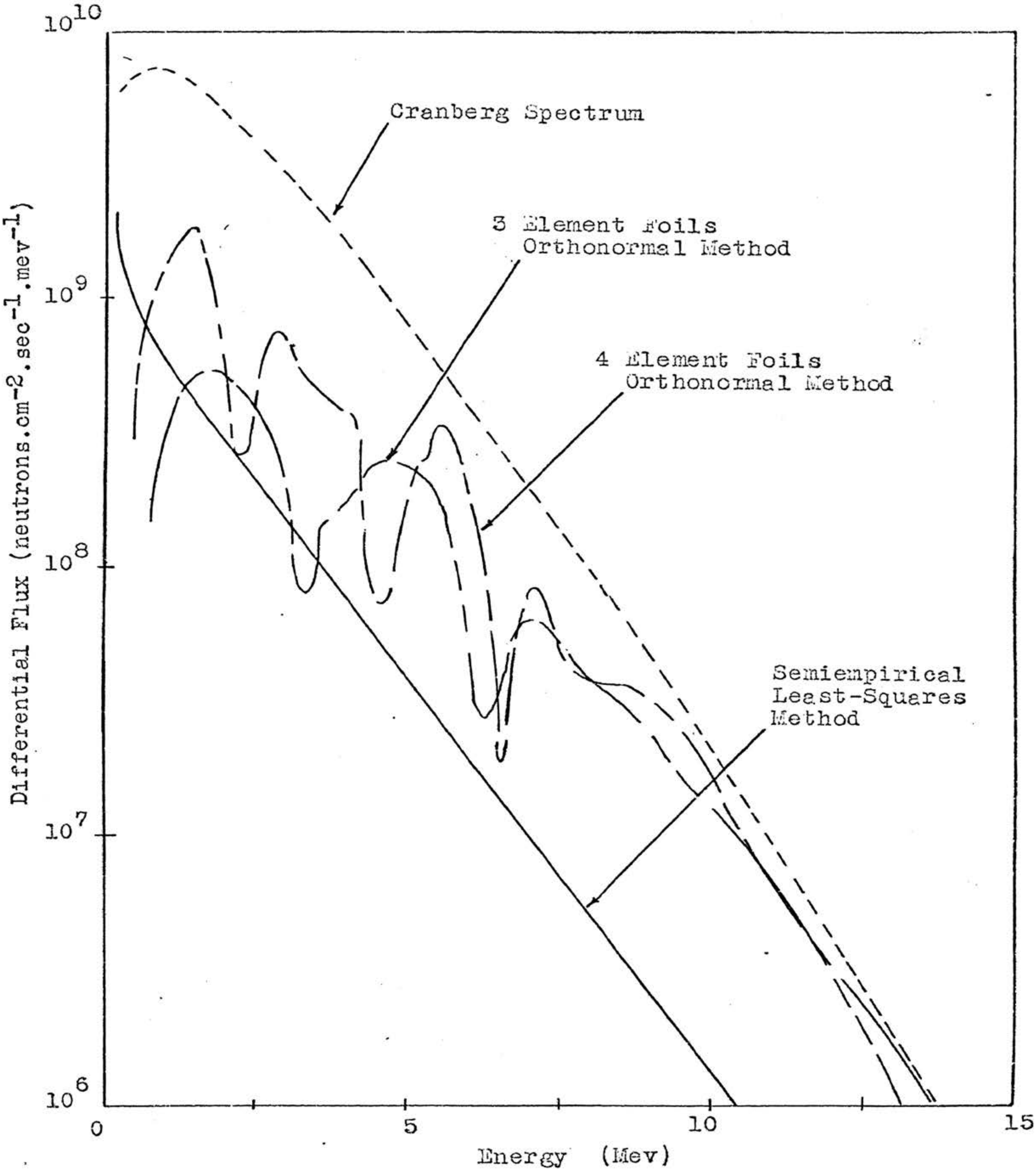

Figure 5.4 Fission Spectrum and Differential Flux of Orthonormal and Semiempirical Least-Squares Methods

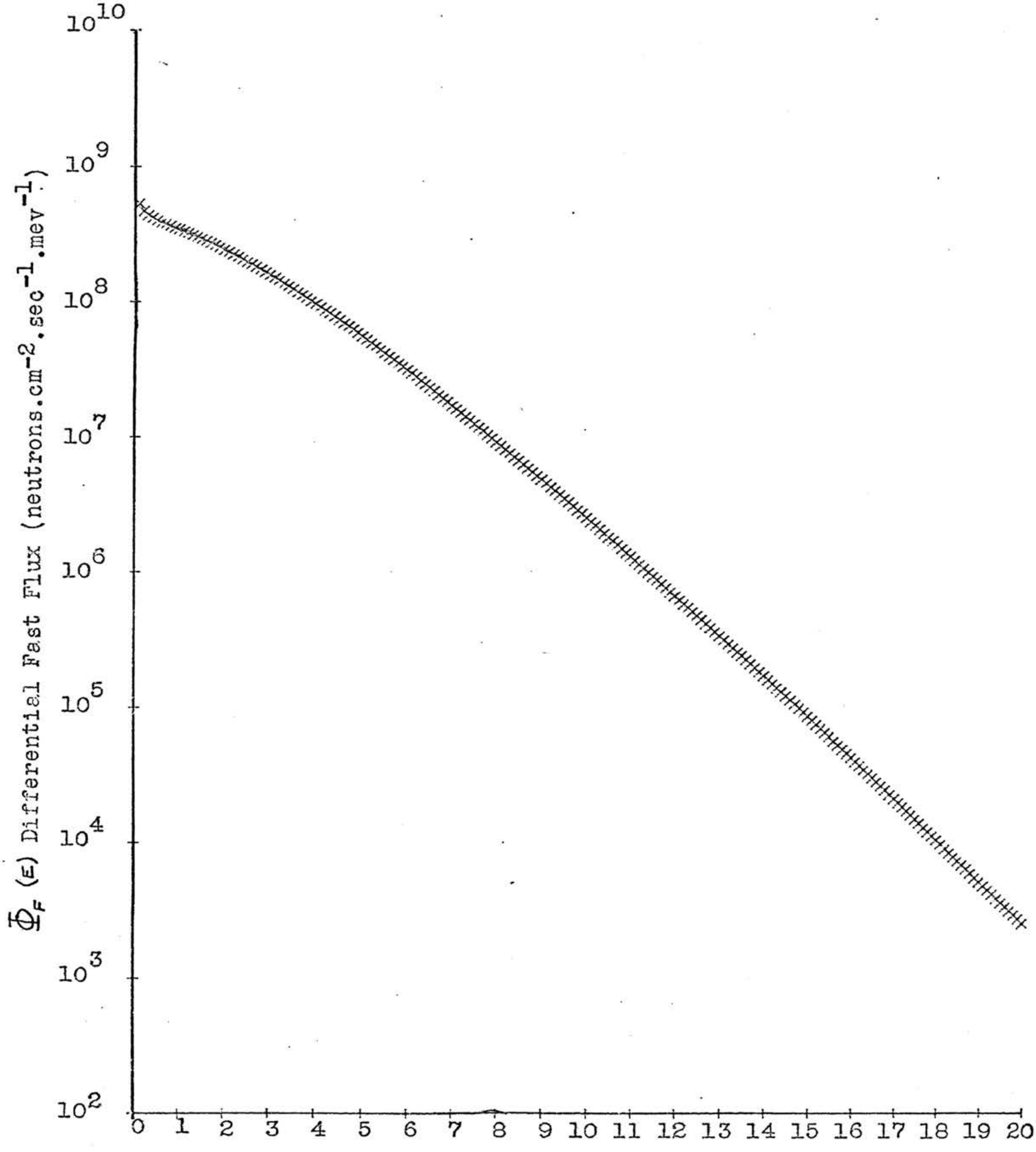

Figure 5.5 Exponent Parameter K
Variation of Position D.7 Results
Kmin=0.1 , Kmax=0.2

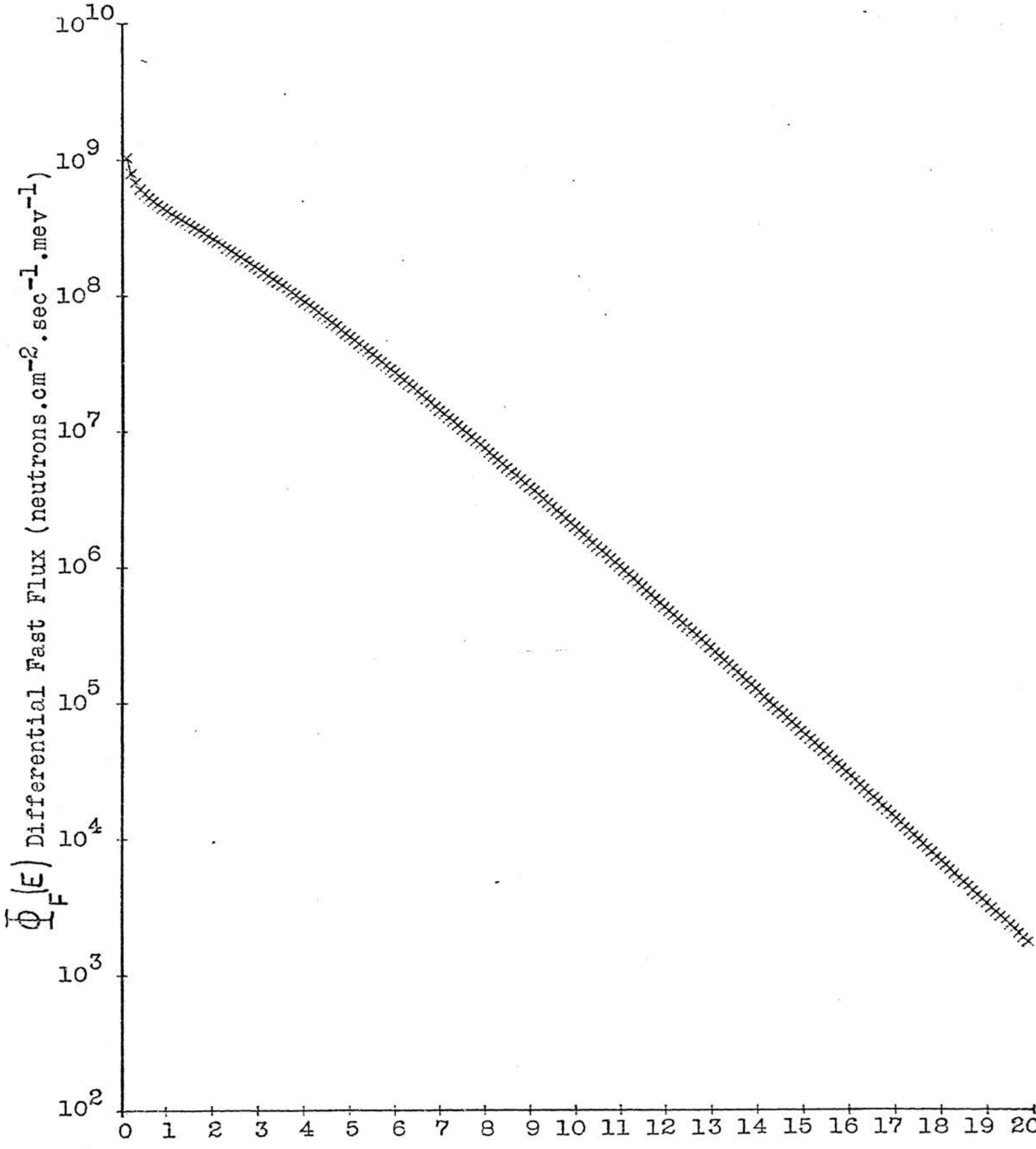

Figure 5.6 Exponent Parameter K
Variation of Position D.7 Results

Kmin=0.2 , Kmax=0.4

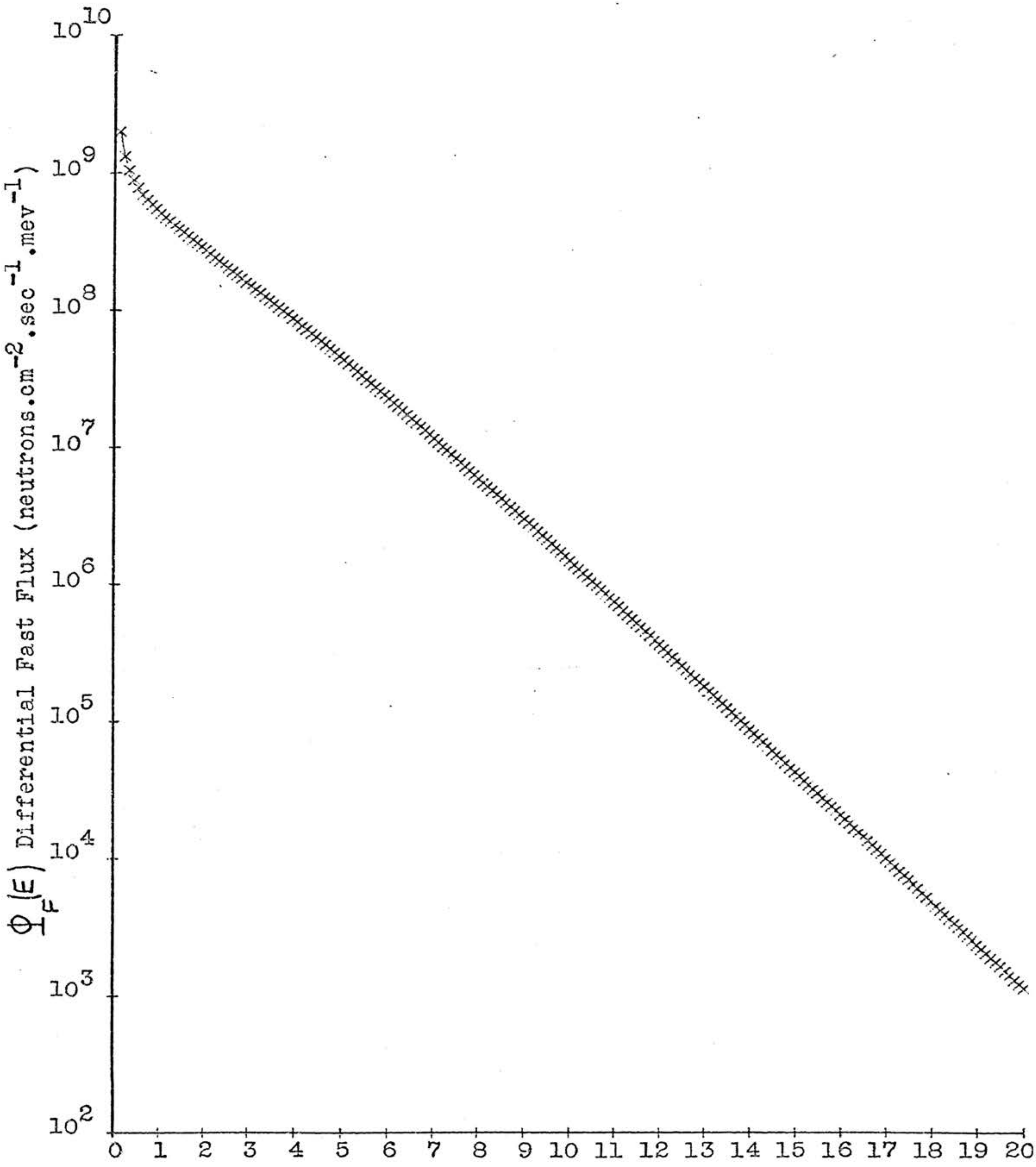

Figure 5.7 Exponent Parameter K
Variation of Position D.7 Results
Kmin=0.4 , Kmax=0.6

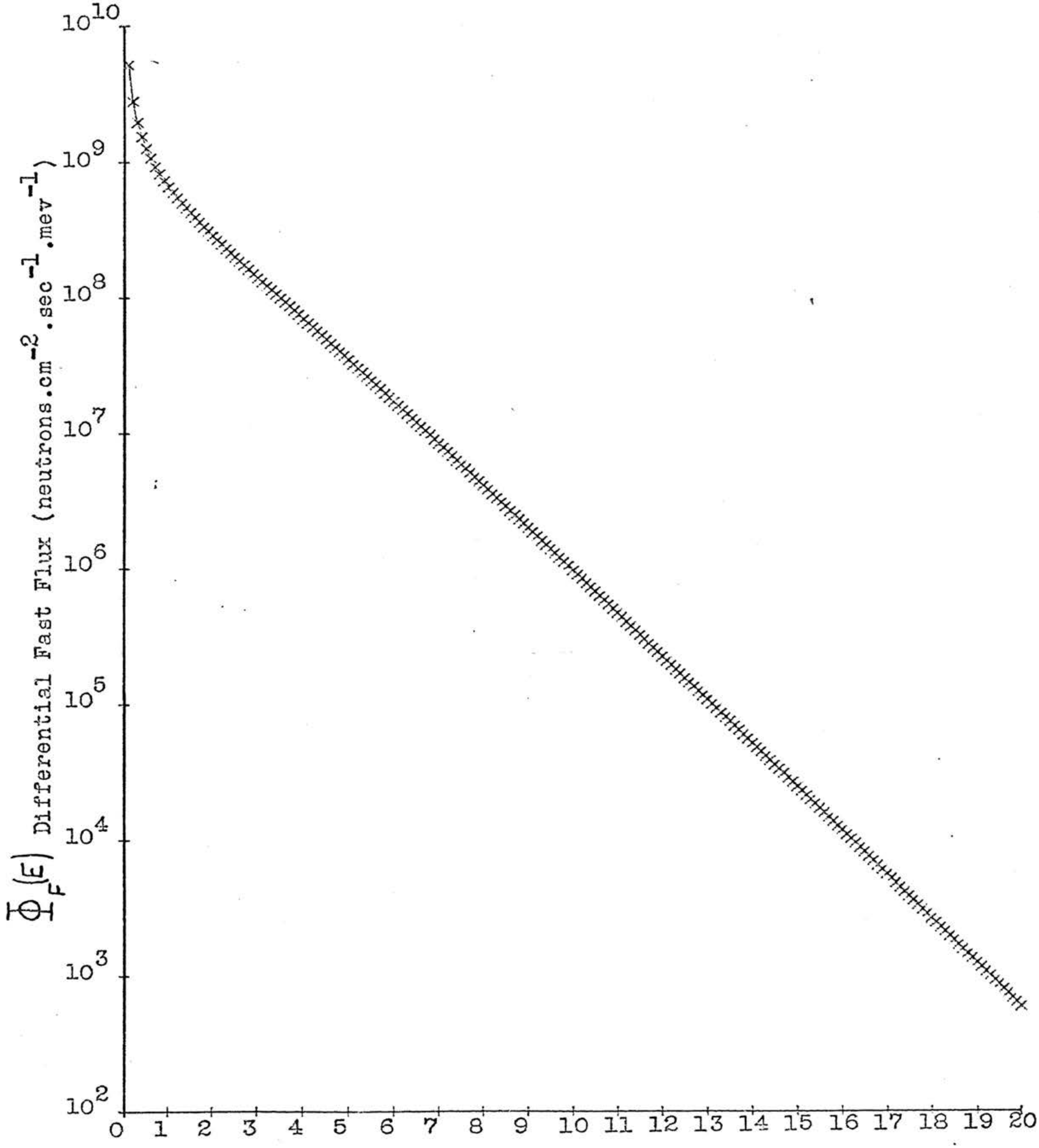

Figure 5.8 Exponent Parameter K
Variation of Position D.7 Results
Kmin=0.8 , Kmax=0.9

Table 5.1

Calculated Activity for Exponent Parameter

Variation of Position D.7 Results

Reaction Product	Measured Activity	Kmin = 0.1 Kmax = 0.2	Kmin = 0.2 Kmax = 0.4	Kmin = 0.4 Kmax = 0.6	Kmin = 0.8 Kmax = 0.9
In-115m	0.237×10^{8}	0.269×10^{8}	0.212×10^{8}	0.272×10^{8}	0.271×10^{8}
Co-58	0.568×10^{6}	0.249×10^{5}	0.228×10^{5}	0.207×10^{5}	0.177×10^{5}
Mn-54	0.141×10^{5}	0.346×10^{2}	0.311×10^{2}	0.277×10^{2}	0.229×10^{2}
Mg-27	0.162×10^{8}	0.103×10^{8}	0.886×10^{7}	0.752×10^{7}	0.577×10^{7}
Mn-56	0.434×10^{7}	0.442×10^{6}	0.360×10^{6}	0.290×10^{6}	0.205×10^{6}
(Mg) Na-24	0.468×10^{6}	0.440×10^{5}	0.350×10^{5}	0.275×10^{5}	0.187×10^{5}
(Al) Na-24	0.481×10^{6}	0.613×10^{5}	0.486×10^{5}	0.380×10^{5}	0.257×10^{5}
Cr-51	0.108×10^{5}	0.168×10^{3}	0.150×10^{3}	0.133×10^{3}	0.111×10^{3}
In-114m	0.648×10^{6}	0.658×10^{2}	0.480×10^{2}	0.345×10^{2}	0.206×10^{2}

Table 5.2

Data Set 2-23

(K-min = 0.6 , K-max = 0.75 , Delta = 0.1)

Reaction	Measured Activity (dis/min)	Calculated Activity (dis/min)	Chi-square Error
In-115(n,n')In-115m	0.1420×10^{7}	0.1380×10^{7}	0.9840×10^{-3}
Ni-58(n,p)Co-58	0.7910×10^{5}	0.8176×10^{3}	
Fe-54(n,p)Mn-54	0.3810×10^{4}	0.3308×10^{2}	
Al-27(n,p)Mg-24	0.1300×10^{6}	0.2736×10^{6}	
Fe-56(n,p)Mn-56	0.1700×10^{6}	0.1096×10^{5}	
Mg-24(n,p)Na-24	0.9070×10^{5}	0.9586×10^{3}	
Al-27(n,α)Na-24	0.7860×10^{5}	0.1299×10^{4}	
Fe-54(n,α)Cr-51	0.2830×10^{4}	0.3660×10^{1}	
In-115(n,2n)In-114m	0.3090×10^{4}	0.2523×10^{-1}	

Table 5.3.

Data Set 3-6

(K-min = 0.6 , K-max = 0.75 , Delta = 0.51)

Reaction	Measured Activity (dis/min)	Calculated Activity (dis/min)	Chi-square Error
In-115(n,n')In-115m	0.1220×10^{7}	0.4241×10^{7}	0.3035×10^{-3}
Ni-58(n,p)Co-58	0.2840×10^{6}	0.2929×10^{4}	
Fe-54(n,p)Mn-54	0.4850×10^{4}	0.4348×10^{1}	
Al-27(n,p)Mg-24	0.9700×10^{7}	0.9957×10^{6}	
Fe-56(n,p)Mn-56	0.1020×10^{7}	0.3716×10^{5}	
Mg-24(n,p)Na-24	0.2000×10^{7}	0.3538×10^{4}	
Al-27(n,α)Na-24	0.2300×10^{6}	0.4727×10^{4}	
Fe-54(n,α)Cr-51	0.1210×10^{5}	0.2098×10^{2}	
In-115(n,2n)In-114m	0.8380×10^{6}	0.4357×10^{1}	

Table 5.4[illegible]

Data Set 3-8

(K-min = 0.60 , K-max = 0.75 , Delta = .08)

Reaction	Measured Activity (dis/min)	Calculated Activity (dis/min)	Chi-square Error
In-115(n,n')In-115m	0.2370×10^{8}	0.2718×10^{8}	0.1684×10^{-3}
Ni-58(n,p)Co-58	0.5680×10^{6}	0.1919×10^{5}	
Fe-54(n,p)Mn-54	0.1410×10^{5}	0.2523×10^{2}	
Al-27(n,p)Mg-24	0.1620×10^{8}	0.6602×10^{7}	
Fe-56(n,p)Mn-56	0.4340×10^{7}	0.2444×10^{6}	
Mg-24(n,p)Na-24	0.4680×10^{6}	0.2277×10^{5}	
Al-27(n,α)Na-24	0.4810×10^{6}	0.5132×10^{5}	
Fe-54(n,α)Cr-51	0.1080×10^{5}	0.1217×10^{3}	
In-115(n,2n)In-114m	0.6480×10^{6}	0.2673×10^{2}	

VI. CONCLUSIONS AND RECOMMENDATIONS

Conclusions reached as a result of this work fall into two categories; conclusions dealing with the results and those regarding the method.

The results obtained may be classified as good considering that analytical foil activation methods are not extremely precise because systematic errors are inherent. Comparing the results of this work to those of a technique previously applied at the UMRR illustrates smoother continuity and greater plausibility in this semiempirical approach. The chi-square error is a spectral consistency indication and depends on the validity of the hypothesis regarding the assumed spectral shape. It gives no information about the accuracy of the flux magnitude, for which experience and knowledge of other regions of the spectrum magnitude aid in extrapolating this estimate. Results from the three locations sampled compared very well.

While it is conceded that none of the analytical foil activation methods are accurate to a great degree, this semi-empirical least-squares approximation is as good as, if not better than, most methods available. A disadvantage of this approach is its restriction to water moderated reactors and its unadaptability to other spectrums. The computer code RUFF, which was developed to perform the necessary calculations, is easy to use and produces a graphical plot of the results of each computation along with tabulated quantities, and a set of calculated activation values for all materials used that are in the code library. These activation values are compared to the measured results. A distinct advantage of this method is its ability to produce results rapidly. Time delays while doing this work occurred in obtaining computer results. With computer priority access, a minimum time estimate for tangible results would be 30 to 36 hours. An important feature to this method is the insensitivity to sporadic inaccurate data, a feature that allows the accurate data to be undisturbed by the faulty data, provided it is sparse.

The threshold detectors applied in this work were used so that information could be extracted from as many reactions as possible. There were five foils of individual materials with nine threshold reactions. Of these only the Fe-54(n,p)Mn-54 reaction could be excluded. An inherent source of error in using foils is the uncertainty of reaction cross-sections for fission neutrons.

The author suggests the following recommendations for future work: other threshold reactions be studied for application as detectors to extend the spectrum investigation range both at the high and low ends. Reaction suggestions are: Rh-103(n,n')Rh-103m ($E_{eff} =$ 0.04 Mev); Cu-63(n,2n)Cu-62 ($E_{eff} =$ 11 Mev); Au-197(n,2n)Au-196 ($E_{eff} =$ 13 Mev); and Al-27(n,2n)Al-26 ($E_{eff} =$ 16 Mev). To gain information of the differential neutron flux below 2 Mev, fission threshold detectors should be utilized producing a (n,f) reaction.

Examples being: U-235 (E_{eff} = 0.3 Mev); Np-237 (E_{eff} = 0.4 Mev); U-236 (E_{eff} = 0.7 Mev); Th-232 (E_{eff} =1.3 Mev; and U-238 (E_{eff} =1.3 Mev).

A detailed parameter study using the program code RUFF to obtain optimum values would be helpful in making this code more effective. Only token attempts along these lines were taken. This parameter study would correct the spectrum below 1 Mev, and the overall magnitude.

APPENDIX A

DERIVATION OF EQUATIONS

A.1 Derivation of Differential Flux Spectrum

The reaction rate or collision density of fission neutrons slowing down and arriving in the energy interval dE from all energies above E is

$$F(E)\,dE = \int_{E}^{E_o} (1-B(E))\,F(E')\,dE'\,\frac{dE}{E'} + S\,\frac{dE}{E_o} \tag{A.1.1}$$

where E_o represents the source neutrons and E' the neutrons having energies higher than E other than the source. The first term on the right side of equation 1.1 is the down-scatter source and the second term is the fission source. The (1-B(E)) multiplier of the down-scatter source term indicates the number of neutrons which survive their first collision. The B(E) term is generally small in a water moderated system so that non-absorption is a reasonably accurate first approximation. Cancelling the dE terms from both sides of the equation and not distinguishing between the source term and the down-scatter, equation 1.1 is reduced to

$$F(E) = \int_{E}^{E_o} \left[\frac{F(E') + S}{E'}\right] dE' \tag{A.1.2}$$

Differentiating with respect to E gives

$$\frac{dF(E)}{dE} = -\frac{F(E')}{E} - \frac{S}{E} \tag{A.1.3}$$

This equation is exact in an infinite medium and could be solved if S and F(E') were known. After rearrangement the following equation is obtained

$$d(E\,F(E)) = -S(E)\,dE \tag{A.1.4}$$

The source term may be approximated by the following

$$-S(E) = a\sqrt{E}\; e^{-bE} \qquad \text{A.1.5}$$

Upon substitution and integration the following form is obtained

$$F(E) = -\frac{a}{E}\int_{E}^{E_o} E^{1/2}\, e^{-bE}\, dE \qquad \text{A.1.6}$$

The fission spectrum suggested by Cranberg is of the form (5)

$$I = -a\int_{E}^{E_o} E^{1/2}\, e^{-bE}\, dE \qquad \text{A.1.7}$$

This is very similar to equation 1.6 developed for a water moderated system. Setting $E = y^2$ and integrating by parts yields

$$I = \frac{ay}{b} e^{-by^2}\Big|_{\sqrt{E}}^{\sqrt{E_o}} - \frac{a}{b}\int_{\sqrt{E}}^{\sqrt{E_o}} e^{-by^2}\, dy \qquad \text{A.1.8}$$

Setting $t = \sqrt{b}\, y$ and substituting in the source term gives

$$I = -\frac{S(E)}{b} - \frac{a}{b^{3/2}}\int_{\sqrt{bE}}^{\sqrt{bE_o}} e^{-t^2}\, dt \qquad \text{A.1.9}$$

The error function, which is denoted by erf(x) is defined by the integral

$$\operatorname{erf}(x) = \frac{2}{\sqrt{\pi}}\int_{0}^{x} e^{-t^2}\, dt$$

The total area under the curve from t equal zero to t equal infinity is unity. Applying the error function to equation 1.9 and substituting for the upper bound gives

$$I = -\frac{S(E)}{b} - \frac{a\sqrt{\pi}}{2b^{3/2}}\left[1 - \operatorname{erf}(\sqrt{bE})\right] \qquad \text{A.1.10}$$

From equations 1.5 and 1.6

Let $I = -EF(E) + S(E)$

then equation 1.10 becomes

$$F(E) = \frac{1}{E}\left[ES(E) + \frac{S(E)}{b} + \frac{a\sqrt{\pi}}{2\,b^{3/2}}\left[1 - \text{erf}(\sqrt{bE})\right]\right] \qquad \text{A.1.11}$$

The reaction rate is

$$F(E) = \Sigma_s(E)\,\phi(E)$$

then

$$\phi(E) = \frac{1}{E\,\Sigma_s(E)}\left[ES(E) + \frac{S(E)}{b} + \frac{a\sqrt{\pi}}{2\,b^{3/2}}\left[1 - \text{erf}(\sqrt{bE})\right]\right] \qquad \text{A.1.12}$$

Resubstituting for the source terms and letting the normalization constant be

$$\phi_0' = \frac{1}{b^{3/2}}$$

Equation 1.12 then becomes

$$\phi(E) = \frac{\phi_0'}{E\Sigma_s(E)}\left[a(bE)^{3/2}e^{-bE} + a\sqrt{bE}\;e^{-bE} + \frac{a\sqrt{\pi}}{2}\left[1 - \text{erf}(\sqrt{bE})\right]\right] \qquad \text{A.1.13}$$

When dealing with an hydrogenous system the following approximations can be made.

$$\Sigma_s \sim \Sigma_s(E_0)\left[\frac{E_0}{E}\right]^k$$

and

$$\phi_0' \sim \Sigma_s(E_0)\,E_0^k\,\phi_0$$

The form of the equation describing the differential energy spectrum of the flux in a pool reactor is

$$\phi(E) = \frac{\phi_0 a}{E^{1-k}}\left[(bE)^{3/2}e^{-bE} + \sqrt{bE}\;e^{-bE} + \frac{\sqrt{\pi}}{2}\left[1 - \text{erf}(\sqrt{bE})\right]\right]$$

Since E^{1-k} is a parameter set by the experimenter, for ease of calculation this can be set to E^k, producing the final results (2).

$$\phi(E) = \frac{\phi_0 a}{E^k}\left[(bE)^{3/2}e^{-bE} + \sqrt{bE}\;e^{-bE} + \frac{\sqrt{\pi}}{2}\left[1 - \text{erf}(\sqrt{bE})\right]\right] \qquad \text{A.1.14}$$

A.2 Least-Squares Approximation for Best Fit of Parameters ϕ_o and k

To determine the exponent parameter k and the normalization constant ϕ_o, a least-squares fit to the data is made. Data came in as foil radioactivity and was fit as well as possible by a least-squares fit of parameters k and ϕ_o by

$$\sum_i \left[A_i - \int_{E_i}^{\infty} \sigma_i \, \phi_o \frac{f(E)}{E^k} dE \right]^2 = q \qquad \text{A.2.1}$$

where:

$$f(E) = \left((bE)^{3/2} e^{-bE} + \sqrt{bE}\, e^{-bE} + \frac{\sqrt{\pi}}{2} \left[1 - \mathrm{erf}\left(\sqrt{bE}\right) \right] \right) \qquad \text{A.2.2}$$

and q ranged from 0.075 to 0.51. For equation 2.1 to be a minimum the partial derivatives of q with respect to k and ϕ_o must equal zero. These equations were then solved for ϕ_o and set equal. The partial derivative of q with respect to ϕ_o is:

$$2\sum_i \left[A_i - \int_{E_i}^{\infty} \sigma_i \, \phi_o \frac{f(E)}{E^k} dE \right] \left[\int_{E_i}^{\infty} \sigma_i \frac{f(E)}{E^k} dE \right] = 0$$

let

$$I_i(k) = \int_{E_i}^{\infty} \sigma_i \frac{f(E)}{E^k} dE \qquad \text{A.2.3}$$

then

$$\sum_i A_i I_i(k) = \phi_o \sum_i I_i^2(k)$$

and solving for ϕ_o

$$\phi_o = \frac{\sum_i A_i I_i(k)}{\sum_i I_i^2(k)} \qquad \text{A.2.4}$$

The derivative of q with respect to k is:

$$-2\sum_i \left[A_i - \phi_o I_i(k)\right]\left[-\frac{\partial}{\partial k}\ \frac{1}{E^k}\right]$$

$$\frac{\partial}{\partial k}\ \frac{1}{E^k} = \frac{\ln E}{E^k}$$

$$\sum_i \left[A_j - \phi_o I_i(k)\right]\left[-\int_{E_j}^{\infty} \frac{\sigma_i f(E) \ln E}{E^k}\right]$$

let

$$I_i'(k) = \int_{E_j}^{\infty} \frac{\sigma_i f(E) \ln E}{E^k}\, dE \qquad \text{A.2.5}$$

and solving for ϕ_o

$$\phi_o = \frac{\sum_i A_i I_i'(k)}{\sum_i I_i(k)\, I_i'(k)} \qquad \text{A.2.6}$$

The flux normalization constant ϕ_o should be the same for both equations 2.4 and 2.6. When this is the case

$$\frac{\sum_i A_i I_i(k)}{\sum_i I_i^2(k)} = \frac{\sum_i A_i I_i'(k)}{\sum_i I_i(k) I_i'(k)}$$

and the parameter k can be solved for exactly. In practice such good results generally do not occur; therefore, the following procedure was used.

$$X(k) = \frac{\sum_i A_i I_i(k)}{\sum_i I_i^2(k)} \qquad \text{A.2.7}$$

$$Y(k) = \frac{\sum_i A_i\ I_i'(k)}{\sum_i I_i(k)\, I_i'(k)} \qquad \text{A.2.8}$$

The results sought were:

$$\left| X(k) - Y(k) \right| \leq \epsilon \qquad A.2.9$$

where ϵ was some arbitrarily small value. If convergence did not occur in three iterations, a new value of k was extrapolated by fitting $X(k)$ and $Y(k)$ to parabolic curves and then obtaining the point of intersection as the best choice for the value k. For example

$$X(k) = A_x k_i^2 + B_x k_i + C_x$$

and

$$Y(k) = A_y k_i^2 + B_y k_i + C_y$$

which were solved by matrices. The intercept of the two parabolas being

$$A_x k^2 + B_x k + C_x = A_y k^2 + B_y k + C_y$$

from which was obtained

$$[A_x - A_y] k^2 + [B_x - B_y] k + [C_x - C_y] = 0$$

and solving this by the quadratic formula gives

$$k = \frac{-(B_x - B_y) \pm \sqrt{(B_x - B_y)^2 - 4(A_x - A_y)(C_x - C_y)}}{2(A_x - A_y)}$$

The radical could not be less than zero but for best results was close to zero on the positive side. This yielded only one answer for the exponent. If two values of k existed the one closest to k_3 was used, and this was substituted into the original equations to make sure they were satisfied.

APPENDIX B

COMPUTER CODES USED IN DETERMINING THE DIFFERENTIAL SPECTRUM

Two computer codes were used in determining the differential fast fission spectra. First a code named Photopeak Analysis (PPA) reduced the gamma spectra to individual foil activities. This information was then used in computer code RUFF to tabulate and plot the resulting spectrum.

B.1 Photopeak Analysis (PPA)

The gamma spectrum of each threshold foil was analyzed using a modified version of the computer code PPA(Photopeak Analysis). The code was originally developed by H. M. Murphy, Jr. of the Air Force Weapons Laboratory and modified by Dr. D. R. Edwards. The activity results reduced by PPA were inserted into the computer code RUFF which determined the differential fast flux spectrum. PPA fits photopeaks with a Gaussian (Normal) distribution function, containing a linear bias term through the use of an iterative, least-squares technique. The following information was produced by the code: the exact channel location of the photopeak; the width of the photopeak at half maximum height; the peak count rate; the integrated photopeak count rate with an optional decay correction. Figure B.1 is a schematic flow diagram of PPA's main program.

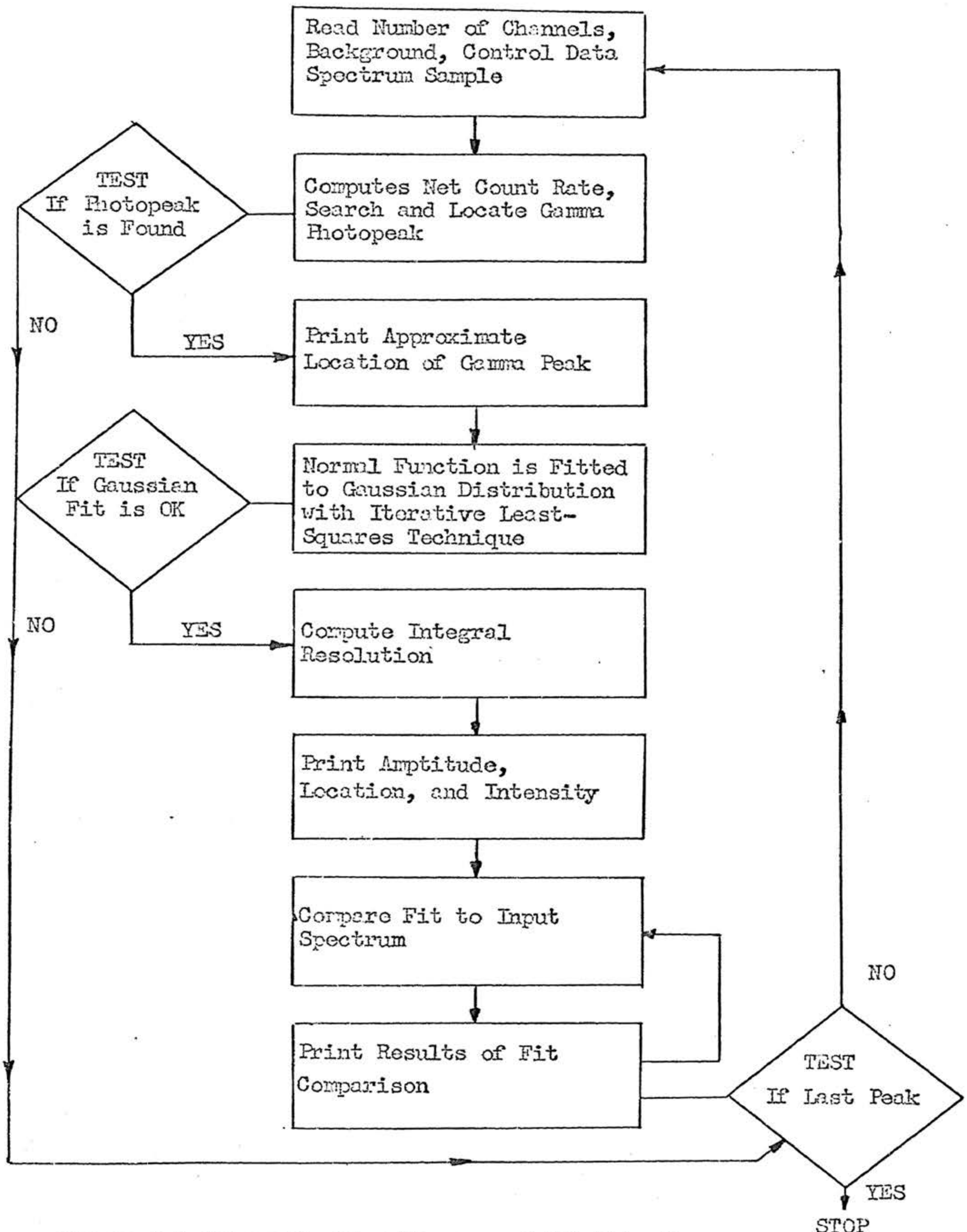

Figure B.1 Schematic Flow Diagram of PPA Main Program

```
      PPA,(PHOTOPEAK ANALYSIS), FITS A GAUSSIAN FUNTION TO SELECTED
      PHOTOPEAKS FOR DETERMINATION OF COUNTRATE UNDER THE PEAK

      DIMENSION BK(400),Y(400),PK(5),HOBB(15),HOBT(15),HOBX(15),HZB(4),
     2HNB(4)
      COMMON HODE(20),KODE(20),AT(3,5),ANV(3,3)

      READ (1,55) HZB,HNB
      READ (1,74) HODE,KODE
      READ (1,57) ((AT(I,J),I=1,3),J=1,5)
      READ (1,75) ((ANV(I,J),I=1,3),J=1,3)

      *RELOAD AND START.

    1 READ (1,54) NC
      IF(NC)45,45,2
    2 IF(NC-401)3,45,45

      *ZEROB

    3 DO 4 I=1,NC
    4 BK(I)=0
      DO 904 I=1,4
  904 HOBB(I)=HZB(I)
      DO 5 I=5,15
    5 HOBB(I)=0
      KBF=0

      READ INPUT DATA.

    6 READ (1,55) HOBX
      J=JTEST(HOBX(1))
      GO TO (7,37,41,43,3,1,46),J

      READ UNKNOWN SPECTRUM.

    7 READ (1,56) TX,TZ,T12,PK
      READ (1,557) (Y(I),I=1,NC)
  557 FORMAT(8(4X,F6.0))
      J=1
      CT=Y(1)/100.
      IF(CT)8,9,9
    8 CT=1.
    9 IF(KBF)10,13,10
   10 DO 12 I=1,NC
      Y(I)=(Y(I)/CT)-BK(I)
      IF(Y(I))11,12,12
   11 Y(I)=0
   12 CONTINUE
      GO TO 15
   13 DO 14 I=1,NC
   14 Y(I)=Y(I)/CT
   15 DT=TX-TZ
      IF(T12)16,16,17
   16 CF=1.
      GO TO 21
   17 IF(DT)18,16,19
   18 DT=-DT
   19 CEXP=0.69314718*DT/T12
```

```
      IF(CFXP-88.)20,16,16
   20 CF=EXP(-CFXP)

      FIT UNKNOWN SPECTRUM AT P(K).

      WRITE (3,59) HOBB
   21 WRITE (3,58) HOBX
      WRITE (3,60) TX,TZ,DT,CF,T12
      WRITE (3,61) CT
      WRITE (3,62) PK(J)
      IB=0.90*PK(J)
      IT=(1.10*PK(J))+0.5
      IF(5-IB)23,23.22
   22 IB=5
   23 IF(IT-NC)25,25,24
   24 IT=NC
   25 D=PEACH(Y,IB,IT,NC)
      IF(D)47,47,26
   26 WRITE (3,63) D
      DDD=D

      CALL DREPK(Y,NC,A,B,C,D,E)

      IF(C)48,48,27
   27 SIGMA=SQRT(-1./(E+E))
      TOTX=2.506628*SIGMA*C
      TOTZ=TOTX/CF
      RES=235.02*SIGMA/D
      WRITE (3,65) C,D
      WRITE (3,66) SIGMA,RES
      WRITE (3,67) TOTX,TOTZ
      WRITE (3,68)
      IF(IB)28,28,29
   28 IB=1
   29 IT=(D+3.*SIGMA)+0.5
      IF(IT-NC)31,31,30
   30 IT=NC
   31 SY=0
      SG=0

      COMPARE RESULTS OF FIT WITH ORIGINAL DATA.

      DO 34 I=IB,IT
      X=I
      DIX=D-X
      YG=C*EXP(E*DIX*DIX)
      YF=A+B*X+YG
      SY=SY+Y(I)
      SG=SG+YG
      IF(KBF)32,32,33
   32 TBK=0
      GO TO 34
   33 TBK=BK(I)
   34 WRITE (3,69) I,TBK,Y(I),YF,YG,SY,SG
   35 J=J+1
      IF(J-6)36,6,6
   36 IF(PK(J))6,6,21

      *BACKG
```

```
 37 READ (1,55) HOBB
    READ (1,57) (BK(I),I=1,NC)
    CT=BK(1)/100.
    IF(CT)38,38,39
 38 CT=1.
 39 DO 40 I=1,NC
 40 BK(I)=BK(I)/CT
    KBF=1
    GO TO 6

    *NOBAC

 41 KBF=0
    DO 42 I=1,15
    HOBT(I)=HOBB(I)
 42 HOBB(I)=0.
    DO 942 I=1,4
942 HOBB(I)=HNB(I)
    GO TO 6

    *RECAL

 43 KBF=1
    DO 44 I=1,15
 44 HOBB(I)=HOBT(I)
    GO TO 6

    ERROR DIAGNOSTICS.

 45 WRITE (3,70) NC
 46 WRITE (3,72)
    CALL EXIT

    PROGRAM EXIT.


    NO PEAK COMMENTC

 47 WRITE (3,64) PK(J)
    GO TO 35

    LIST INPUT DATA ON WHICH GAUSS FAILED TO CONVERGE.

 48 WRITE (3,73)
    IB=0.85*DDD
    IT=1.15*DDD+0.5
    IF(IB)49,49,50
 49 IB=1
 50 IF(IT-NC)52,52,51
 51 IT=NC
 52 DO 53 I=IB,IT
 53 WRITE (3,69) I,BK(I),Y(I)
    GO TO 35

                   =====   FORMATS   =====

 54 FORMAT (I3)
 55 FORMAT (15A4)
 56 FORMAT (8E10.4)
 57 FORMAT(10F8.0)
```

```
 58 FORMAT (9H1        PPA 2X 15A4/1X)
 59 FORMAT (11X 15A4/1X)
 60 FORMAT (6X 4HTX = F10.4,3X 4HTZ = F10.4,3X 4HDT = F9.4/6X 18HTHE D
   2ECAY FACTOR = F13.8,3X 6HT1/2 = F9.3,6H DAYS.)
 61 FORMAT (6X 17HTHE COUNT TIME IS F7.2,9H MINUTES.)
 62 FORMAT (6X 31HTHE PEAK IS EXPECTED IN CHANNEL F7.2,1H./31H0       ST
   2ART PHOTOPEAK ANALYSIS./1X)
 63 FORMAT (6X 35HTHE PEAK APPEARS TO BE NEAR CHANNEL F7.2,1H.)
 64 FORMAT (33H0       NO PEAK EXISTS NEAR CHANNEL F7.2,1H.)
 65 FORMAT (27H0       THE PEAK AMPLITUDE IS F8.2,19H CPM/CH AT CHANNEL
   2F7.2,1H.)
 66 FORMAT (6X 25HTHE STANDARD DEVIATION IS F6.2,12H CHANNELS, ( F6.2,
   215H PERCENT FWHM).)
 67 FORMAT (6X 27HTHE PHOTOPEAK COUNT-RATE IS F9.2,29H CPM AT TX, WHIC
   2H CORRESPONDS/6X 18HTO A COUNT-RATE OF   E11.4,11H CPM AT TZ.)
 68 FORMAT (9H0          I 6X 4HB(I) 6X 4HY(I) 7X 3HFIT 5X 5HGAUSS 6X 4HS
   2UMY 8X 2HSG/1X)
 69 FORMAT (5X I4,4F10.2,2F10.1)
 70 FORMAT (42H1       THE NUMBER OF CHANNELS IS INCORRECT./6X 4HNC = I4
   2/1H0)
 72 FORMAT (25H0       END OF COMPUTATION./1H1)
 73 FORMAT (9H0          I 6X 4HB(I) 6X 4HY(I)/1X)
 74 FORMAT (20A4,/ 20I3)
 75 FORMAT (4E15.8)
    END
    FUNCTION JTEST(HARD)

    FUNCTION JTEST TESTS THE WORD HARD TO SEE IF IT IS A SPECIAL
    CONTROL WORD.
    COMMON HODE(20),KODE(20),AT(3,5),ANV(3,3)

  2 DO 4 I=1,20
    IF(HARD-HODE(I)) 4,3,4
  3 JTEST=KODE(I)
    GO TO 5
  4 CONTINUE
    JTEST=1
  5 RETURN
    END
    FUNCTION PEACH(Y,NB,NT,NC)

    FUNCTION PEACH LOCATES THE PEAK (IF ANY) IN THE BAND NB-NT OF THE
    SPECTRUM Y. THE OUTPUT IS FLOATING AND NOT TRUNCATED.

    DIMENSION Y(400),VY(5),VN(3),C(3)
    COMMON HODE(20),KODE(20),AT(3,5),ANV(3,3)
    EQUIVALENCE (C(3),C3),(C(2),C2),(C(1),C1),(VY(5),VY5)


    START AND INITIAL TESTS.

101 IF(5-NC)1,1,17
  1 IF(1-NB)2,2,17
  2 IF(NT-NC)3,3,17
  3 IF(NB+4-NT)5,5,4
  4 NB=NB-1
    NT=NT+1
    GO TO 1
```

```
 5 NL=NB-2
   DO 6 J=2,5
   K=NL+J
 6 VY(J)=Y(K)
   BIGY=0
   BIGX=0
   NL=NT-4

   MAIN ITERATION STARTS HERE.

   DO 16 I=NB,NL

   PUSH WINDOW DOWN AND ENTER NEXT Y VALUE IN TOP LOCATION.

   DO 7 J=1,4
 7 VY(J)=VY(J+1)
   VY5=Y(I+4)

   PRE-MULTIPLY WINDOW BY TRANSPOSE MATRIX TO OBTAIN NORMAL VECTOR.

   DO 9 J=1,3
   SUM=0
   DO 8 K=1,5
 8 SUM=SUM+AT(J,K)*VY(K)
 9 VN(J)=SUM

   PRE-MULTIPLY NORMAL VECTOR BY INVERSE MATRIX TO OBTAIN SECOND-
   ORDER POLYNOMIAL CONSTANTS.

   DO 11 J=1,3
   SUM=0
   DO 10 K=1,3
10 SUM=SUM+ANV(J,K)*VN(K)
11 C(J)=SUM

   TEST SECOND DERIVATIVE.

   IF(C3)12,16,16

   EVALUATE PEAK LOCATION TO DETERMINE IF IT IS IN WINDOW LIMITS.

12 XP=-C2/(C3+C3)
   IF(1.-XP)13,14,16
13 IF(XP-5.)14,14,16

   EVALUATE PEAK AMPLITUDE TO SEE IF IT IS A MAXIMUM.

14 YP=((C3*XP)+C2)*XP+C1
   IF(YP-BIGY)16,16,15
15 BIGY=YP
   XI=I-1
   BIGX=XP+XI
16 CONTINUE

   END MAIN ITERATION AND EXIT.

   PEACH =BIGX
   RETURN
```

```
   ERROR RETURN.

17 WRITE (3,18) NB,NT,NC
   PEACH=-1.

                 =====   FORMATS     =====

   RETURN
18 FORMAT (18H0       PEACH ERROR./6X 4HNB = I4/6X 4HNT = I4/6X 4HNC =
  2I4/1H0)
   END
   SUBROUTINE DREPK(Y,NC,A,B,C,D,E)

   THIS ROUTINE FITS A MODIFIED GAUSSIAN FUNCTION TO PHOTOPEAKS
   OBTAINED ON A SCINTILLATION PULSE HEIGHT ANALYZER.

   F(X,A,B,C,D,E)=A+B*X+C*EXP(E*(D-X)**2)

   DIMENSION Y(400),YW(100),XW(100),YF(100),X(100,5),AA(5,6),AROW(6)

   EQUIVALENCE (AA(1,6),DA),(AA(2,6),DB),(AA(3,6),DC),(AA(4,6),DD),
  2(AA(5,6),DE)

   START AND INITIAL GUESSES

   Q=1.E6
 1 I=D+0.5
   JIG=0
   A=0
   B=0
   C=Y(I)
   SIG=0.323+0.0314*D
   E=-0.5/(SIG*SIG)
   CCC=C
   DDD=D
   EEE=E
   Z=1
   ISIG=SIG+SIG+0.5
   IF(ISIG)2,2,3
 2 ISIG=1
 3 IB=I-3
   IT=I+3
   I=ISIG
   IF(IB*(NC-IT))41,41,4
 4 IBB=IB-1
   ITT=IT+1
   IF(IBB*(NC-ITT))8,8,5
 5 IF(Y(IB)-Y(IBB))8,8,6
 6 IF(Y(IT)-Y(ITT))8,8,7
 7 IB=IBB
   IT=ITT
   I=I-1
   IF(I)8,8,4

   LOAD X AND Y WINDOWS AND PREPARE FIRST TWO COLUMNS OF MATRIX X.

 8 J=0
   DO 9 I=IB,IT
   J=J+1
   XW(J)=I
```

```
      YW(J)=Y(I)
      X(J,1)=1
    9 X(J,2)=XW(J)
      IMAX=J
      IPASS=1

      MAIN ITERATION STARTS HERE.
      PREPARE LAST THREE COLUMNS OF MATRIX X AND LOAD VECTOR YF FOR
      LEAST SQUARE SOLUTION FOR CORRECTION TERMS.

   10 DO 11 I=1,IMAX
      DIX=D-XW(I)
      EXPON=EXP(E*DIX*DIX)
      X(I,3)=EXPON
      X(I,4)=2.*E*C*DIX*EXPON
      X(I,5)=C*DIX*DIX*EXPON
   11 YF(I)=YW(I)-(A+B*XW(I)+C*EXPON)

      PREPARE NORMAL EQUATIONS IN MATRIX AA.

      DO 15 I=1,5
      DO 13 J=1,5
      SUM=0
      DO 12 K=1,IMAX
   12 SUM=SUM+X(K,I)*X(K,J)
   13 AA(I,J)=SUM
      SUM=0
      DO 14 K=1,IMAX
   14 SUM=SUM+X(K,I)*YF(K)
   15 AA(I,6)=SUM

      SOLVE SYSTEM OF LINEAR NORMAL EQUATIONS BY MEANS OF THE JORDAN
      ALGORITHM.

      DO 24 I=1,5
      BIG=ABS(AA(I,I))
      KBIG=0
      DO 17 K=I,5
      T=ABS(AA(K,I))
      IF(T-BIG)17,17,16
   16 BIG=T
      KBIG=K
   17 CONTINUE
      IF(BIG)1,38,18
   18 IF(KBIG)1,21,19
   19 DO 20 J=I,6
      T=AA(I,J)
      AA(I,J)=AA(KBIG,J)
   20 AA(KBIG,J)=T
   21 T=1./AA(I,I)
      DO 22 J=I,6
   22 AROW(J)=T*AA(I,J)
      DO 23 K=1,5
      T=AA(K,I)
      DO 23 J=I,6
   23 AA(K,J)=AA(K,J)-T*AROW(J)
      DO 24 J=I,6
   24 AA(I,J)=AROW(J)

      END OF LINEAR EQUATION SOLUTION.
```

```
   APPLY CORRECTION TERMS TO A,B,C,D, AND E, OBSERVING SIGN
   RESTRICTIONS.

   A=A+(DA*Z)
   B=B+(DB*Z)
   C=C+(DC*Z)
   IF(C)25,26,26
25 C=0
26 D=D+(DD*Z)
   IF(D-1.)27,28,28
27 D=1
28 E=E+(DE*Z)
   IF(E)30,30,29
29 E=0

   TEST RELATIVE CORRECTION TERMS FOR CONVERGENCE.

30 IF(ABS(A/Q)-ABS(DA)) 36,36,31
31 IF(ABS(B/Q)-ABS(DB)) 36,36,32
32 IF(ABS(C/Q)-ABS(DC)) 36,36,33
33 IF(ABS(D/Q)-ABS(DD)) 36,36,34
34 IF(ABS(E/Q)-ABS(DE)) 36,36,35
35 WRITE (3,42) IPASS
   RETURN

   NOT YET CONVERGED.  INCREMENT IPASS AND TRY AGAIN.

36 IPASS=IPASS+1
   IF(IPASS-33)10,37,37
37 IPASS=IPASS-1
   WRITE (3,43) IPASS
   RETURN

   INCONSISTENT EQUATIONS. RESET CONSTANTS FOR A SECOND TRY.

38 IF(JIG)41,39,41
39 IF(IPASS)41,41,40
40 JIG=1
   A=0
   B=0
   C=CCC
   D=DDD
   E=EEE
   Z=0.5
   WRITE (3,45) IPASS
   IPASS=0
   GO TO 10

   INCONSISTENT CORRECTION EQUATIONS ERROR RETURN.

41 WRITE (3,44)
   A=0
   B=0
   C=0
   RETURN

                 =====    FORMATS    =====

42 FORMAT (6X I2,12H ITERATIONS.)
43 FORMAT (6X 49HWARNING.  SUBROUTINE GAUSS DID NOT CONVERGE AFTER I2
```

```
  2,12H ITERATIONS.)
44 FORMAT (62H0      SUBROUTINE GAUSS CANNOT OBTAIN A SOLUTION FOR THI
  2S DATA./1X)
45 FORMAT (6X 29HSUBROUTINE GAUSS FAILED AFTER I3,12H ITERATIONS./6X
  256HTHE CONVERGENCE RATE HAS BEEN RETARDED FOR A SECOND TRY.)
   END
```

B.2 Spectrum Code RUFF

RUFF was used in determining the differential fast flux spectrum. It is a computerization of what was presented under Section III. (Theoretical Analysis) and Appendix A. (Derivation of Equations). It was written by Dr. D. R. Edwards in Fortran IV G. A flow diagram of the program is illustrated in Figure B.2.

There is a cross-section library for nine reactions extending in energy from 0.1 to 20 Mev, in 100 Kev increments. The reaction cross-section values were the latest available, and are given in Tables C.1 thru C.9 (31). The reactions and sequence used were: In-115(n,n')In-115m; Ni-58(n,p)Co-58; Fe-54(n,p)Mn-54; Al-27(n,p)Mg-27; Fe-56(n,p)Mn-56; Mg-24(n,p)Na-24; Al-27(n,α)Na-24; Fe-54(n,α)Cr-51; and In-115(n,2n)In-114m.

There is a simple plotter routine built into the RUFF code that plots the log of the flux as a function of energy. The energy units are linear and extend along the abscissa from 0 to 20 Mev. The flux extends along the ordinate axis eight cycles whose area of coverage can be raised or lowered easily by changing two IBM cards, the CALL ORIGIN, and CALL YSCALE..

The program code RUFF has the following features:

(1) It allows the differential flux spectrum to be obtained by use of nine foils. This can be increased by merely adding the desired cross-section libraries.

(2) The degree of fit for the flux spectrum can be set by the experimenter. The code iterates until this accuracy is achieved or the maximum number of 100 iterations is exceeded. A chi-square error is produced.

(3) It provides a calculated activity and compares it with the measured activity for each foil.

(4) It tabulates and plots the flux spectrum.

The sequence of operations was contained in the following steps.

(1) F(I) was determined as a function of energy. F(I) is the calculated differential energy spectrum, equation 2.2.

(2) The number of foils and the cross-section library as a function of energy were read in.

(3) Data necessary for the determination of the activity concentration CON(I), was read in. Specifically these values are A(I), W(I), TIR(I), PC(I), PA(I), EP(I), GPD(I), THALF(I) and Z(I).

(4) The minimum and maximum energy exponent parameters were read in.

(5) Subroutine INTEGER was called for the calculation of integrals, equations 2.3 and 2.5.

(6) A least-squares approximation was made to determine the best fit of the exponent parameter and the normalization parameter.

(7) Iteration occurred until the criteria for a best fit was satisfied. Then the flux as a function of energy was printed out.

The data information read into the program were: NFOIL (The number of reactions used, the number used was 9. As many as desired are possible); DELTA (the best fit criteria for the least squares approximation); SIG (cross-sections as a function of energy); A(I) (foil activations which are obtained from the program PPA); W(I) (Foil weight); TIR(I) (irradiation time); PC(I) (percentage concentration of the target element); PA(I) (percent abundance of target element); EP(I) (efficiency of the detector as a function of gamma energy); GPD(I) (gammas per disintegration); THALF(I) (the half-life of the reaction product isotope); Z(I) (the atomic weight of the reaction produced isotope); EX(1) and EX(2) (the lower and upper limits of the energy exponent parameter 0.6 and 0.75 respectively). The values A(I), TIR(I), and W(I) are variables that change with each irradiation and new set of foils. The values PC(I), PA(I), EP(I), GPD(I), THAL(I), and Z(I) are constant once the foils and reactions are chosen, and are listed in Table B.1.

The information printed out is:

(1) the number of iterations

(2) the energy exponent

(3) Integral A

(4) Integral B

(5) Calculated Activity

(6) Chi-Square error

(7) Degrees of freedom

(8) Tabulated flux spectrum

(9) Graphical plot of flux spectrum

Table B.1

Constants for RUFF Activity Concentration

Foil	PC(I)	PA(I)	EP(I)	GPD(I)	THALF(I) (min)	Z(I)
In-115(n,n')In-115m	.100E01	.958E00	.970E00	.100E01	.270E03	.115E03
Ni-58(n,p)Co-58	.100E01	.678E00	.835E00	.990E00	.103E06	.580E02
Fe-54(n,p)Mn-54	.100E01	.063E00	.835E00	.100E01	.419E06	.540E02
Al-27(n,p)Mg-27	.100E01	.100E01	.775E00	.100E01	.900E01	.270E02
Fe-56(n,p)Mn-56	.100E01	.917E00	.814E00	.100E01	.155E03	.560E02
Mg-24(n,p)Na-24	.100E01	.786E00	.688E00	.100E01	.900E03	.240E02
Al-27(n,α)Na-24	.100E01	.100E01	.688E00	.100E01	.900E03	.240E02
Fe-54(n,α)Cr-51	.100E01	.100E01	.970E00	.090E00	.389E05	.510E02
In-115(n,2n)In-114m	.100E01	.958E00	.100E01	.965E00	.706E05	.114E03

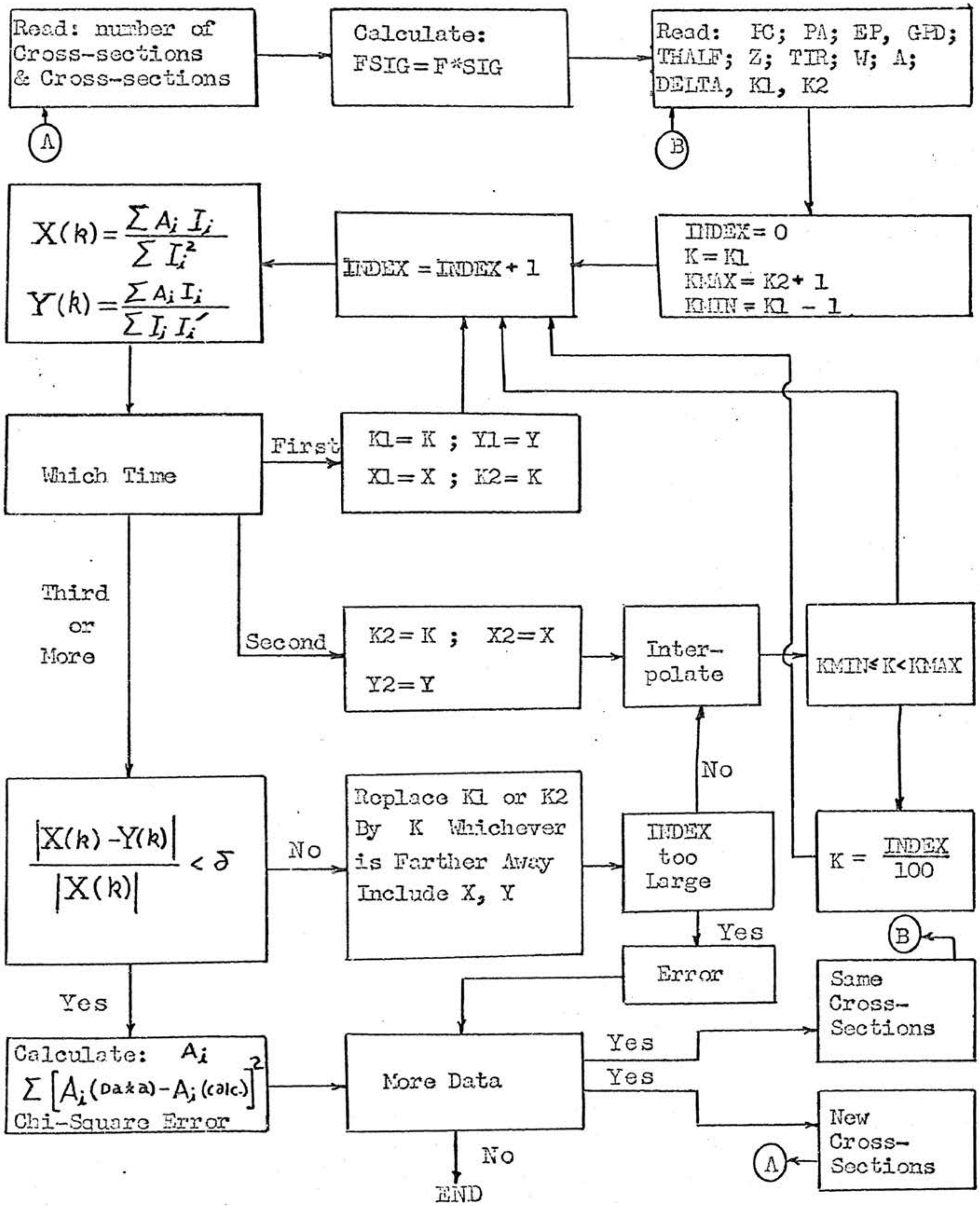

Figure B.2 Flow Diagram of Computer Code RUFF

```
      RUFF--A PROGRAM TO ESTIMATE THE FAST FLUX SPECTRUM FROM A LIMITED
      NUMBER OF FOIL MEASUREMENTS

      DIMENSION E(200),F(200),SIG(200,10),FSIG(200,10),A(10),THALF(10),
     2Z(10),TIR(10),W(10),PA(10),PC(10),EP(10),GPD(10),EX(3),X(3),Y(3),
     3CON(10),ENT(10),ENTP(10),PHI(200),PHII(200)
      CALL PENPOS('TILL,HENRY',10,0)
      B=0.775
      PI=3.14159
      SPI=SQRT(PI)
      DO 10 I=1,200
      E(I)=0.1*I
      BE=B*E(I)
      F(I)=SQRT(BE)*(1.+BE)*EXP(-BE)+SPI*(1.-ERF(SQRT(BE)))/2
   10 CONTINUE

      READ CROSS SECTIONS AS PREPARED BY 'CROSS'

   20 READ(1,1000)
      WRITE (3,1000)
      READ (1,1010) NFOIL,MORE
      DO 30 J=1,NFOIL
      READ (1,1020) (SIG(I,J),I=1,200)
      DO 25 I=1,200
      FSIG(I,J)=F(I)*SIG(I,J)
   25 CONTINUE
   30 CONTINUE
      GO TO 50
   40 READ (1,1000)
      WRITE (3,1000)
      READ (1,1010) NFOIL,MORE
   50 DO 60 I=1,NFOIL
      READ(1,1030) PC(I), PA(I), EP(I), GPD(I), THALF(I), Z(I),
     2TIR(I), W(I), A(I)
      CON(I)=W(I)*PA(I)*PC(I)*EP(I)*(1-EXP(-.693*TIR(I)/THALF(I)))/(Z(I)
     2*GPD(I))
   60 CONTINUE
      READ (1,1020) DELTA
      READ (1,1030) EX(1),EX(2)
      EXMIN=EX(1)-1
      EZ=EX(1)
      INDEX=-2
      EMAX=EX(2)+1
      WRITE (3,2000)
   70 INDEX=INDEX+1
      XA=0
      CALL INTEGR(EZ,FSIG,E,NFOIL,ENT,ENTP)
      XA=A(1)*CON(1)*ENT(1)
      XB=(CON(1)*ENT(1))**2
      YA=A(1)*CON(1)*ENTP(1)
      YB=CON(1)**2*ENT(1)*ENTP(1)
      DO 80 I=2,NFOIL
      XA=XA+A(I)*CON(I)*ENT(I)
      XB=XB+(CON(I)*ENT(I))**2
      YA=YA+A(I)*CON(I)*ENTP(I)
   80 YB=YB+CON(I)**2*ENT(I)*ENTP(I)
      XA=XA/XB
      YA=YA/YB
      WRITE(3,217) YA
```

```
217 FORMAT(E12.6)
    WRITE (3,2010) INDEX,EZ,XA,XB
    IF(INDEX) 90,100,110
 90 EX(1)=EZ
    X(1)=XA
    Y(1)=YA
    EZ=EX(2)
    GO TO 70
100 EX(2)=EZ
    X(2)=XA
    Y(2)=YA
    GO TO 70
110 IF(ABS(1-YA/XA)-DELTA) 200,200,120

    REPLACEMENT OF ONE X,Y,AND EX VALUE FOR NEXT INTERPOLATION
    THE VALUE CLOSEST TO EZ IS REPLACED

120 IF(ABS(EX(1)-EZ)-ABS(EX(2)-EZ)) 130,130,140
130 EX(1)=EZ
    X(1)=XA
    Y(1)=YA
    GO TO 150
140 EX(2)=EZ
    X(2)=XA
    Y(2)=YA
150 IF(INDEX-100) 170,170,160
160 WRITE (3,2020)
    GO TO 230
170 EZ=(EX(1)*(Y(2)-X(2))-EX(2)*(Y(1)-X(1)))/(Y(1)-Y(2)-X(1)+X(2))
    EZ=EZ-0.1
    IF(EZ-EMAX) 180,70,190
180 IF(EZ-EMIN) 190,70,70
190 EZ=INDEX/100.
    GO TO 70
200 PHIZ=(XA+YA)/2
    CHI=0
    WRITE (3,2030)
    DO 210 I=1,NFOIL
    AP=PHIZ*CON(I)*ENT(I)
    CHI=CHI+((AP/A(I)-1)**2)/A(I)
210 WRITE (3,2040) I,A(I),AP
    NN=NFOIL-2
    WRITE (3,2050) CHI,NN
    DO 220 I=1,200
    E(I)=0.1*I
    PHI(I)=PHIZ*E(I)/(E(I)**EZ)
220 CONTINUE
    WRITE (3,2060)
    WRITE(3,2070) (E(I),PHI(I),I=1,200)
    DO 237 I=1,200
237 PHII(I)=ALOG10(PHI(I))
    CALL NEWPLT(1.0,1.5,8.0)
    CALL ORIGIN(0.0,2.0)
    CALL XSCALE(0.0,20.0,6.0)
    CALL YSCALE(2.0,10.0,8.0)
    CALL XAXIS(1.0)
    CALL YAXIS(1.0)
    CALL XYPLT(E,PHII,200,1,4)
    CALL ENDPLT
230 IF(MORE) 20,40,240
```

```
 240 CONTINUE
     CALL LSTPLT
     CALL EXIT

     FORMAT STATEMENTS

1000 FORMAT ('
    2                          ')
1010 FORMAT (10I5)
1020 FORMAT (5E12.4)
1030 FORMAT(6F12.3)
2000 FORMAT ('0' 7X 'ITERATION' 7X 'EXPONENT' 8X 'INTEGRAL-A' 7X 'INTE
    2RAL-B' /)
2010 FORMAT (8X I5, 3(5X E12.6))
2020 FORMAT ('0' 4X 'NUMBER OF ITERATIONS EXCESSIVE')
2030 FORMAT ('1' 13X 'FOIL' 29X 'ACTIVITY'/ 13X 'NUMBER' 15X 'MEASURED
    2 16X 'CALCULATED' /)
2040 FORMAT (11X I5, 16X E12.6, 13X E12.6)
2050 FORMAT ('0' 4X 'CHI-SQUARED =' E12.6,/ 5X 'DEGREES OF FREEDOM ='
    2I3)
2060 FORMAT (/ 4(3X 'E' 8X 'PHI'5X) /)
2070 FORMAT (4(1X F5.1,2X E12.6))
     END

     SUBROUTINE INTEGR(EZ,FSIG,E,NFOIL,ENT,ENTP)

     CALCULATES INTEGRALS FOR RUFF

     DIMENSION FSIG(200,10),E(200),ENT(10),ENTP(10)

     DO 20 I=1,NFOIL
     ENT(I)=0
     ENTP(I)=0
     DO 10 J=1,199,2
     X=FSIG(J,I)/(E(J)**EZ)
     Y=FSIG(J+1,I)/(E(J+1)**EZ)
     ENT(I)=ENT(I)+4*X+2*Y
     ENTP(I)=ENTP(I)+4*X*ALOG(E(J))+2*Y*ALOG(E(J+1))
  10 CONTINUE
     X=E(2)-E(1)
     ENT(I)=(ENT(I)-Y)*X/3
     ENTP(I)=(ENTP(I)-Y*ALOG(E(200)))*X/3
  20 CONTINUE
     RETURN
     END

     FUNCTION ERF(X)

  10 IF(ABS(X)-3.7) 30,20,20
  20 ERF=1
     GO TO 55
  30 XX=ABS(X)
     IF(XX-1.E-5) 40,40,50
  40 ERF=1.12838*XX
     GO TO 55
  50 ERF=1.-1./(1.+XX*(.14112821+XX*(.08864027+XX*(.02743349+XX*
    2(-.00039446+XX*.00328975)))))**8
  55 IF(X) 60,70,70
  60 ERF=-ERF
  70 RETURN
```

END

CROSS-SECTION LIBRARIES USED IN PROGRAM CODE RUFF
LIBRARY ENERGY RANGE 0.1 THRU 20 MEV. IN INCEMENTS OF 100 KEV

CROSS-SECTION LIBRARY FOR IN115(N,N')IN115M REACTION

.0000E00	.0000E00	.0000E00	.0000E00	.0000E00
.1500E01	.4000E01	.1105E02	.1900E02	.3500E02
.5000E02	.1200E03	.1320E03	.1400E03	.1540E03
.1860E03	.1980E03	.2270E03	.2820E03	.2700E03
.2860E03	.2860E03	.3150E03	.3320E03	.3400E03
.3750E03	.3780E03	.3700E03	.3600E03	.3540E03
.3500E03	.3400E03	.3350E03	.3250E03	.3150E03
.3000E03	.3200E03	.3400E03	.3200E03	.3050E03
.2900E03	.2920E03	.2950E03	.2980E03	.2950E03
.2900E03	.2800E03	.2760E03	.2740E03	.2580E03
.2480E03	.2400E03	.2300E03	.2310E03	.2300E03
.2200E03	.2170E03	.2140E03	.2120E03	.2090E03
.2070E03	.1950E03	.1900E03	.1830E03	.1820E03
.1750E03	.1700E03	.1650E03	.1600E03	.1580E03
.1530E03	.1450E03	.1350E03	.1330E03	.1320E03
.1280E03	.1250E03	.1200E03	.1150E03	.1100E03
.1070E03	.1040E03	.1000E03	.9500E02	.9000E02
.8200E02	.7000E02	.6500E02	.6000E02	.5700E02
.5000E02	.4500E02	.4100E02	.3900E02	.3500E02
.3200E02	.2000E02	.1500E02	.1000E02	.7000E01
.0000E00	.0000E00	.0000E00	.0000E00	.0000E00
.0000E00	.0000E00	.0000E00	.0000E00	.0000E00
.0000E00	.0000E00	.0000E00	.0000E00	.0000E00
.0000E00	.0000E00	.0000E00	.0000E00	.0000E00
.0000E00	.0000E00	.0000E00	.0000E00	.0000E00
.0000E00	.0000E00	.0000E00	.0000E00	.0000E00
.0000E00	.0000E00	.0000E00	.0000E00	.0000E00
.0000E00	.0000E00	.0000E00	.0000E00	.0000E00
.0000E00	.0000E00	.0000E00	.0000E00	.0000E00
.0000E00	.0000E00	.0000E00	.0000E00	.0000E00
.0000E00	.0000E00	.0000E00	.0000E00	.0000E00
.0000E00	.0000E00	.0000E00	.0000E00	.0000E00
.0000E00	.0000E00	.0000E00	.0000E00	.0000E00
.0000E00	.0000E00	.0000E00	.0000E00	.0000E00
.0000E00	.0000E00	.0000E00	.0000E00	.0000E00
.0000E00	.0000E00	.0000E00	.0000E00	.0000E00
.0000E00	.0000E00	.0000E00	.0000E00	.0000E00
.0000E00	.0000E00	.0000E00	.0000E00	.0000E00
.0000E00	.0000E00	.0000E00	.0000E00	.0000E00
.0000E00	.0000E00	.0000E00	.0000E00	.0000E00

CROSS-SECTION LIBRARY FOR NI58(N,P)CO58 REACTION

.0000E00	.0000E00	.0000E00	.0000E00	.0000E00
.0000E00	.0000E00	.0000E00	.0000E00	.0000E00
.0000E00	.5000E01	.0500E01	.5000E01	.1000E02
.1800E02	.2000E02	.2500E02	.3000E02	.4000E02
.5000E02	.6000E02	.7000E02	.8000E02	.9000E02
.1000E03	.1200E03	.1500E03	.2000E03	.2600E03
.2300E03	.2150E03	.4550E03	.3450E03	.3000E03
.1800E03	.2100E03	.1850E03	.3200E03	.3500E03
.3700E03	.3950E03	.4100E03	.4300E03	.4600E03
.4680E03	.4750E03	.4900E03	.5030E03	.5160E03

.5250E03	.5400E03	.5525E03	.5650E03	.5750E03
.5800E03	.5900E03	.6000E03	.6100E03	.6150E03
.6200E03	.6250E03	.6300E03	.6350E03	.6380E03
.6400E03	.6450E03	.6450E03	.6460E03	.6450E03
.6440E03	.6420E03	.6400E03	.6400E03	.6400E03
.6400E03	.6400E03	.6400E03	.6450E03	.6450E03
.6450E03	.6450E03	.6450E03	.6400E03	.6400E03
.6400E03	.6400E03	.6400E03	.6375E03	.6325E03
.6300E03	.6300E03	.6275E03	.6275E03	.6250E03
.6250E03	.6210E03	.6180E03	.6160E03	.6140E03
.6120E03	.6100E03	.6080E03	.6050E03	.6020E03
.6000E03	.6000E03	.5980E03	.5950E03	.5920E03
.5900E03	.5800E03	.5730E03	.5700E03	.5680E03
.5650E03	.5640E03	.5630E03	.5620E03	.5610E03
.5600E03	.5575E03	.5500E03	.5475E03	.5450E03
.5400E03	.5375E03	.5325E03	.5300E03	.5250E03
.5200E03	.5150E03	.5100E03	.5050E03	.5000E03
.4950E03	.4900E03	.4850E03	.4750E03	.4650E03
.4550E03	.4400E03	.4300E03	.4200E03	.4100E03
.4000E03	.3950E03	.3900E03	.3850E03	.3800E03
.3700E03	.3600E03	.3500E03	.3400E03	.3200E03
.3100E03	.3000E03	.2900E03	.2800E03	.2700E03
.2600E03	.2400E03	.2200E03	.2100E03	.2000E03
.1800E03	.1600E03	.1400E03	.1200E03	.1000E03
.9000E02	.8000E02	.7000E02	.6000E02	.5000E02
.4500E02	.4600E02	.4700E02	.4800E02	.4900E02
.5000E02	.4900E02	.4800E02	.4700E02	.4600E02
.4500E02	.4400E02	.4300E02	.4200E02	.4100E02
.4000E02	.3900E02	.3800E02	.3900E02	.3900E02
.4000E02	.4000E02	.4100E02	.4150E02	.4200E02

CROSS-SECTION LIBRARY FOR FE54(N,P)MN54 REACTION

.0000E00	.0000E00	.0000E00	.0000E00	.0000E00
.0000E00	.0000E00	.0000E00	.0000E00	.0000E00
.0000E00	.0000E00	.0000E00	.0000E00	.0000E00
.0000E00	.0000E00	.0000E00	.0000E00	.0000E00
.0000E01	.0000E01	.3500E02	.4000E02	.5000E02
.6000E02	.7000E02	.8500E02	.1000E03	.1150E03
.1250E03	.1350E03	.1500E03	.1650E03	.1900E03
.2000E03	.2150E03	.2300E03	.2500E03	.2650E03
.2850E03	.3000E03	.3100E03	.3250E03	.3450E03
.3550E03	.3700E03	.3800E03	.3950E03	.4100E03
.4200E03	.4250E03	.4450E03	.4500E03	.4550E03
.4700E03	.4750E03	.4800E03	.4850E03	.5000E03
.5100E03	.5150E03	.5200E03	.5200E03	.5250E03
.5300E03	.5350E03	.5350E03	.5400E03	.5400E03
.5450E03	.5450E03	.5450E03	.5450E03	.5450E03
.5500E03	.5500E03	.5500E03	.5500E03	.5500E03
.5500E03	.5500E03	.5500E03	.5500E03	.5500E03
.5500E03	.5500E03	.5500E03	.5500E03	.5500E03
.5500E03	.5450E03	.5450E03	.5450E03	.5400E03
.5400E03	.5400E03	.5350E03	.5350E03	.5350E03
.5350E03	.5300E03	.5280E03	.5250E03	.5240E03
.5200E03	.5190E03	.5170E03	.5150E03	.5120E03
.5100E03	.5050E03	.5000E03	.4980E03	.4970E03
.4950E03	.4900E03	.4850E03	.4830E03	.4800E03
.4750E03	.4730E03	.4700E03	.4650E03	.4630E03
.4600E03	.4550E03	.4500E03	.4450E03	.4400E03
.4350E03	.4300E03	.4250E03	.4230E03	.4200E03

.4150E03	.4100E03	.4050E03	.4000E03	.3950E03
.3900E03	.3850E03	.3800E03	.3750E03	.3700E03
.3650E03	.3600E03	.3550E03	.3500E03	.3450E03
.3400E03	.3350E03	.3300E03	.3250E03	.3200E03
.3150E03	.3100E03	.3050E03	.3000E03	.2950E03
.2850E03	.2800E03	.2750E03	.2700E03	.2650E03
.2600E03	.2550E03	.2500E03	.2450E03	.2400E03
.2300E03	.2250E03	.2200E03	.2150E03	.2100E03
.2050E03	.2000E03	.1500E03	.1250E03	.1100E03
.1000E03	.9000E02	.8000E02	.7000E02	.6000E02
.5000E02	.4000E02	.3000E02	.2000E02	.1000E02
.9000E01	.8000E01	.7000E01	.6000E01	.5000E01
.4500E01	.4000E01	.3500E01	.3000E01	.2500E01

CROSS-SECTION LIBRARY FOR AL27(N,P)MG27 REACTION

.0000E00	.0000E00	.0000E00	.0000E00	.0000E00
.0000E00	.0000E00	.0000E00	.0000E00	.0000E00
.0000E00	.0000E00	.0000E00	.0000E00	.0000E00
.0000E00	.0000E00	.0000E00	.0000E00	.0000E00
.0000E00	.0000E00	.0000E00	.0000E00	.0000E00
.0000E00	.0000E00	.1500E01	.1500E01	.1500E01
.2000E01	.2500E01	.2500E01	.3500E01	.5000E01
.1000E02	.5000E01	.9000E01	.7500E01	.7000E01
.7000E01	.7000E01	.1000E02	.1500E02	.1500E02
.1700E02	.2200E02	.2000E02	.1600E02	.1750E02
.2000E02	.2600E02	.2700E02	.3500E02	.3550E02
.3600E02	.3800E02	.4000E02	.4200E02	.4500E02
.4650E02	.4800E02	.4950E02	.5200E02	.5300E02
.5350E02	.5400E02	.5450E02	.5500E02	.5800E02
.5900E02	.6350E02	.6550E02	.6750E02	.7000E02
.7250E02	.7500E02	.7600E02	.7850E02	.8000E02
.8150E02	.8300E02	.8450E02	.8500E02	.8600E02
.8600E02	.8600E02	.8700E02	.8900E02	.8950E02
.9000E02	.9000E02	.9100E02	.9150E02	.9200E02
.9200E02	.9250E02	.9300E02	.9350E02	.9400E02
.9500E02	.9700E02	.9800E02	.9850E02	.9900E02
.1000E03	.1010E03	.1020E03	.1030E02	.1030E02
.1010E03	.9900E02	.9700E02	.9500E02	.9400E02
.9300E02	.9200E02	.9000E02	.8900E02	.8750E02
.8750E02	.8600E02	.8500E02	.8200E02	.8000E02
.7900E02	.7900E02	.7750E02	.7750E02	.7600E02
.7550E02	.7500E02	.7500E02	.7400E02	.7250E02
.7200E02	.7150E02	.6950E02	.6750E02	.6500E02
.6450E02	.6400E02	.6350E02	.6300E02	.6250E02
.6200E02	.6175E02	.6100E02	.6050E02	.6000E02
.6000E02	.5925E02	.5800E02	.5725E02	.5600E02
.5525E02	.5400E02	.5350E02	.5300E02	.5275E02
.5250E02	.5175E02	.5100E02	.5025E02	.4950E02
.4875E02	.4800E02	.4725E02	.4650E02	.4600E02
.4500E02	.4425E02	.4350E02	.4275E02	.4200E02
.4125E02	.4050E02	.3975E02	.3900E02	.3825E02
.3750E02	.3725E02	.3700E02	.3675E02	.3650E02
.3625E02	.3600E02	.3575E02	.3550E02	.3525E02
.3500E02	.3450E02	.3400E02	.3350E02	.3300E02
.3250E02	.3200E02	.3150E02	.3100E02	.3000E02

CROSS-SECTION LIBRARY FOR FE56(N,P)MN56 REACTION

.0000E00	.0000E00	.0000E00	.0000E00	.0000E00

.0000E00	.0000E00	.0000E00	.0000E00	.0000E00
.0000E00	.0000E00	.0000E00	.0000E00	.0000E00
.0000E00	.0000E00	.0000E00	.0000E00	.0000E00
.0000E00	.0000E00	.0000E00	.0000E00	.0000E00
.0000E00	.0000E00	.0000E00	.0000E00	.0000E00
.0000E00	.0000E00	.0000E00	.0000E00	.0000E00
.0000E00	.0000E00	.0000E00	.0000E00	.0000E00
.0000E00	.0000E00	.0000E00	.0000E00	.0000E00
.0000E00	.0000E00	.0000E00	.0000E00	.0000E00
.2000E01	.3000E01	.4000E01	.6000E01	.8000E01
.1000E02	.1200E02	.1300E02	.1300E02	.1350E02
.1400E02	.1500E02	.1800E02	.1900E02	.2000E02
.2200E02	.2400E02	.2600E02	.2700E02	.2900E02
.3100E02	.3300E02	.3500E02	.3600E02	.3800E02
.3900E02	.4000E02	.4100E02	.4600E02	.4800E02
.4800E02	.4800E02	.5000E02	.5200E02	.5300E02
.5400E02	.5600E02	.5700E02	.5800E02	.5950E02
.6200E02	.6350E02	.6500E02	.6600E02	.6800E02
.6900E02	.7100E02	.7300E02	.7400E02	.7500E02
.7600E02	.7700E02	.7900E02	.8000E02	.8100E02
.8300E02	.8450E02	.8600E02	.8750E02	.8900E02
.9000E02	.9150E02	.9300E02	.9450E02	.9500E02
.9600E02	.9700E02	.9700E02	.9800E02	.1000E03
.1030E03	.1045E03	.1060E03	.1075E03	.1080E03
.1090E03	.1100E03	.1110E03	.1120E03	.1130E03
.1140E03	.1140E03	.1145E03	.1150E03	.1153E03
.1157E03	.1153E03	.1150E03	.1140E03	.1130E03
.1120E03	.1110E03	.1100E03	.1090E03	.1070E03
.1050E03	.1030E03	.1010E03	.9900E02	.9800E02
.9800E02	.9650E02	.9500E02	.9350E02	.9200E02
.9000E02	.8800E02	.8600E02	.8400E02	.8200E02
.8100E02	.8000E02	.7900E02	.7800E02	.7700E02
.7600E02	.7500E02	.7400E02	.7300E02	.7100E02
.7000E02	.6900E02	.6800E02	.6700E02	.6600E02
.6500E02	.6400E02	.6300E02	.6200E02	.6100E02
.6000E02	.5900E02	.5800E02	.5700E02	.5600E02
.5500E02	.5400E02	.5300E02	.5250E02	.5175E02
.5100E02	.5050E02	.5000E02	.4925E02	.4850E02
.4800E02	.4750E02	.4700E02	.4600E02	.4500E02

CROSS-SECTION LIBRARY FOR MG24(N,P)NA24 REACTION

.0000E00	.0000E00	.0000E00	.0000E00	.0000E00
.0000E00	.0000E00	.0000E00	.0000E00	.0000E00
.0000E00	.0000E00	.0000E00	.0000E00	.0000E00
.0000E00	.0000E00	.0000E00	.0000E00	.0000E00
.0000E00	.0000E00	.0000E00	.0000E00	.0000E00
.0000E00	.0000E00	.0000E00	.0000E00	.0000E00
.0000E00	.0000E00	.0000E00	.0000E00	.0000E00
.0000E00	.0000E00	.0000E00	.0000E00	.0000E00
.0000E00	.0000E00	.0000E00	.0000E00	.0000E00
.0000E00	.0000E00	.0000E00	.0000E00	.0000E00
.0000E00	.0000E00	.0000E00	.0000E00	.0000E00
.0000E00	.0000E00	.0000E00	.0000E00	.0000E00
.1250E01	.1250E01	.2000E01	.2500E01	.4000E01
.7500E01	.1100E02	.2500E02	.4100E02	.3700E02
.3700E02	.4200E02	.5000E02	.5000E02	.5000E02
.5200E02	.6000E02	.7750E02	.1070E03	.1115E03
.1130E03	.1170E03	.1200E03	.1230E03	.1250E03
.1255E03	.1255E03	.1255E03	.1255E03	.1255E03

.1255E03	.1270E03	.1280E03	.1290E03	.1300E03
.1300E03	.1370E03	.1400E03	.1420E03	.1430E03
.1480E03	.1500E03	.1550E03	.1550E03	.1590E03
.1590E03	.1600E03	.1600E03	.1600E03	.1610E03
.1610E03	.1650E03	.1680E03	.1700E03	.1730E03
.1750E03	.1765E03	.1790E03	.1810E03	.1830E03
.1850E03	.1860E03	.1880E03	.1890E03	.1910E03
.1920E03	.1930E03	.1950E03	.1975E03	.2000E03
.2010E03	.2020E03	.2030E03	.2040E03	.2050E03
.2040E03	.2000E03	.1970E03	.1960E03	.1950E03
.1910E03	.1880E03	.1830E03	.1770E03	.1750E03
.1730E03	.1700E03	.1680E03	.1650E03	.1600E03
.1600E03	.1590E03	.1580E03	.1560E03	.1540E03
.1520E03	.1510E03	.1490E03	.1480E03	.1460E03
.1450E03	.1420E03	.1390E03	.1380E03	.1370E03
.1350E03	.1330E03	.1310E03	.1290E03	.1270E03
.1250E03	.1240E03	.1220E03	.1210E03	.1190E03
.1175E03	.1160E03	.1150E03	.1140E03	.1130E03
.1100E03	.1090E03	.1080E03	.1070E03	.1060E03
.1050E03	.1030E03	.1010E03	.9900E02	.9700E02
.9500E02	.9300E02	.9100E02	.8900E02	.8700E02
.8600E02	.8500E02	.8400E02	.8350E02	.8250E02

CROSS-SECTION LIBRARY FOR AL27(N,ALPHA)NA24 REACTION

.0000E00	.0000E00	.0000E00	.0000E00	.0000E00
.0000E00	.0000E00	.0000E00	.0000E00	.0000E00
.0000E00	.0000E00	.0000E00	.0000E00	.0000E00
.0000E00	.0000E00	.0000E00	.0000E00	.0000E00
.0000E00	.0000E00	.0000E00	.0000E00	.0000E00
.0000E00	.0000E00	.0000E00	.0000E00	.0000E00
.0000E00	.0000E00	.0000E00	.0000E00	.0000E00
.0000E00	.0000E00	.0000E00	.0000E00	.0000E00
.0000E00	.0000E00	.0000E00	.0000E00	.0000E00
.0000E00	.0000E00	.0000E00	.0000E00	.0000E00
.0000E00	.0000E00	.0000E00	.0000E00	.0000E00
.0000E00	.0000E00	.0000E00	.0000E00	.0000E00
.2000E01	.3000E01	.4000E01	.6000E01	.6000E01
.6000E01	.6000E01	.7000E01	.1000E02	.1200E02
.1700E02	.1800E02	.2000E02	.3200E02	.2500E02
.2800E02	.3000E02	.3400E02	.3800E02	.4100E02
.4300E02	.4400E02	.4500E02	.4900E02	.5300E02
.5600E02	.5700E02	.6000E02	.6500E02	.6700E02
.7000E02	.7200E02	.7400E02	.7600E02	.7800E02
.8000E02	.8200E02	.8400E02	.8600E02	.8800E02
.9000E02	.9200E02	.9400E02	.9600E02	.9800E02
.1000E03	.1010E03	.1020E03	.1040E03	.1060E03
.1080E03	.1100E03	.1200E03	.1130E03	.1140E03
.1150E03	.1165E03	.1175E03	.1190E03	.1200E03
.1220E03	.1240E03	.1260E03	.1280E03	.1290E03
.1300E03	.1310E03	.1315E03	.1320E03	.1325E03
.1330E03	.1330E03	.1320E03	.1310E03	.1290E03
.1280E03	.1270E03	.1260E03	.1250E03	.1245E03
.1240E03	.1220E03	.1210E03	.1200E03	.1190E03
.1180E03	.1160E03	.1140E03	.1120E03	.1100E03
.1100E03	.1080E03	.1060E03	.1040E03	.1020E03
.1000E03	.9900E02	.9800E02	.9700E02	.9500E02
.9300E02	.9200E02	.9000E02	.8800E02	.8000E02
.8000E02	.8050E02	.8000E02	.7800E02	.7600E02
.7600E02	.7800E02	.7600E02	.7400E02	.7200E02

.7100E02	.7000E02	.6700E02	.6400E02	.6850E02
.6600E02	.6500E02	.5900E02	.6350E02	.5800E02
.5700E02	.5650E02	.5500E02	.5350E02	.5250E02
.5200E02	.5100E02	.4900E02	.4800E02	.4700E02
.4600E02	.4500E02	.4400E02	.4200E02	.4000E02

CROSS-SECTION LIBRARY FOR FE54(N,ALPHA)CR51 REACTION

.0000E00	.0000E00	.0000E00	.0000E00	.0000E00
.0000E00	.0000E00	.0000E00	.0000E00	.0000E00
.0000E00	.0000E00	.0000E00	.0000E00	.0000E00
.0000E00	.0000E00	.0000E00	.0000E00	.0000E00
.3000E01	.3000E01	.3000E01	.3000E01	.3000E01
.3000E01	.3000E01	.3000E01	.3500E01	.4000E01
.4000E01	.4000E01	.4000E01	.4500E01	.4500E01
.5000E01	.5000E01	.5000E01	.5500E01	.5500E01
.6000E01	.6000E01	.6000E01	.6500E01	.6500E01
.7000E01	.7000E01	.7500E01	.8000E01	.8500E01
.9000E01	.9000E01	.9500E01	.9500E01	.1000E02
.1000E02	.1050E02	.1100E02	.1200E02	.1300E02
.1350E02	.1350E02	.1400E02	.1500E02	.1600E02
.1650E02	.1700E02	.1700E02	.1800E02	.1900E02
.2000E02	.2100E02	.2200E02	.2300E02	.2400E02
.2500E02	.2600E02	.2700E02	.2800E02	.2900E02
.3000E02	.3100E02	.3200E02	.3300E02	.3400E02
.3500E02	.3700E02	.3800E02	.4000E02	.4050E02
.4100E02	.4300E02	.4400E02	.4600E02	.4700E02
.4800E02	.4900E02	.5000E02	.5100E02	.5200E02
.5300E02	.5400E02	.5500E02	.5600E02	.5700E02
.5800E02	.6000E02	.6100E02	.6200E02	.6300E02
.6400E02	.6500E02	.6600E02	.6700E02	.6800E02
.6900E02	.7000E02	.7200E02	.7300E02	.7350E02
.7400E02	.7500E02	.7600E02	.7700E02	.7800E02
.7850E02	.7900E02	.8000E02	.8100E02	.8200E02
.8300E02	.8400E02	.8500E02	.8600E02	.8650E02
.8700E02	.8800E02	.8850E02	.8900E02	.8950E02
.9000E02	.9100E02	.9200E02	.9250E02	.9300E02
.9350E02	.9400E02	.9500E02	.9600E02	.9650E02
.9700E02	.9750E02	.9800E02	.9850E02	.9900E02
.1000E03	.1010E03	.1015E03	.1020E03	.1025E03
.1030E03	.1035E03	.1040E03	.1045E03	.1050E03
.1055E03	.1060E03	.1065E03	.1070E03	.1075E03
.1080E03	.1085E03	.1090E03	.1093E03	.1095E03
.1098E03	.1100E03	.1105E03	.1110E03	.1115E03
.1120E03	.1125E03	.1130E03	.1133E03	.1135E03
.1140E03	.1145E03	.1148E03	.1150E03	.1155E03
.1160E03	.1165E03	.1170E03	.1175E03	.1180E03
.1182E03	.1184E03	.1185E03	.1190E03	.1190E03

CROSS-SECTION LIBRARY FOR IN115(N,2N)IN114M REACTION

.0000E00	.0000E00	.0000E00	.0000E00	.0000E00
.0000E00	.0000E00	.0000E00	.0000E00	.0000E00
.0000E00	.0000E00	.0000E00	.0000E00	.0000E00
.0000E00	.0000E00	.0000E00	.0000E00	.0000E00
.0000E00	.0000E00	.0000E00	.0000E00	.0000E00
.0000E00	.0000E00	.0000E00	.0000E00	.0000E00
.0000E00	.0000E00	.0000E00	.0000E00	.0000E00
.0000E00	.0000E00	.0000E00	.0000E00	.0000E00
.0000E00	.0000E00	.0000E00	.0000E00	.0000E00

.0000E00	.0000E00	.0000E00	.0000E00	.0000E00
.0000E00	.0000E00	.0000E00	.0000E00	.0000E00
.0000E00	.0000E00	.0000E00	.0000E00	.0000E00
.0000E00	.0000E00	.0000E00	.0000E00	.0000E00
.0000E00	.0000E00	.0000E00	.0000E00	.0000E00
.0000E00	.0000E00	.0000E00	.0000E00	.0000E00
.0000E00	.0000E00	.0000E00	.0000E00	.0000E00
.0000E00	.0000E00	.0000E00	.0000E00	.0000E00
.0000E00	.0000E00	.0000E00	.0000E00	.0000E00
.0000E00	.0000E00	.0000E00	.0000E00	.0000E00
.0000E00	.0000E00	.0000E00	.0000E00	.0000E00
.0000E00	.0000E00	.0000E00	.0000E00	.0000E00
.0000E00	.0000E00	.0000E00	.0000E00	.0000E00
.0000E00	.0000E00	.0000E00	.0000E00	.0000E00
.0000E00	.0000E00	.0000E00	.0000E00	.0000E00
.1060E03	.1060E03	.1160E03	.1200E03	.1220E03
.1240E03	.1280E03	.1300E03	.1340E03	.1360E03
.1380E03	.1400E03	.1420E03	.1440E03	.1460E03
.1460E03	.1470E03	.1480E03	.1500E03	.1510E03
.1520E03	.1530E03	.1540E03	.1540E03	.1540E03
.1540E03	.1540E03	.1540E03	.1540E03	.1540E03
.1540E03	.1540E03	.1540E03	.1540E03	.1540E03
.1530E03	.1520E03	.1520E03	.1520E03	.1520E03
.1520E03	.1510E03	.1510E03	.1500E03	.1500E03
.1500E03	.1500E03	.1490E03	.1490E03	.1480E03
.1480E03	.1470E03	.1460E03	.1450E03	.1450E03
.1450E03	.1440E03	.1440E03	.1440E03	.1430E03
.1420E03	.1420E03	.1410E03	.1400E03	.1400E03
.1400E03	.1390E03	.1380E03	.1380E03	.1380E03
.1370E03	.1360E03	.1360E03	.1350E03	.1340E03
.1340E03	.1320E03	.1320E03	.1310E03	.1310E03

APPENDIX C

CROSS-SECTION AND DECAY INFORMATION

1 Cross Sections

Program code RUFF contains a library of threshold cross-ctions for nine reactions which ranges from 0.1 to 20 Mev 100 Kev increments. The following order sequence was used: -115(n,n')In-115m; Ni-58(n,p)Co-58; Fe-54(n,p)Mn-54; -27(n,p)Mg-27; Fe-56(n,p)Mn-56; Mg-24(n,p)Na-24; -27(n, α)Na-24; Fe-54(n, α)Cr-51; and In-115(n,2n)In-114. bles C.1 through C.9 are tabulated values of these threshold oss-sections (24,25,26,30). There are the values that were d in determining the differential flux. All energies rresponding to zero cross-section values were deleted. gures C.1 through C.9 are graphical illustrations of the spective tables to aid in visualizing the shape of the in-idual cross-sections (9,24,25,26).

Gamma Spectra and Decay of Reaction Products

Gamma spectra of the reaction product decay are illus-ted in Figures C.10 through C.15. The gamma energy is ended along the abscissa and the relative count rate along ordinate. These spectra were produced by dual 3" diameter " thick right cylindrical sodium-iodide (thallium activated) stals in conjunction with a 400 channel pulse height lyzer, and were expanded along the abscissa to give a better w of the peaks.

Included with the decay gamma spectra are nuclear transformation energy level diagrams containing the identifying gamma transitions and energies. These schematics are illustrated in Figures C.16 through C.23. Gamma transitions are denoted by vertical downward arrows, negatron emission by arrows slanted downward to the right, and positron and electron capture by arrows directed downward and to the left. Double arrows drawn from the ground state to a higher level of the nucleus indicate that the higher level has been coulomb excited. The figures to the right of the horizontal lines designate the energy levels and those to the left the spin or quantum numbers (29,32).

Table C.1

In-115(n,n')In-115m Library

E (Mev)	σ (mb)	E (Mev)	σ (mb)	E (Mev)	σ (mb)
.5	1.50	3.7	340.00	6.9	158.00
.6	4.00	3.8	320.00	7.0	153.00
.7	11.05	3.9	305.00	7.1	145.00
.8	19.00	4.0	290.00	7.2	135.00
.9	35.00	4.1	292.00	7.3	133.00
1.0	50.00	4.2	295.00	7.4	132.00
1.1	120.00	4.3	298.00	7.5	128.00
1.2	132.00	4.4	295.00	7.6	125.00
1.3	140.00	4.5	290.00	7.7	120.00
1.4	154.00	4.6	280.00	7.8	115.00
1.5	186.00	4.7	276.00	7.9	110.00
1.6	198.00	4.8	274.00	8.0	107.00
1.7	227.00	4.9	258.00	8.1	104.00
1.8	282.00	5.0	248.00	8.2	100.00
1.9	270.00	5.1	240.00	8.3	95.00
2.0	286.00	5.2	230.00	8.4	90.00
2.1	286.00	5.3	231.00	8.5	82.00
2.2	315.00	5.4	230.00	8.6	70.00
2.3	332.00	5.5	220.00	8.7	65.00
2.4	340.00	5.6	217.00	8.8	60.00
2.5	375.00	5.7	214.00	8.9	57.00
2.6	378.00	5.8	212.00	9.0	50.00
2.7	370.00	5.9	209.00	9.1	45.00
2.8	360.00	6.0	207.00	9.2	41.00
2.9	354.00	6.1	195.00	9.3	39.00
3.0	350.00	6.2	190.00	9.4	35.00
3.1	340.00	6.3	188.00	9.5	32.00
3.2	335.00	6.4	182.00	9.6	20.00
3.3	325.00	6.5	175.00	9.7	15.00
3.4	315.00	6.6	170.00	9.8	10.00
3.5	300.00	6.7	165.00	9.9	7.00
3.6	320.00	6.8	160.00		

Table C.2

Ni-58(n,p)Co-58 Library

E (Mev)	σ (mb)	E (Mev)	σ (mb)	E (Mev)	σ (mb)
1.1	5.00	4.3	430.00	7.5	640.00
1.2	5.00	4.4	460.00	7.6	640.00
1.3	5.00	4.5	468.00	7.7	640.00
1.4	10.00	4.6	475.00	7.8	645.00
1.5	18.00	4.7	490.00	7.9	645.00
1.6	20.00	4.8	503.00	8.0	645.00
1.7	25.00	4.9	516.00	8.1	645.00
1.8	30.00	5.0	525.00	8.2	645.00
1.9	40.00	5.1	540.00	8.3	640.00
2.0	50.00	5.2	552.50	8.4	640.00
2.1	60.00	5.3	565.00	8.5	640.00
2.2	70.00	5.4	575.00	8.6	640.00
2.3	80.00	5.5	580.00	8.7	640.00
2.4	90.00	5.6	590.00	8.8	637.50
2.5	100.00	5.7	600.00	8.9	632.50
2.6	120.00	5.8	610.00	9.0	630.00
2.7	150.00	5.9	615.00	9.1	630.00
2.8	200.00	6.0	620.00	9.2	627.50
2.9	260.00	6.1	625.00	9.3	627.50
3.0	230.00	6.2	630.00	9.4	625.00
3.1	215.00	6.3	635.00	9.5	625.00
3.2	455.00	6.4	638.00	9.6	621.00
3.3	345.00	6.5	640.00	9.7	618.00
3.4	300.00	6.6	645.00	9.8	616.00
3.5	180.00	6.7	645.00	9.9	614.00
3.6	210.00	6.8	646.00	10.0	612.00
3.7	185.00	6.9	645.00	10.1	610.00
3.8	320.00	7.0	644.00	10.2	608.00
3.9	350.00	7.1	642.00	10.3	605.00
4.0	370.00	7.2	640.00	10.4	602.00
4.1	395.00	7.3	640.00	10.5	600.00
4.2	410.00	7.4	640.00	10.6	600.00

Table C.2

Ni-58(n,p)Co-58 Continued

E (Mev)	σ (mb)	E (Mev)	σ (mb)	E (Mev)	σ (mb)
10.7	598.00	13.8	475.00	16.9	100.00
10.8	595.00	13.9	465.00	17.0	90.00
10.9	592.00	14.0	455.00	17.1	80.00
11.0	590.00	14.1	440.00	17.2	70.00
11.1	580.00	14.2	430.00	17.3	60.00
11.2	573.00	14.3	420.00	17.4	50.00
11.3	570.00	14.4	410.00	17.5	45.00
11.4	568.00	14.5	400.00	17.6	46.00
11.5	565.00	14.6	395.00	17.7	47.00
11.6	564.00	14.7	390.00	17.8	48.00
11.7	563.00	14.8	385.00	17.9	49.00
11.8	562.00	14.9	380.00	18.0	50.00
11.9	561.00	15.0	370.00	18.1	49.00
12.0	560.00	15.1	360.00	18.2	48.00
12.1	557.50	15.2	350.00	18.3	47.00
12.2	550.00	15.3	340.00	18.4	46.00
12.3	547.50	15.4	320.00	18.5	45.00
12.4	545.00	15.5	310.00	18.6	44.00
12.5	540.00	15.6	300.00	18.7	43.00
12.6	537.50	15.7	290.00	18.8	42.00
12.7	532.50	15.8	280.00	18.9	41.00
12.8	530.00	15.9	270.00	19.0	40.00
12.9	525.00	16.0	260.00	19.1	39.00
13.0	520.00	16.1	240.00	19.2	38.00
13.1	515.00	16.2	220.00	19.3	39.00
13.2	510.00	16.3	210.00	19.4	39.00
13.3	505.00	16.4	200.00	19.5	40.00
13.4	500.00	16.5	180.00	19.6	40.00
13.5	495.00	16.6	160.00	19.7	41.00
13.6	490.00	16.7	140.00	19.8	41.50
13.7	485.00	16.8	120.00	19.9	42.00

Table C.3

Fe-54(n,p)Mn-54 Library

E (Mev)	σ (mb)	E (Mev)	σ (mb)	E (Mev)	σ (mb)
2.2	35.00	5.2	445.00	8.2	550.00
2.3	40.00	5.3	450.00	8.3	550.00
2.4	50.00	5.4	455.00	8.4	550.00
2.5	60.00	5.5	470.00	8.5	550.00
2.6	70.00	5.6	475.00	8.6	550.00
2.7	85.00	5.7	480.00	8.7	550.00
2.8	100.00	5.8	485.00	8.8	550.00
2.9	115.00	5.9	500.00	8.9	550.00
3.0	125.00	6.0	510.00	9.0	550.00
3.1	135.00	6.1	515.00	9.1	545.00
3.2	150.00	6.2	520.00	9.2	545.00
3.3	165.00	6.3	520.00	9.3	545.00
3.4	190.00	6.4	525.00	9.4	540.00
3.5	200.00	6.5	530.00	9.5	540.00
3.6	215.00	6.6	535.00	9.6	540.00
3.7	230.00	6.7	535.00	9.7	535.00
3.8	250.00	6.8	540.00	9.8	535.00
3.9	265.00	6.9	540.00	9.9	535.00
4.0	285.00	7.0	545.00	10.0	535.00
4.1	300.00	7.1	545.00	10.1	530.00
4.2	310.00	7.2	545.00	10.2	528.00
4.3	325.00	7.3	545.00	10.3	525.00
4.4	345.00	7.4	545.00	10.4	524.00
4.5	355.00	7.5	550.00	10.5	520.00
4.6	370.00	7.6	550.00	10.6	519.00
4.7	380.00	7.7	550.00	10.7	517.00
4.8	395.00	7.8	550.00	10.8	515.00
4.9	410.00	7.9	550.00	10.9	512.00
5.0	420.00	8.0	550.00	11.0	510.00
5.1	425.00	8.1	550.00	11.1	505.00

Table C.3

Fe-54(n,p)Mn-54 Continued

E (Mev)	σ (mb)	E (Mev)	σ (mb)	E (Mev)	σ (mb)
11.2	500.00	14.2	380.00	17.1	225.00
11.3	498.00	14.3	375.00	17.2	220.00
11.4	497.00	14.4	370.00	17.3	215.00
11.5	495.00	14.5	365.00	17.4	210.00
11.6	490.00	14.6	360.00	17.5	205.00
11.7	485.00	14.7	355.00	17.6	200.00
11.8	483.00	14.8	350.00	17.7	150.00
11.9	480.00	14.9	345.00	17.8	125.00
12.0	475.00	15.0	340.00	17.9	110.00
12.1	473.00	15.1	335.00	18.0	100.00
12.2	470.00	15.2	330.00	18.1	90.00
12.3	465.00	15.3	325.00	18.2	80.00
12.4	463.00	15.4	320.00	18.3	70.00
12.5	460.00	15.5	315.00	18.4	60.00
12.6	455.00	15.6	310.00	18.5	50.00
12.7	450.00	15.7	305.00	18.6	40.00
12.8	445.00	15.8	300.00	18.7	30.00
12.9	440.00	15.9	295.00	18.8	20.00
13.0	435.00	16.0	285.00	18.9	10.00
13.1	430.00	16.1	280.00	19.0	9.00
13.2	425.00	16.2	275.00	19.1	8.00
13.3	423.00	16.3	270.00	19.2	7.00
13.4	420.00	16.4	265.00	19.3	6.00
13.5	415.00	16.5	260.00	19.4	5.00
13.6	410.00	16.6	255.00	19.5	4.50
13.7	405.00	16.7	250.00	19.6	4.00
13.8	400.00	16.8	245.00	19.7	3.50
13.9	395.00	16.9	240.00	19.8	3.00
14.0	390.00	17.0	230.00	19.9	2.50
14.1	385.00				

Table C.4

Al-27(n,p)Mg-27 Library

E (Mev)	σ (mb)	E (Mev)	σ (mb)	E (Mev)	σ (mb)
2.7	1.50	5.7	40.00	8.7	87.00
2.8	1.50	5.8	42.00	8.8	89.00
2.9	1.50	5.9	45.00	8.9	89.50
3.0	2.00	6.0	46.50	9.0	90.00
3.1	2.50	6.1	48.00	9.1	90.00
3.2	2.50	6.2	49.50	9.2	91.00
3.3	3.50	6.3	52.00	9.3	91.50
3.4	5.00	6.4	53.00	9.4	92.00
3.5	10.00	6.5	53.50	9.5	92.00
3.6	5.00	6.6	54.00	9.6	92.50
3.7	9.00	6.7	54.50	9.7	93.00
3.8	7.50	6.8	55.00	9.8	93.50
3.9	7.00	6.9	58.00	9.9	94.00
4.0	7.00	7.0	59.00	10.0	95.00
4.1	7.00	7.1	63.50	10.1	97.00
4.2	10.00	7.2	65.50	10.2	98.00
4.3	15.00	7.3	67.50	10.3	98.50
4.4	15.00	7.4	70.00	10.4	99.00
4.5	17.00	7.5	72.50	10.5	100.00
4.6	22.00	7.6	75.00	10.6	101.00
4.7	20.00	7.7	76.00	10.7	102.00
4.8	16.00	7.8	78.50	10.8	103.00
4.9	17.50	7.9	80.00	10.9	103.00
5.0	20.00	8.0	81.50	11.0	101.00
5.1	26.00	8.1	83.00	11.1	99.00
5.2	27.00	8.2	84.50	11.2	97.00
5.3	35.00	8.3	85.00	11.3	95.00
5.4	35.50	8.4	86.00	11.4	94.00
5.5	36.00	8.5	86.00	11.5	93.00
5.6	38.00	8.6	86.00	11.6	92.00

Table C.4

Al-27(n,p)Mg-27 Continued

E (Mev)	σ (mb)	E (Mev)	σ (mb)	E (Mev)	σ (mb)
11.7	90.00	14.5	62.00	17.3	42.75
11.8	89.00	14.6	61.75	17.4	42.00
11.9	87.50	14.7	61.00	17.5	41.25
12.0	87.50	14.8	60.50	17.6	40.50
12.1	86.00	14.9	60.00	17.7	39.75
12.2	85.00	15.0	60.00	17.8	39.00
12.3	82.00	15.1	59.25	17.9	38.25
12.4	80.00	15.2	58.00	18.0	37.50
12.5	79.00	15.3	57.25	18.1	37.25
12.6	79.00	15.4	56.00	18.2	37.00
12.7	77.50	15.5	55.25	18.3	36.75
12.8	77.50	15.6	54.00	18.4	36.50
12.9	76.00	15.7	53.50	18.5	36.25
13.0	75.50	15.8	53.00	18.6	36.00
13.1	75.00	15.9	52.75	18.7	35.75
13.2	75.00	16.0	52.50	18.8	35.50
13.3	74.00	16.1	51.75	18.9	35.25
13.4	72.50	16.2	51.00	19.0	35.00
13.5	72.00	16.3	50.25	19.1	34.50
13.6	71.50	16.4	49.50	19.2	34.00
13.7	69.50	16.5	48.75	19.3	33.50
13.8	67.50	16.6	48.00	19.4	33.00
13.9	65.00	16.7	47.25	19.5	32.50
14.0	64.50	16.8	46.50	19.6	32.00
14.1	64.00	16.9	46.00	19.7	31.50
14.2	63.50	17.0	45.00	19.8	31.00
14.3	63.00	17.1	44.25	19.9	30.00
14.4	62.50	17.2	43.50		

Table C.5

Fe-56(n,p)Mn-56 Library

E (Mev)	σ (mb)	E (Mev)	σ (mb)	E (Mev)	σ (mb)
5.0	2.00	7.5	39.00	10.0	76.00
5.1	3.00	7.6	40.00	10.1	77.00
5.2	4.00	7.7	41.00	10.2	79.00
5.3	6.00	7.8	46.00	10.3	80.00
5.4	8.00	7.9	48.00	10.4	81.00
5.5	10.00	8.0	48.00	10.5	83.00
5.6	12.00	8.1	48.00	10.6	84.50
5.7	13.00	8.2	50.00	10.7	86.00
5.8	13.00	8.3	52.00	10.8	87.50
5.9	13.50	8.4	53.00	10.9	89.00
6.0	14.00	8.5	54.00	11.0	90.00
6.1	15.00	8.6	56.00	11.1	91.50
6.2	18.00	8.7	57.00	11.2	93.00
6.3	19.00	8.8	58.00	11.3	94.50
6.4	20.00	8.9	59.50	11.4	95.00
6.5	22.00	9.0	62.00	11.5	96.00
6.6	24.00	9.1	63.50	11.6	97.00
6.7	26.00	9.2	65.00	11.7	97.00
6.8	27.00	9.3	66.00	11.8	98.00
6.9	29.00	9.4	68.00	11.9	100.00
7.0	31.00	9.5	69.00	12.0	103.00
7.1	33.00	9.6	71.00	12.1	104.50
7.2	35.00	9.7	73.00	12.2	106.00
7.3	36.00	9.8	74.00	12.3	107.50
7.4	38.00	9.9	75.00	12.4	108.00

Table C.5

Fe-56(n,p)Mn-56 Continued

E (Mev)	σ (mb)	E (Mev)	σ (mb)	E (Mev)	σ (mb)
12.5	109.00	15.0	98.00	17.5	65.00
12.6	110.00	15.1	96.50	17.6	64.00
12.7	111.00	15.2	95.00	17.7	63.00
12.8	112.00	15.3	93.50	17.8	62.00
12.9	113.00	15.4	92.00	17.9	61.00
13.0	114.00	15.5	90.00	18.0	60.00
13.1	114.00	15.6	88.00	18.1	59.00
13.2	114.50	15.7	86.00	18.2	58.00
13.3	115.00	15.8	84.00	18.3	57.00
13.4	115.30	15.9	82.00	18.4	56.00
13.5	115.70	16.0	81.00	18.5	55.00
13.6	115.30	16.1	80.00	18.6	54.00
13.7	115.00	16.2	79.00	18.7	53.00
13.8	114.00	16.3	78.00	18.8	52.50
13.9	113.00	16.4	77.00	18.9	51.75
14.0	112.00	16.5	76.00	19.0	51.00
14.1	111.00	16.6	75.00	19.1	50.50
14.2	110.00	16.7	74.00	19.2	50.00
14.3	109.00	16.8	73.00	19.3	49.25
14.4	107.00	16.9	71.00	19.4	48.50
14.5	105.00	17.0	70.00	19.5	48.00
14.6	103.00	17.1	69.00	19.6	47.50
14.7	101.00	17.2	68.00	19.7	47.00
14.8	99.00	17.3	67.00	19.8	46.00
14.9	98.00	17.4	66.00	19.9	45.00

Table C.6

Mg-24(n,p)Na-24 Library

E (Mev)	σ (mb)	E (Mev)	σ (mb)	E (Mev)	σ (mb)
6.0	1.25	10.7	160.00	15.4	154.00
6.1	1.25	10.8	160.00	15.5	152.00
6.2	2.00	10.9	161.00	15.6	151.00
6.3	2.50	11.0	161.00	15.7	149.00
6.4	4.00	11.1	165.00	15.8	148.00
6.5	7.50	11.2	168.00	15.9	146.00
6.6	11.00	11.3	170.00	16.0	145.00
6.7	25.00	11.4	173.00	16.1	142.00
6.8	41.00	11.5	175.00	16.2	139.00
6.9	37.00	11.6	176.50	16.3	138.00
7.0	37.00	11.7	179.00	16.4	137.00
7.1	42.00	11.8	181.00	16.5	135.00
7.2	50.00	11.9	183.00	16.6	133.00
7.3	50.00	12.0	185.00	16.7	131.00
7.4	50.00	12.1	186.00	16.8	129.00
7.5	52.00	12.2	188.00	16.9	127.00
7.6	60.00	12.3	189.00	17.0	125.00
7.7	77.50	12.4	191.00	17.1	124.00
7.8	107.00	12.5	192.00	17.2	122.00
7.9	111.50	12.6	193.00	17.3	121.00
8.0	113.00	12.7	195.00	17.4	110.00
8.1	117.00	12.8	197.50	17.5	117.50
8.2	120.00	12.9	200.00	17.6	116.00
8.3	123.00	13.0	201.00	17.7	115.00
8.4	125.00	13.1	202.00	17.8	114.00
8.5	125.50	13.2	203.00	17.9	113.00
8.6	125.50	13.3	204.00	18.0	110.00
8.7	125.50	13.4	205.00	18.1	109.00
8.8	125.50	13.5	204.00	18.2	108.00
8.9	125.50	13.6	200.00	18.3	107.00
9.0	125.50	13.7	197.00	18.4	106.00
9.1	127.00	13.8	196.00	18.5	105.00
9.2	128.00	13.9	195.00	18.6	103.00
9.3	129.00	14.0	191.00	18.7	101.00
9.4	130.00	14.1	188.00	18.8	99.00
9.5	130.00	14.2	183.00	18.9	97.00
9.6	137.00	14.3	177.00	19.0	95.00
9.7	140.00	14.4	175.00	19.1	93.00
9.8	142.00	14.5	173.00	19.2	91.00
9.9	143.00	14.6	170.00	19.3	89.00
10.0	148.00	14.7	168.00	19.4	87.00
10.1	150.00	14.8	165.00	19.5	86.00
10.2	155.00	14.9	160.00	19.6	85.00
10.3	155.00	15.0	160.00	19.7	84.00
10.4	159.00	15.1	159.00	19.8	83.50
10.5	159.00	15.2	158.00	19.9	82.50
10.6	160.00	15.3	156.00		

Table C.7

Al-27(n,α)Na-24 Library

E (Mev)	σ (mb)	E (Mev)	σ (mb)	E (Mev)	σ (mb)
6.0	2.00	10.7	102.00	15.4	102.00
6.1	3.00	10.8	104.00	15.5	100.00
6.2	4.00	10.9	106.00	15.6	99.00
6.3	6.00	11.0	108.00	15.7	98.00
6.4	6.00	11.1	110.00	15.8	97.00
6.5	6.00	11.2	120.00	15.9	95.00
6.6	6.00	11.3	113.00	16.0	93.00
6.7	7.00	11.4	114.00	16.1	92.00
6.8	10.00	11.5	115.00	16.2	90.00
6.9	12.00	11.6	116.50	16.3	88.00
7.0	17.00	11.7	117.50	16.4	80.00
7.1	18.00	11.8	119.00	16.5	80.00
7.2	20.00	11.9	120.00	16.6	80.50
7.3	32.00	12.0	122.00	16.7	80.00
7.4	25.00	12.1	124.00	16.8	78.00
7.5	28.00	12.2	126.00	16.9	76.00
7.6	30.00	12.3	128.00	17.0	76.00
7.7	34.00	12.4	129.00	17.1	78.00
7.8	38.00	12.5	130.00	17.2	76.00
7.9	41.00	12.6	131.00	17.3	74.00
8.0	43.00	12.7	131.50	17.4	72.00
8.1	44.00	12.8	132.00	17.5	71.00
8.2	45.00	12.9	132.50	17.6	70.00
8.3	49.00	13.0	133.00	17.7	67.00
8.4	53.00	13.1	133.00	17.8	64.00
8.5	56.00	13.2	132.00	17.9	68.50
8.6	57.00	13.3	131.00	18.0	66.00
8.7	60.00	13.4	129.00	18.1	65.00
8.8	65.00	13.5	128.00	18.2	59.00
8.9	67.00	13.6	127.00	18.3	63.50
9.0	70.00	13.7	126.00	18.4	58.00
9.1	72.00	13.8	125.00	18.5	57.00
9.2	74.00	13.9	124.50	18.6	56.50
9.3	76.00	14.0	124.00	18.7	55.00
9.4	78.00	14.1	122.00	18.8	53.50
9.5	80.00	14.2	121.00	18.9	52.50
9.6	82.00	14.3	120.00	19.0	52.00
9.7	84.00	14.4	119.00	19.1	51.00
9.8	86.00	14.5	118.00	19.2	49.00
9.9	88.00	14.6	116.00	19.3	48.00
10.0	90.00	14.7	114.00	19.4	47.00
10.1	92.00	14.8	112.00	19.5	46.00
10.2	94.00	14.9	110.00	19.6	45.00
10.3	96.00	15.0	110.00	19.7	44.00
10.4	98.00	15.1	108.00	19.8	42.00
10.5	100.00	15.2	106.00	19.9	40.00
10.6	101.00	15.3	104.00		

Table C.8

Fe-54(n, α)Cr-51 Library

E (Mev)	σ (mb)	E (Mev)	σ (mb)	E (Mev)	σ (mb)
2.0	3.00	5.0	9.00	8.0	30.00
2.1	3.00	5.1	9.00	8.1	31.00
2.2	3.00	5.2	9.50	8.2	32.00
2.3	3.00	5.3	9.50	8.3	33.00
2.4	3.00	5.4	10.00	8.4	34.00
2.5	3.00	5.5	10.00	8.5	35.00
2.6	3.00	5.6	10.50	8.6	37.00
2.7	3.00	5.7	11.00	8.7	38.00
2.8	3.50	5.8	12.00	8.8	40.00
2.9	4.00	5.9	13.00	8.9	40.50
3.0	4.00	6.0	13.50	9.0	41.00
3.1	4.00	6.1	13.50	9.1	43.00
3.2	4.00	6.2	14.00	9.2	44.00
3.3	4.50	6.3	15.00	9.3	46.00
3.4	4.50	6.4	16.00	9.4	47.00
3.5	5.00	6.5	16.50	9.5	48.00
3.6	5.00	6.6	17.00	9.6	49.00
3.7	5.00	6.7	17.00	9.7	50.00
3.8	5.50	6.8	18.00	9.8	51.00
3.9	5.50	6.9	19.00	9.9	52.00
4.0	6.00	7.0	20.00	10.0	53.00
4.1	6.00	7.1	21.00	10.1	54.00
4.2	6.00	7.2	22.00	10.2	55.00
4.3	6.50	7.3	23.00	10.3	56.00
4.4	6.50	7.4	24.00	10.4	57.00
4.5	7.00	7.5	25.00	10.5	58.00
4.6	7.00	7.6	26.00	10.6	60.00
4.7	7.50	7.7	27.00	10.7	61.00
4.8	8.00	7.8	28.00	10.8	62.00
4.9	8.50	7.9	29.00	10.9	63.00

Table C.8

Fe-54(n, α)Cr-51 Continued

E (Mev)	σ (mb)	E (Mev)	σ (mb)	E (Mev)	σ (mb)
11.0	64.00	14.0	90.00	17.0	108.00
11.1	65.00	14.1	91.00	17.1	108.50
11.2	66.00	14.2	92.00	17.2	109.00
11.3	67.00	14.3	92.50	17.3	109.30
11.4	68.00	14.4	93.00	17.4	109.50
11.5	69.00	14.5	93.50	17.5	109.80
11.6	70.00	14.6	94.00	17.6	110.00
11.7	72.00	14.7	95.00	17.7	110.50
11.8	73.00	14.8	96.00	17.8	111.00
11.9	73.50	14.9	96.50	17.9	111.50
12.0	74.00	15.0	97.00	18.0	112.00
12.1	75.00	15.1	97.50	18.1	112.50
12.2	76.00	15.2	98.00	18.2	113.00
12.3	77.00	15.3	98.50	18.3	113.30
12.4	78.00	15.4	99.00	18.4	113.50
12.5	78.50	15.5	100.00	18.5	114.00
12.6	79.00	15.6	101.00	18.6	114.50
12.7	80.00	15.7	101.50	18.7	114.80
12.8	81.00	15.8	102.00	18.8	115.00
12.9	82.00	15.9	102.50	18.9	115.50
13.0	83.00	16.0	103.00	19.0	116.00
13.1	84.00	16.1	103.50	19.1	116.50
13.2	85.00	16.2	104.00	19.2	117.00
13.3	86.00	16.3	104.50	19.3	117.50
13.4	86.50	16.4	105.00	19.4	118.00
13.5	87.00	16.5	105.50	19.5	118.20
13.6	88.00	16.6	106.00	19.6	118.40
13.7	88.50	16.7	106.50	19.7	118.50
13.8	89.00	16.8	107.00	19.8	119.00
13.9	89.50	16.9	107.50	19.9	119.00

Table C.9

In-115(n,2n)In-114m Library

E (Mev)	σ (mb)	E (Mev)	σ (mb)	E (Mev)	σ (mb)
12.0	1060.00	14.7	1540.00	17.4	1450.00
12.1	1060.00	14.8	1540.00	17.5	1450.00
12.2	1160.00	14.9	1540.00	17.6	1440.00
12.3	1200.00	15.0	1540.00	17.7	1440.00
12.4	1220.00	15.1	1540.00	17.8	1440.00
12.5	1240.00	15.2	1540.00	17.9	1430.00
12.6	1280.00	15.3	1540.00	18.0	1420.00
12.7	1300.00	15.4	1540.00	18.1	1420.00
12.8	1340.00	15.5	1530.00	18.2	1410.00
12.9	1360.00	15.6	1520.00	18.3	1400.00
13.0	1380.00	15.7	1520.00	18.4	1400.00
13.1	1400.00	15.8	1520.00	18.5	1400.00
13.2	1420.00	15.9	1520.00	18.6	1390.00
13.3	1440.00	16.0	1520.00	18.7	1380.00
13.4	1460.00	16.1	1510.00	18.8	1380.00
13.5	1460.00	16.2	1510.00	18.9	1380.00
13.6	1470.00	16.3	1500.00	19.0	1370.00
13.7	1480.00	16.4	1500.00	19.1	1360.00
13.8	1500.00	16.5	1500.00	19.2	1360.00
13.9	1510.00	16.6	1500.00	19.3	1350.00
14.0	1520.00	16.7	1490.00	19.4	1340.00
14.1	1530.00	16.8	1490.00	19.5	1340.00
14.2	1540.00	16.9	1480.00	19.6	1320.00
14.3	1540.00	17.0	1480.00	19.7	1320.00
14.4	1540.00	17.1	1470.00	19.8	1310.00
14.5	1540.00	17.2	1460.00	19.9	1310.00
14.6	1540.00	17.3	1450.00	20.0	1300.00

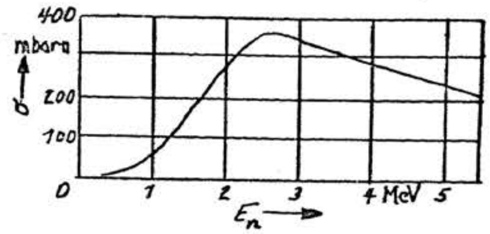

Fig. C.1 The cross-section for the reaction In-115(n,n')In-115m as a function of neutron energy

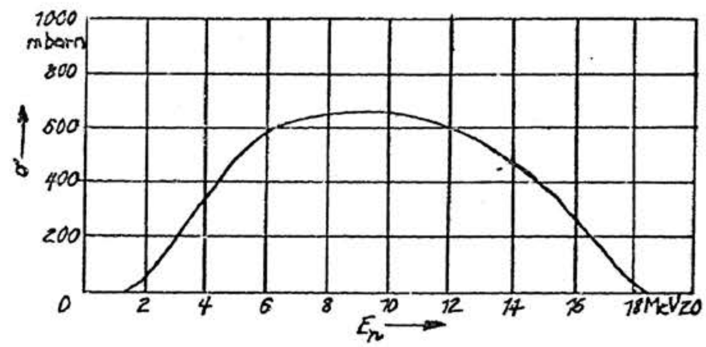

Fig. C.2 The cross-section for the reaction Ni-58(n,p)Co-58 as a function of neutron energy

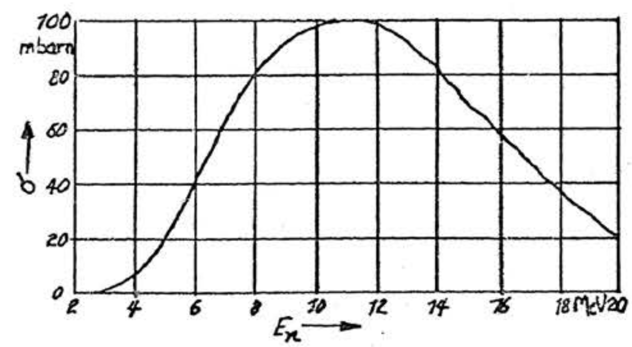

Fig. C.3 The cross-section for the reaction Al-27(n,p)Mg-27 as a function of neutron energy

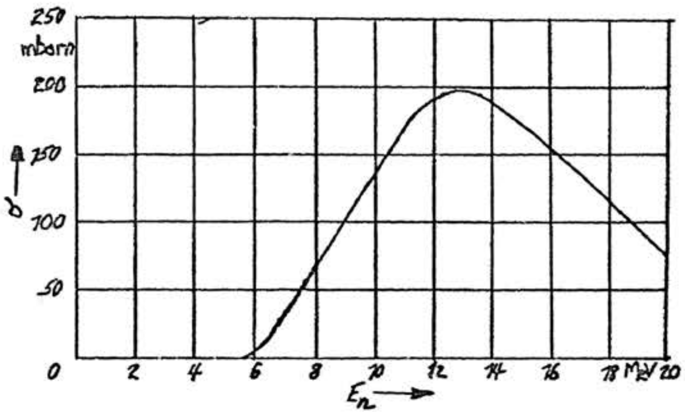

Fig. C.4. The cross-section for the reaction Mg-24(n,p)Na-24 as a function of neutron energy

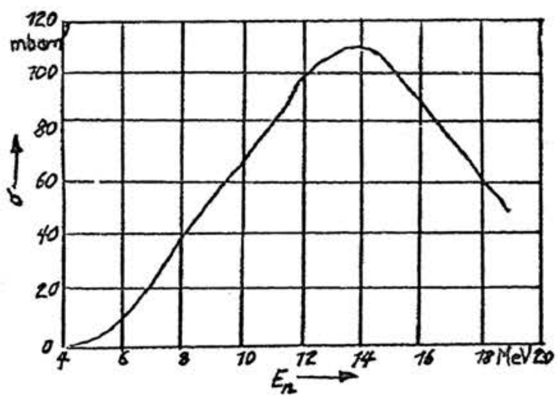

Fig. C.5. The cross-section for the reaction Fe-56(n,p)Mn-56 as a function of neutron energy

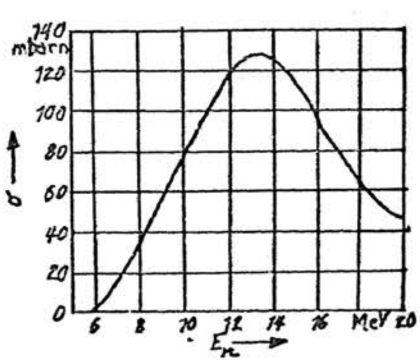

Fig. C.6. The cross-section for the reaction Al-27(n,α)Na-24 as a function of neutron energy

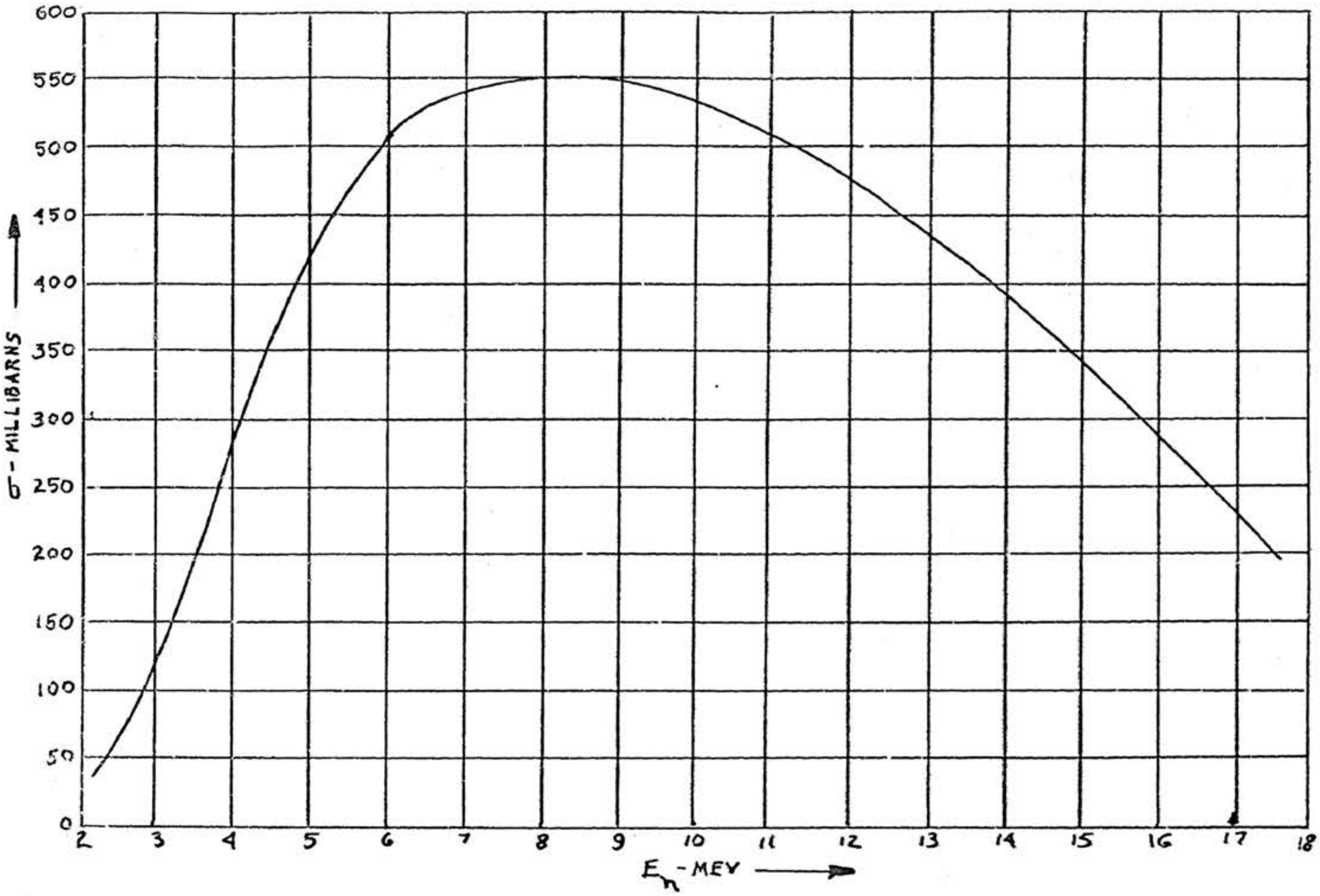

Fig. C.7. The cross-section for the reaction Fe-54(n,p)Mn-54 as a function of neutron energy

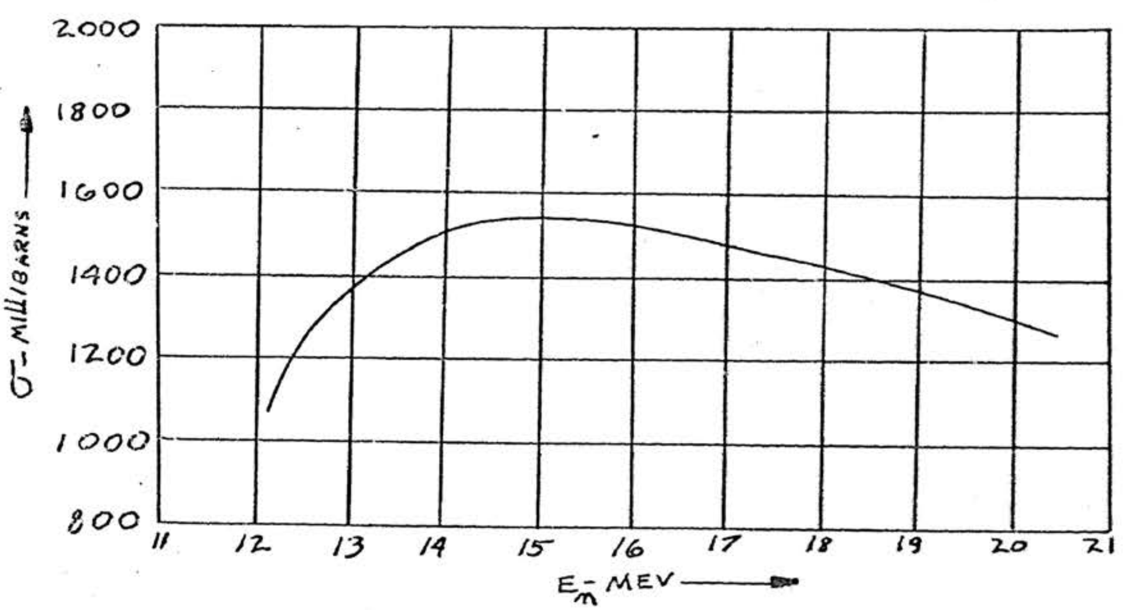

Fig. C.8. The cross-section for the reaction In-115(n,2n)In-114m as a function of neutron energy

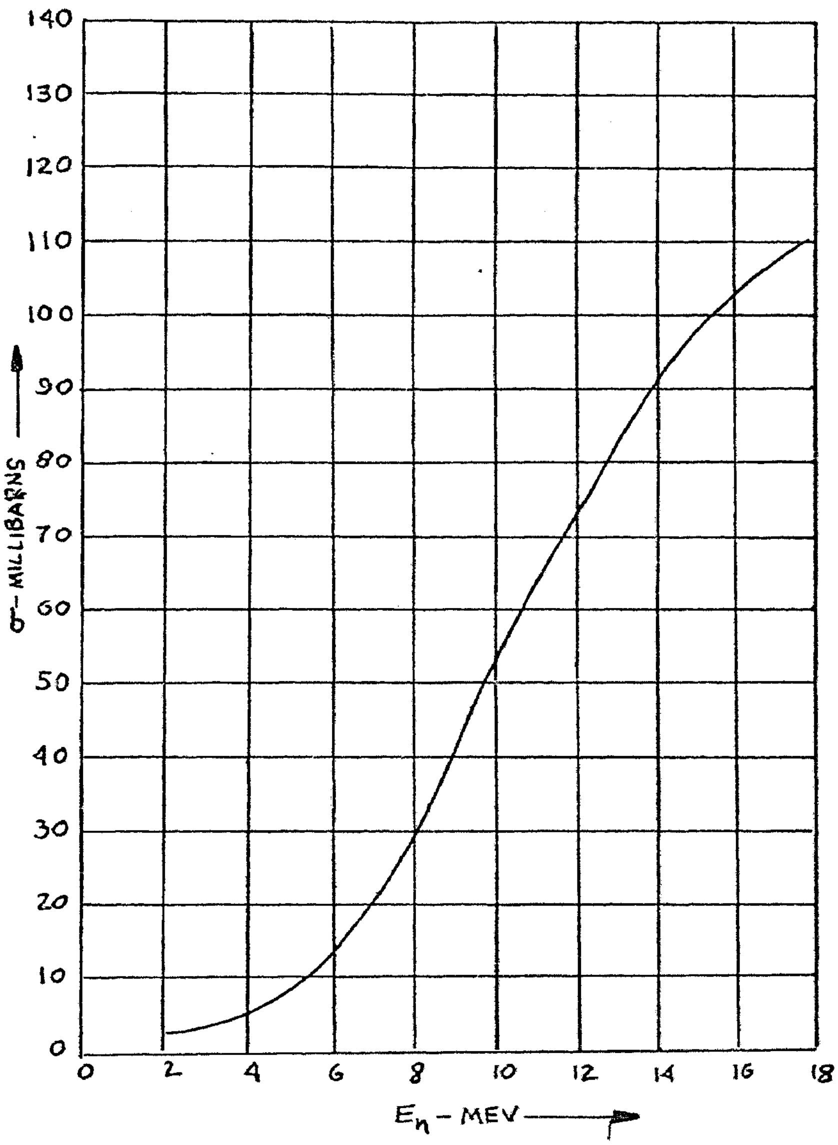

Fig. C.9 The cross-section for the reaction Fe-54(n,α)Cr-51 as a function of neutron energy

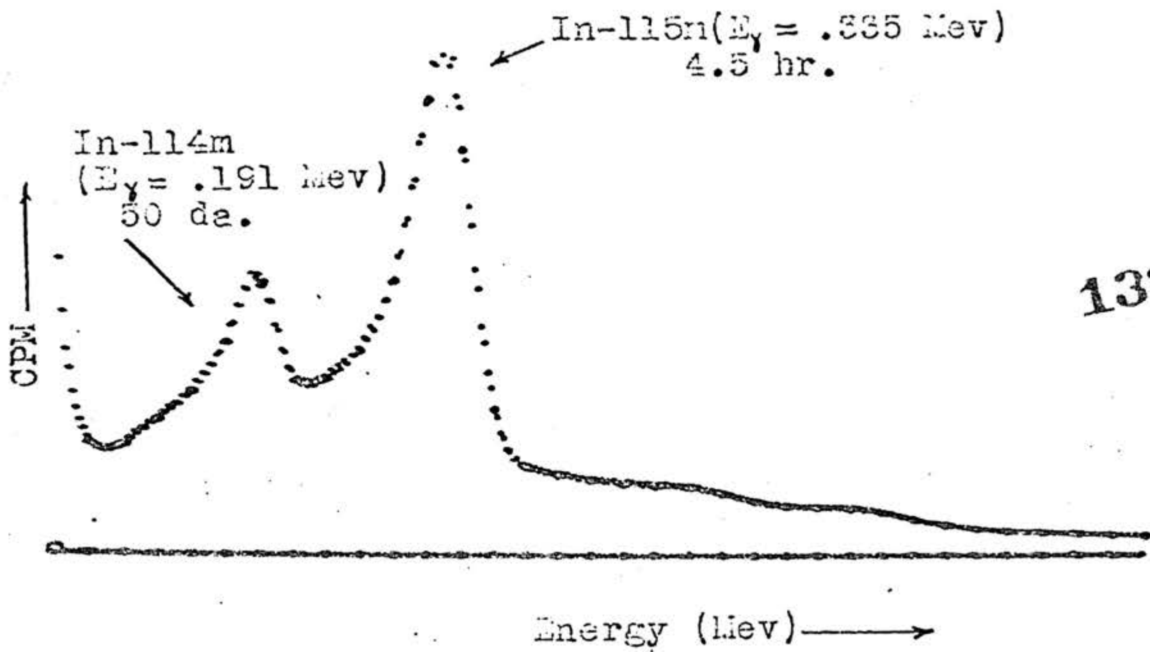

Figure C.10 Gamma Spectrum of In-114m and In-115m after 28 hour Decay

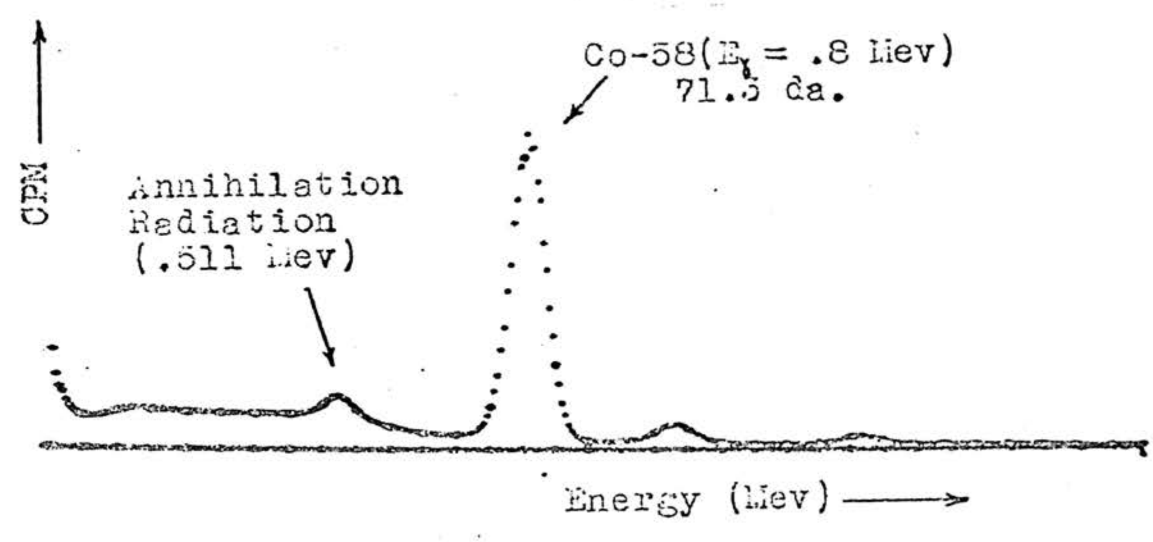

Figure C.11 Gamma Spectrum of Co-58 after 10 hour Decay

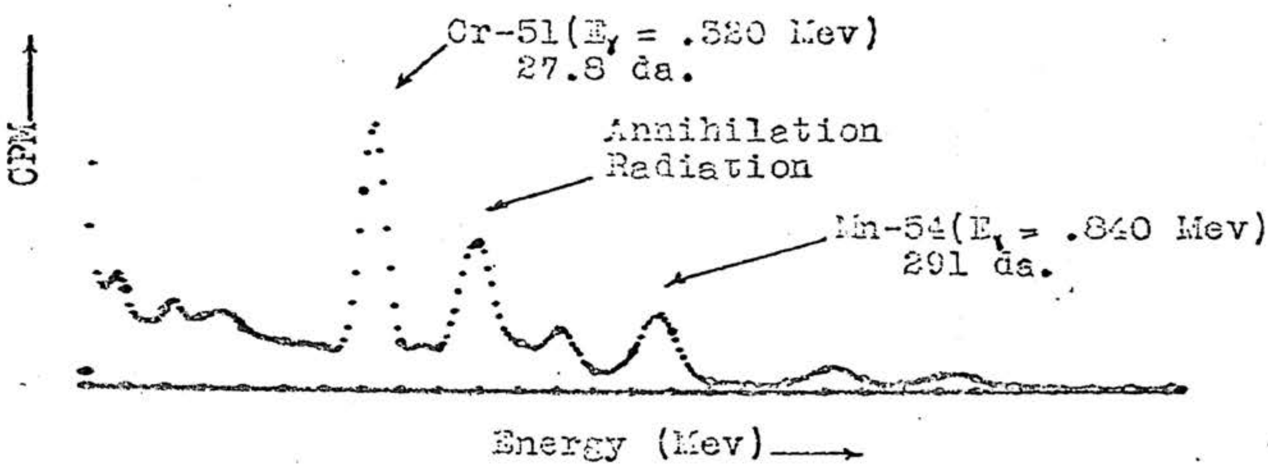

Figure C.12 Gamma Spectrum of Mn-54 and Cr-51 after 94 hour Decay

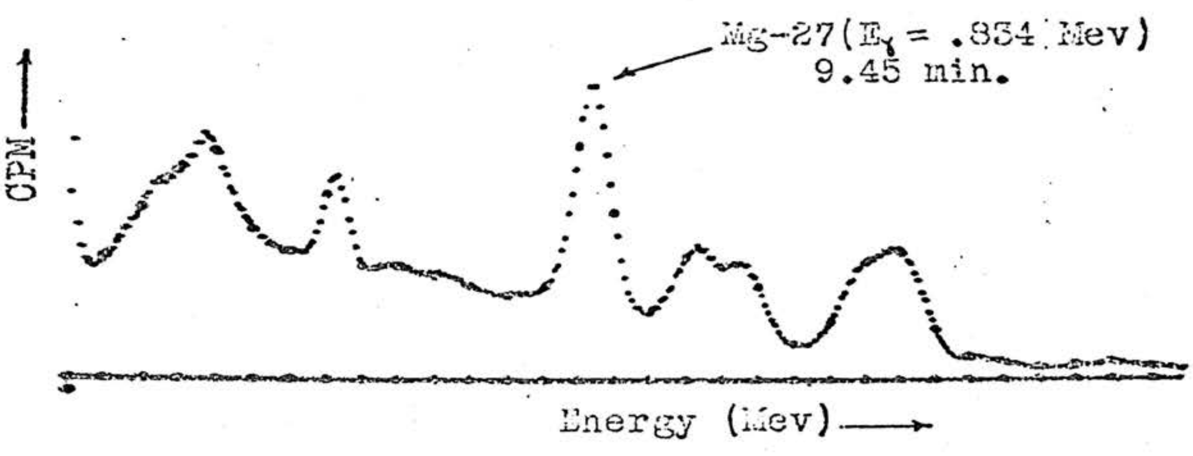

Figure C.13 Gamma Spectrum of Mg-27 after 45 minute Decay

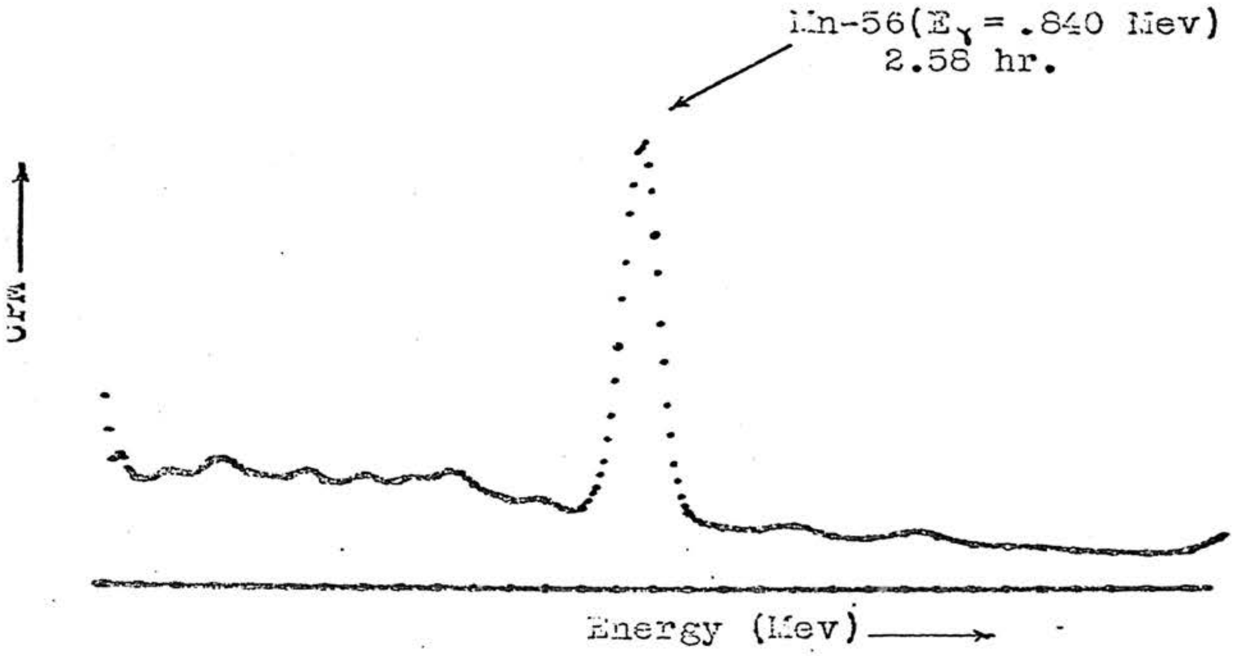

Figure C.14 Gamma Spectrum of Mn-56
after 10 hour Decay

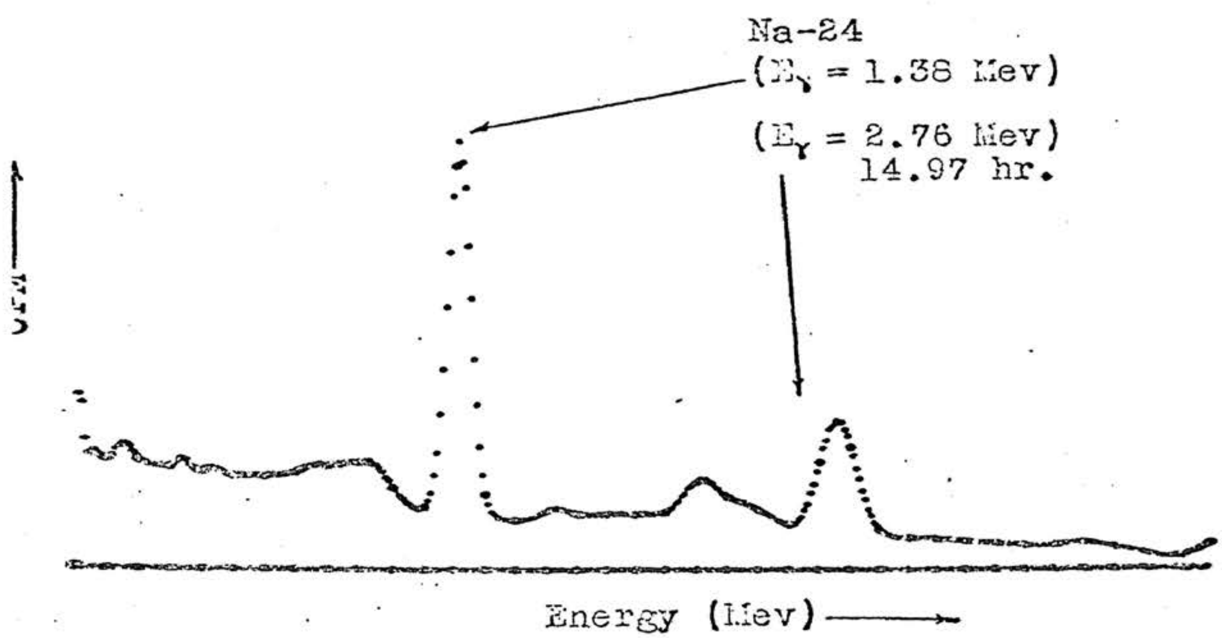

Figure C.15 Gamma Spectrum of Na-24
after 9 hour Decay

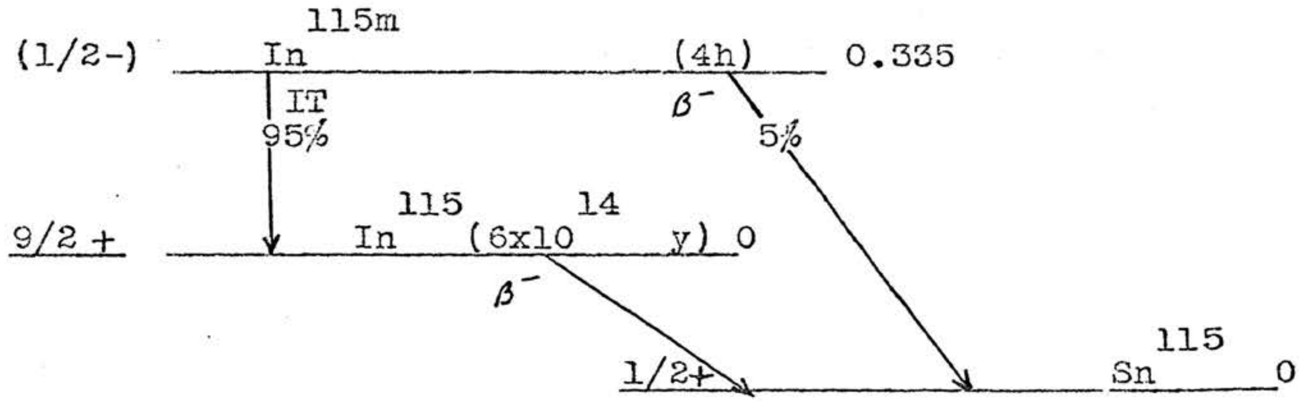

Figure C.16 Diagram of In-115m Decay

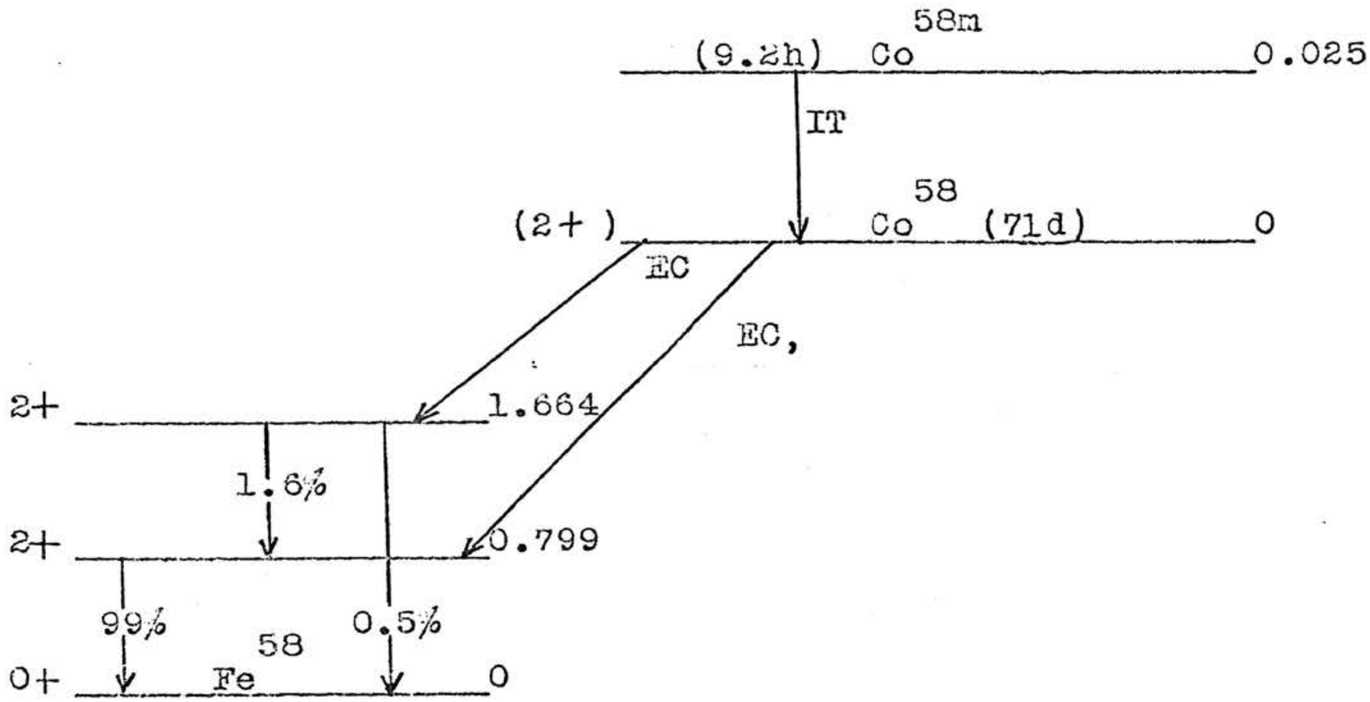

Figure C.17 Diagram of Co-58m Decay

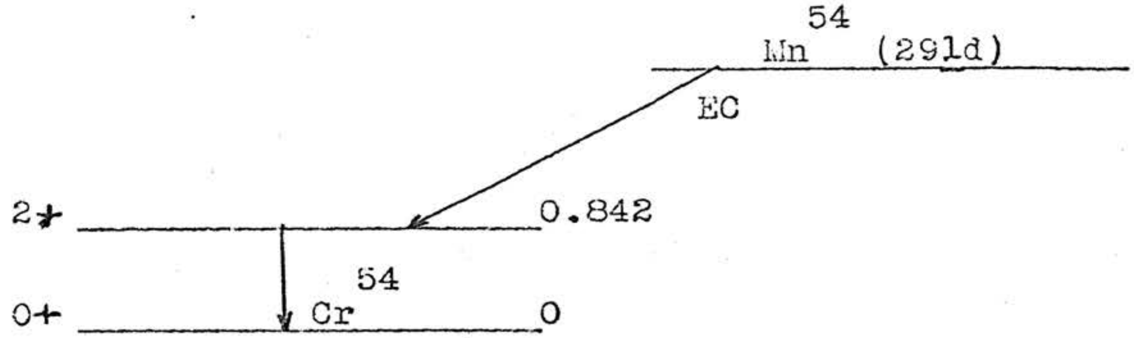

Figure C.18 Diagram of Mn-54 Decay

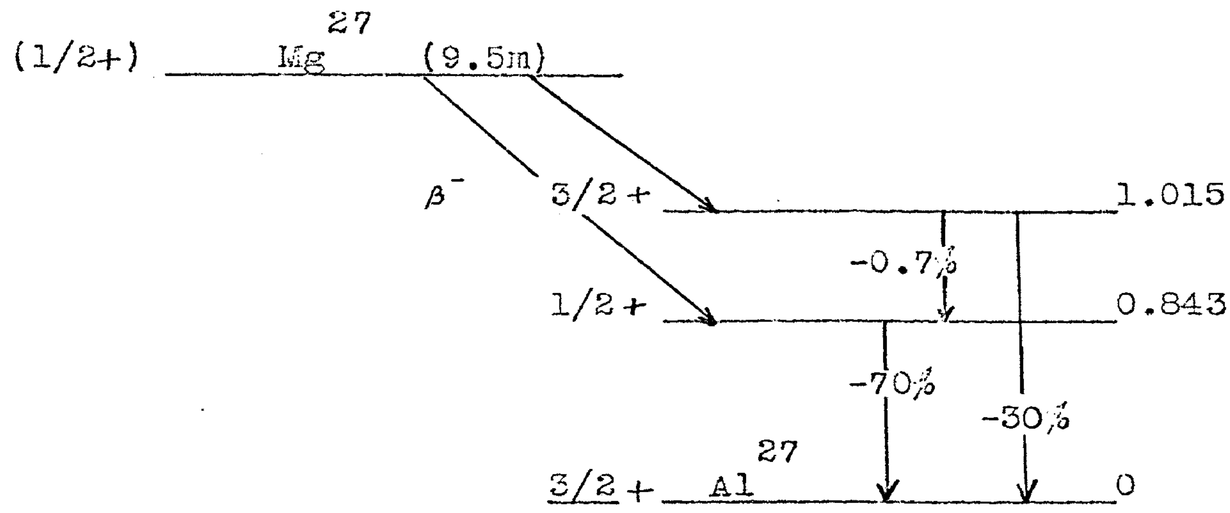

Figure C.19 Diagram of Mg-27 Decay

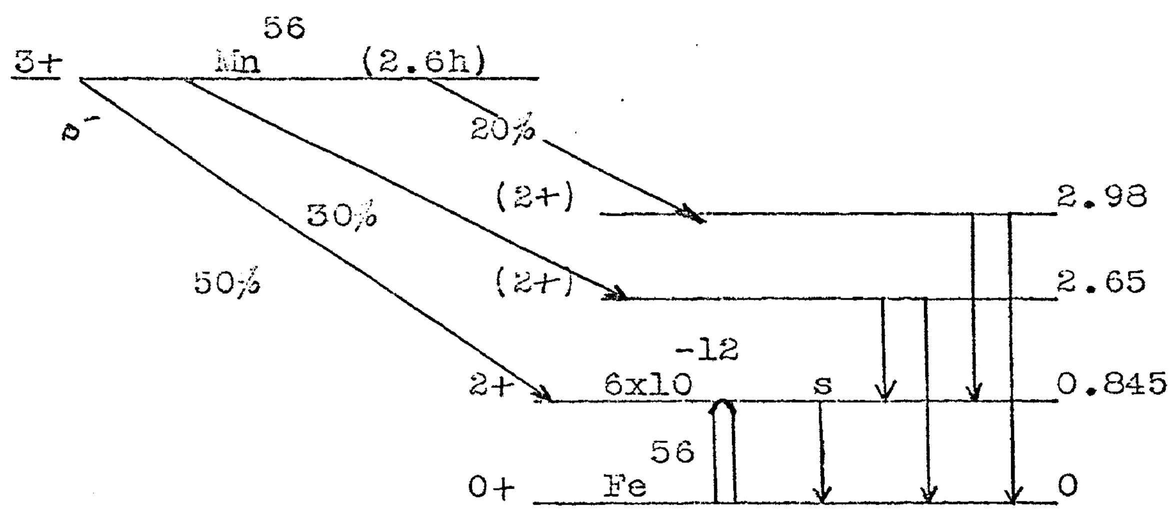

Figure C.20 Diagram of Mn-56 Decay

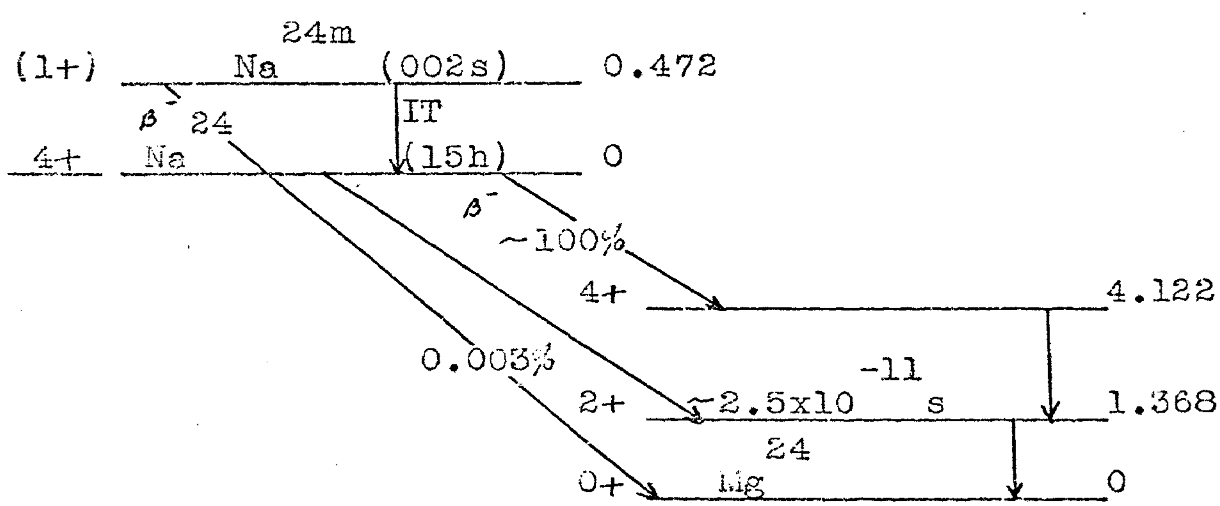

Figure C.21 Diagram of Na-24 Decay

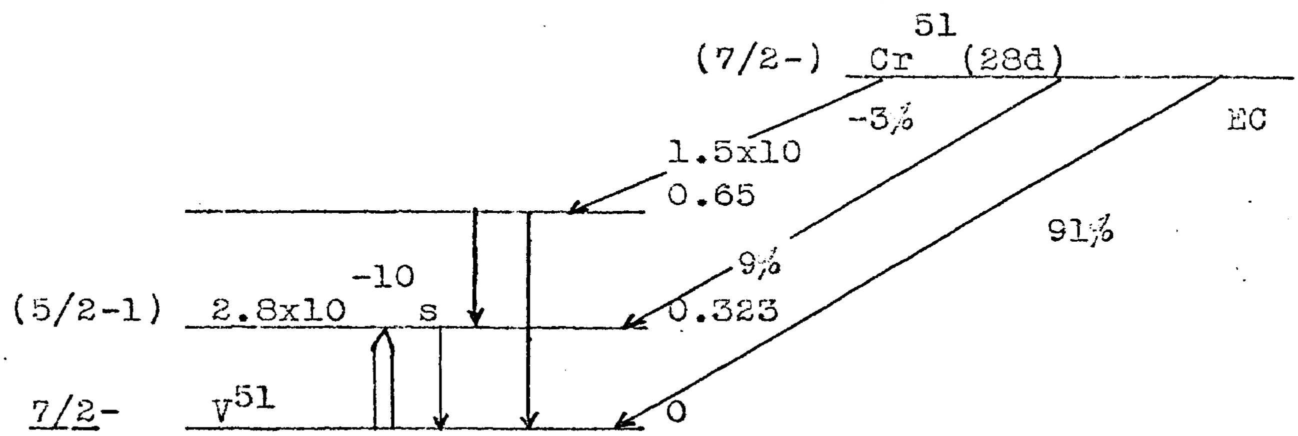

Figure C.22 Diagram of Cr-51 Decay

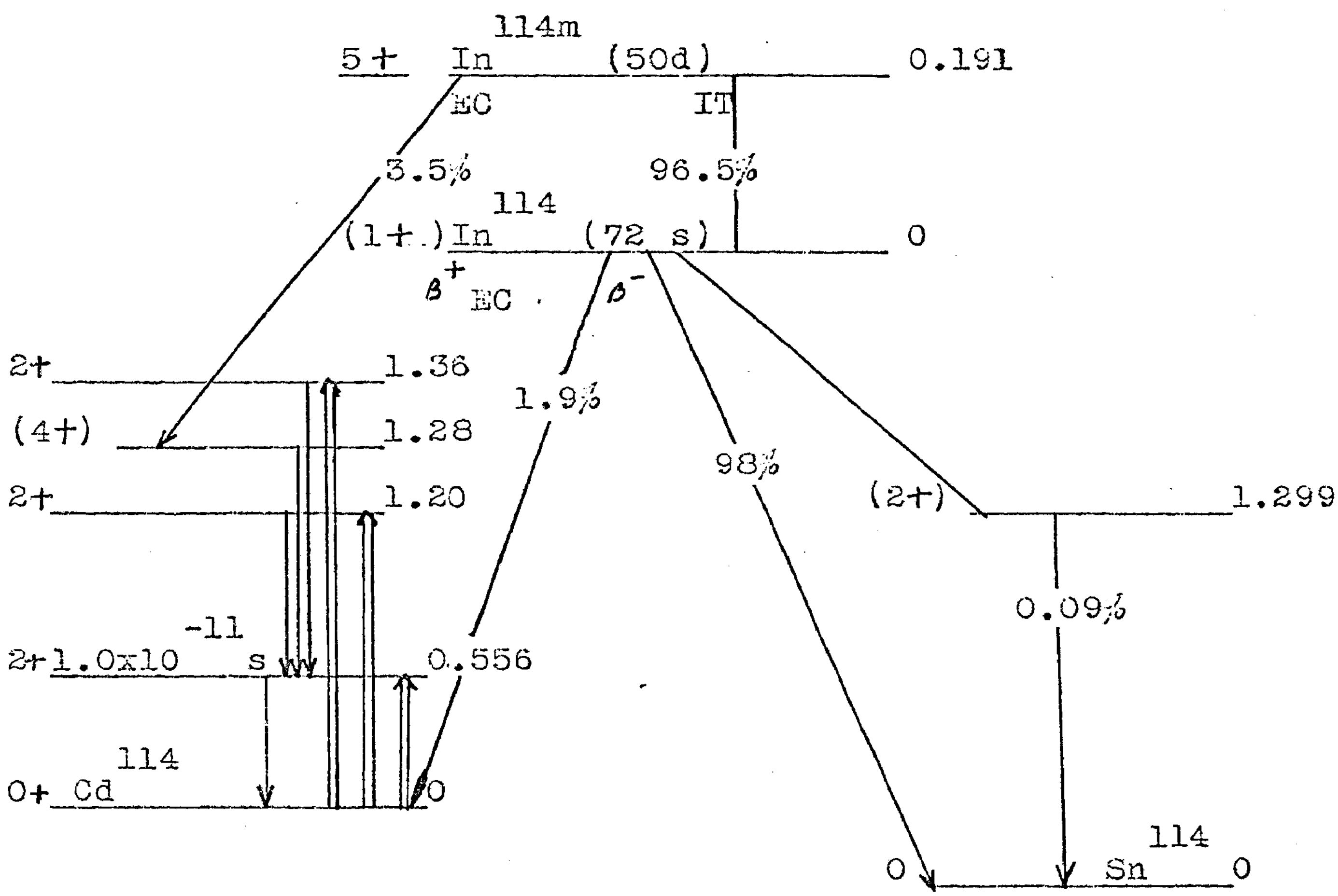

Figure C.23 Diagram of In-114m Decay

APPENDIX D

DESCRIPTION OF FACILITY AND EQUIPMENT

D.1 Reactor Facility and Core

The University of Missouri at Rolla Reactor is a 200 Kw, heterogeneous, thermal, pool-type, research and training reactor. The pool of the reactor is 9' wide, 19' long, 27' deep, and holds approximately 32,000 gallons of high purity demineralized water.

An aluminum tower is suspended from a bridge which spans the pool. At the lower end of this tower is a heavy aluminum grid plate with holes to receive the nose pieces of the fuel elements which form the core of the reactor. The bridge structure and core are wheel mounted on tracks located parallel to the long axis of the pool along the pool top. The bridge can be moved along its rails for a distance of approximately 6' from its normal operating position, thus providing maximum graphite reflection when desired. The overall size of a fuel element is 3" x 3" x about 36". A standard fuel element has 10 plates approximately 1/16" thick, and each plate is an aluminum-uranium oxide-aluminum sandwich with 17 grams of Uranium-235. The control elements are composed of six of these plates with a space along the vertical axis of the element so that they can receive one of the three boron-carbide, shim safety rods or the stainless steel regulating rod.

Experimental facilities of the UMRR include a thermal column for irradiations requiring low energy neutrons, a beam tube for experiments which require a collimated beam of neutrons at the external face of the reactor, and activations can be performed in or near the core by direct insertion or via the pneumatic injection system.

The use of any of the above experimental facilities or the movement of the core position in the pool could change the reactivity and fission spectrum.

Some of the more important characteristics of the reactor are tabulated in Table D.1 (33).

During the course of the experiment, the reactor core loading was designated as 31T. Figure D.1 is a diagram of this loading. A key to the fuel prefixes is:

F Standard Elements
C Control Elements
HF Half Front Element
HR Half Rear Element
CA Core Access Element
IP Isotope Production Element
S Source Holder

D.2 Equipment

The detectors were two RIDL Model 10-9 Harshaw Integral Line Detectors in hermetically sealed assemblies which include the Thallium-activated Sodium Iodide crystals and mating photomultiplier tubes. This was connected into a RIDL Model 10-17 two transistor preamplifier and a standard cylindrical housing. The design is such as to provide extremely low noise and permits the complete detector-preamplifier to be used in measurements of low energy radiation. The dual detectors are centrally located in a 23" x 51" x 23" steel-lead combination shield container. Background radiation inside the counting chamber ranged from 3 to 5 cpm/channel with the reactor operating at 200 Kw. The purpose for noting the effect of the reactor power level was because the detector and shield assembly are situated in the reactor room, with the multichannel analyzer in an adjacent room.

The Multi-Channel Analyzer is composed of the proper combination of instrument modules in the Nuclear-Chicago Model 34-27 Scientific Analyzer System. The memory unit being a RIDL Model 24-2 400 word memory. The choice of spectrum output is: IBM Typewriter, Tally Tape, or Plotter Assembly.

Table D.1

Characteristics of the University of Missouri
at Rolla Reactor

Type:	Swimming Pool (modified BSR-type)
Core:	Heterogeneous-uranium, aluminum, water
Al/H_2O Volume Ratio:	0.7 ± .05
Moderator:	Light Water
Reflector:	Light Water and Graphite
Coolant:	Light water with free convection flow
Biological Shield:	Light water and normal concrete
Critical Mass:	2.7kg U-235 for water reflector
Power Level:	Up to 200 Kw.
Average Thermal Flux:	1.6 x 10^{12} n/cm^2 - sec at 200 Kw with an H_2O reflector.

Figure D.1

Diagram of UMRR Core Loading 31T

	1	2	3	4	5	6	7	8	9
A									
B					S				
C				F12	F8	C4			
D			F22	C1	F15	F11	F18	F2	
E			F5	C2	F15	C13	F3	F14	
F			Bare Rabbit	F21	F10	F7	Cd Covered Rabbit		

APPENDIX E

DIFFERENTIAL FLUX TABULATED RESULTS

Tables E.1, E.2, and E.3 are the tabulated results of determinations at core positions C.3, F.7, and D.7 respectively. The energy increment corresponding to the values is 100 Kev, the same increment used for developing the graphs in Figures 5.1, 5.2, and 5.3.

Tables E.4 through E.7 are the tabulated results for variation of the slope parameter. These values correspond to graphs in Figures 5.5, 5.6, 5.7, and 5.8, and the energy increment is 500 Kev.

Table E.1

Tabulated Results for Differential Flux at C.3

E	Flux	E	Flux	E	Flux	E	Flux
0.1	0.155×10^9	0.2	0.813×10^8	0.3	0.605×10^8	0.4	0.492×10^8
0.5	0.418×10^8	0.6	0.366×10^8	0.7	0.326×10^8	0.8	0.294×10^8
0.9	0.267×10^8	1.0	0.245×10^8	1.1	0.226×10^8	1.2	0.209×10^8
1.3	0.194×10^8	1.4	0.180×10^8	1.5	0.168×10^8	1.6	0.156×10^8
1.7	0.146×10^8	1.8	0.136×10^8	1.9	0.127×10^8	2.0	0.119×10^8
2.1	0.112×10^8	2.2	0.104×10^8	2.3	0.978×10^7	2.4	0.916×10^7
2.5	0.858×10^7	2.6	0.804×10^7	2.7	0.753×10^7	2.8	0.705×10^7
2.9	0.661×10^7	3.0	0.619×10^7	3.1	0.580×10^7	3.2	0.543×10^7
3.3	0.509×10^7	3.4	0.477×10^7	3.5	0.446×10^7	3.6	0.418×10^7
3.7	0.391×10^7	3.8	0.366×10^7	3.9	0.343×10^7	4.0	0.321×10^7
4.1	0.300×10^7	4.2	0.281×10^7	4.3	0.263×10^7	4.4	0.246×10^7
4.5	0.230×10^7	4.6	0.215×10^7	4.7	0.201×10^7	4.8	0.188×10^7
4.9	0.176×10^7	5.0	0.164×10^7	5.1	0.154×10^7	5.2	0.144×10^7
5.3	0.134×10^7	5.4	0.126×10^7	5.5	0.117×10^7	5.6	0.110×10^7
5.7	0.102×10^7	5.8	0.956×10^6	5.9	0.893×10^6	6.0	0.834×10^6
6.1	0.779×10^6	6.2	0.727×10^6	6.3	0.679×10^6	6.4	0.634×10^6
6.5	0.592×10^6	6.6	0.552×10^6	6.7	0.515×10^6	6.8	0.481×10^6
6.9	0.449×10^6	7.0	0.419×10^6	7.1	0.391×10^6	7.2	0.364×10^6
7.3	0.340×10^6	7.4	0.317×10^6	7.5	0.296×10^6	7.6	0.276×10^6
7.7	0.257×10^6	7.8	0.240×10^6	7.9	0.224×10^6	8.0	0.209×10^6
8.1	0.194×10^6	8.2	0.181×10^6	8.3	0.169×10^6	8.4	0.157×10^6
8.5	0.147×10^6	8.6	0.137×10^6	8.7	0.127×10^6	8.8	0.119×10^6
8.9	0.111×10^6	9.0	0.103×10^6	9.1	0.961×10^5	9.2	0.895×10^5
9.3	0.834×10^5	9.4	0.777×10^5	9.5	0.724×10^5	9.6	0.674×10^5
9.7	0.628×10^5	9.8	0.585×10^5	9.9	0.545×10^5	10.0	0.507×10^5

Table E.1 (continued)

Tabulated Results for Differential Flux at C.3

E	Flux	E	Flux	E	Flux	E	Flux
10.1	$0.472x10^5$	10.2	$0.440x10^5$	10.3	$0.409x10^5$	10.4	$0.381x10^5$
10.5	$0.355x10^5$	10.6	$0.330x10^5$	10.7	$0.308x10^5$	10.8	$0.286x10^5$
10.9	$0.267x10^5$	11.0	$0.248x10^5$	11.1	$0.231x10^5$	11.2	$0.215x10^5$
11.3	$0.200x10^5$	11.4	$0.186x10^5$	11.5	$0.173x10^5$	11.6	$0.161x10^5$
11.7	$0.150x10^5$	11.8	$0.140x10^5$	11.9	$0.130x10^5$	12.0	$0.121x10^5$
12.1	$0.112x10^5$	12.2	$0.105x10^5$	12.3	$0.973x10^4$	12.4	$0.906x10^4$
12.5	$0.842x10^4$	12.6	$0.784x10^4$	12.7	$0.729x10^4$	12.8	$0.678x10^4$
12.9	$0.631x10^4$	13.0	$0.587x10^4$	13.1	$0.546x10^4$	13.2	$0.507x10^4$
13.3	$0.472x10^4$	13.4	$0.439x10^4$	13.5	$0.408x10^4$	13.6	$0.380x10^4$
13.7	$0.353x10^4$	13.8	$0.329x10^4$	13.9	$0.305x10^4$	14.0	$0.284x10^4$
14.1	$0.264x10^4$	14.2	$0.245x10^4$	14.3	$0.817x10^4$	14.4	$0.760x10^4$
14.5	$0.706x10^4$	14.6	$0.657x10^4$	14.7	$0.610x10^4$	14.8	$0.158x10^4$
14.9	$0.147x10^4$	15.0	$0.137x10^4$	15.1	$0.127x10^4$	15.2	$0.118x10^4$
15.3	$0.110x10^4$	15.4	$0.102x10^4$	15.5	$0.950x10^3$	15.6	$0.883x10^3$
15.7	$0.821x10^3$	15.8	$0.763x10^3$	15.9	$0.709x10^3$	16.0	$0.659x10^3$
16.1	$0.612x10^3$	16.2	$0.569x10^3$	16.3	$0.529x10^3$	16.4	$0.491x10^3$
16.5	$0.457x10^3$	16.6	$0.424x10^3$	16.7	$0.394x10^3$	16.8	$0.366x10^3$
16.9	$0.340x10^3$	17.0	$0.316x10^3$	17.1	$0.294x10^3$	17.2	$0.273x10^3$
17.3	$0.254x10^3$	17.4	$0.236x10^3$	17.5	$0.219x10^3$	17.6	$0.203x10^3$
17.7	$0.188x10^3$	17.8	$0.175x10^3$	17.9	$0.162x10^3$	18.0	$0.151x10^3$
18.1	$0.140x10^4$	18.2	$0.130x10^3$	18.3	$0.121x10^3$	18.4	$0.112x10^3$
18.5	$0.104x10^3$	18.6	$0.968x10^2$	18.7	$0.899x10^2$	18.8	$0.835x10^2$
18.9	$0.775x10^2$	19.0	$0.720x10^2$	19.1	$0.669x10^2$	19.2	$0.621x10^2$
19.3	$0.577x10^2$	19.4	$0.536x10^2$	19.5	$0.498x10^2$	19.6	$0.462x10^2$
19.7	$0.429x10^2$	19.8	$0.340x10^2$	19.9	$0.370x10^2$	20.0	$0.344x10^2$

Table E.2

Tabulated Results for Differential Flux at F.7

E	Flux	E	Flux	E	Flux	E	Flux
0.1	0.485×10^{9}	0.2	0.291×10^{9}	0.3	0.217×10^{9}	0.4	0.176×10^{9}
0.5	0.150×10^{9}	0.6	0.131×10^{9}	0.7	0.117×10^{9}	0.8	0.105×10^{9}
0.9	0.958×10^{8}	1.0	0.878×10^{8}	1.1	0.809×10^{8}	1.2	0.748×10^{8}
1.3	0.693×10^{8}	1.4	0.644×10^{8}	1.5	0.600×10^{8}	1.6	0.560×10^{8}
1.7	0.522×10^{8}	1.8	0.488×10^{8}	1.9	0.456×10^{8}	2.0	0.427×10^{8}
2.1	0.400×10^{8}	2.2	0.374×10^{8}	2.3	0.350×10^{8}	2.4	0.328×10^{8}
2.5	0.307×10^{8}	2.6	0.288×10^{8}	2.7	0.270×10^{8}	2.8	0.253×10^{8}
2.9	0.237×10^{8}	3.0	0.222×10^{8}	3.1	0.208×10^{8}	3.2	0.195×10^{8}
3.3	0.182×10^{8}	3.4	0.171×10^{8}	3.5	0.160×10^{8}	3.6	0.150×10^{8}
3.7	0.140×10^{8}	3.8	0.131×10^{8}	3.9	0.123×10^{8}	4.0	0.115×10^{8}
4.1	0.108×10^{8}	4.2	0.101×10^{8}	4.3	0.942×10^{7}	4.4	0.881×10^{7}
4.5	0.824×10^{7}	4.6	0.771×10^{7}	4.7	0.721×10^{7}	4.8	0.674×10^{7}
4.9	0.630×10^{7}	5.0	0.589×10^{7}	5.1	0.551×10^{7}	5.2	0.515×10^{7}
5.3	0.481×10^{7}	5.4	0.450×10^{7}	5.5	0.420×10^{7}	5.6	0.392×10^{7}
5.7	0.367×10^{7}	5.8	0.342×10^{7}	5.9	0.320×10^{7}	6.0	0.299×10^{7}
6.1	0.279×10^{7}	6.2	0.260×10^{7}	6.3	0.243×10^{7}	6.4	0.227×10^{7}
6.5	0.212×10^{7}	6.6	0.198×10^{7}	6.7	0.185×10^{7}	6.8	0.172×10^{7}
6.9	0.161×10^{7}	7.0	0.150×10^{7}	7.1	0.140×10^{7}	7.2	0.131×10^{7}
7.3	0.122×10^{7}	7.4	0.114×10^{7}	7.5	0.106×10^{7}	7.6	0.988×10^{6}
7.7	0.921×10^{6}	7.8	0.860×10^{6}	7.9	0.801×10^{6}	8.0	0.747×10^{6}
8.1	0.696×10^{6}	8.2	0.649×10^{6}	8.3	0.605×10^{6}	8.4	0.564×10^{6}
8.5	0.526×10^{6}	8.6	0.490×10^{6}	8.7	0.457×10^{6}	8.8	0.425×10^{6}
8.9	0.396×10^{6}	9.0	0.369×10^{6}	9.1	0.344×10^{6}	9.2	0.321×10^{6}
9.3	0.299×10^{6}	9.4	0.278×10^{6}	9.5	0.259×10^{6}	9.6	0.241×10^{6}
9.7	0.225×10^{6}	9.8	0.209×10^{6}	9.9	0.195×10^{6}	10.0	0.182×10^{6}

Table E.2 (continued)

Tabulated Results for Differential Flux at F.7

E	Flux	E	Flux	E	Flux	E	Flux
10.1	0.169×10^6	10.2	0.158×10^6	10.3	0.147×10^6	10.4	0.137×10^6
10.5	0.127×10^6	10.6	0.118×10^6	10.7	0.110×10^6	10.8	0.103×10^6
10.9	0.955×10^5	11.0	0.889×10^5	11.1	0.827×10^5	11.2	0.770×10^5
11.3	0.717×10^5	11.4	0.667×10^5	11.5	0.621×10^5	11.6	0.578×10^5
11.7	0.537×10^5	11.8	0.500×10^5	11.9	0.465×10^5	12.0	0.433×10^5
12.1	0.403×10^5	12.2	0.375×10^5	12.3	0.349×10^5	12.4	0.324×10^5
12.5	0.302×10^5	12.6	0.281×10^5	12.7	0.261×10^5	12.8	0.243×10^5
12.9	0.226×10^5	13.0	0.210×10^5	13.1	0.195×10^5	13.2	0.182×10^5
13.3	0.169×10^5	13.4	0.157×10^5	13.5	0.146×10^5	13.6	0.136×10^5
13.7	0.126×10^5	13.8	0.118×10^5	13.9	0.109×10^5	14.0	0.102×10^5
14.1	0.945×10^4	14.2	0.879×10^4	14.3	0.817×10^4	14.4	0.760×10^4
14.5	0.706×10^4	14.6	0.657×10^4	14.7	0.610×10^4	14.8	0.567×10^4
14.9	0.528×10^4	15.0	0.490×10^4	15.1	0.456×10^4	15.2	0.424×10^4
15.3	0.394×10^4	15.4	0.366×10^4	15.5	0.340×10^4	15.6	0.316×10^4
15.7	0.294×10^4	15.8	0.273×10^4	15.9	0.254×10^4	16.0	0.236×10^4
16.1	0.219×10^4	16.2	0.204×10^4	16.3	0.189×10^4	16.4	0.176×10^4
16.5	0.164×10^4	16.6	0.152×10^4	16.7	0.141×10^4	16.8	0.131×10^4
16.9	0.122×10^4	17.0	0.113×10^4	17.1	0.105×10^4	17.2	0.978×10^3
17.3	0.909×10^3	17.4	0.844×10^3	17.5	0.785×10^3	17.6	0.729×10^3
17.7	0.673×10^3	17.8	0.625×10^3	17.9	0.581×10^3	18.0	0.540×10^3
18.1	0.501×10^3	18.2	0.466×10^3	18.3	0.433×10^3	18.4	0.402×10^3
18.5	0.373×10^3	18.6	0.347×10^3	18.7	0.322×10^3	18.8	0.299×10^3
18.9	0.278×10^3	19.0	0.258×10^3	19.1	0.240×10^3	19.2	0.223×10^3
19.3	0.207×10^3	19.4	0.192×10^3	19.5	0.178×10^3	19.6	0.166×10^3
19.7	0.154×10^3	19.8	0.143×10^3	19.9	0.133×10^3	20.0	0.123×10^3

Table E.3

Tabulated Results for Differential Flux at D.7

E	Flux	E	Flux	E	Flux	E	Flux
0.1	0.321×10^{10}	0.2	0.193×10^{10}	0.3	0.144×10^{10}	0.4	0.117×10^{10}
0.5	0.993×10^{9}	0.6	0.868×10^{9}	0.7	0.773×10^{9}	0.8	0.698×10^{9}
0.9	0.635×10^{9}	1.0	0.582×10^{9}	1.1	0.536×10^{9}	1.2	0.496×10^{9}
1.3	0.460×10^{9}	1.4	0.427×10^{9}	1.5	0.398×10^{9}	1.6	0.371×10^{9}
1.7	0.346×10^{9}	1.8	0.324×10^{9}	1.9	0.303×10^{9}	2.0	0.283×10^{9}
2.1	0.265×10^{9}	2.2	0.248×10^{9}	2.3	0.232×10^{9}	2.4	0.218×10^{9}
2.5	0.204×10^{9}	2.6	0.191×10^{9}	2.7	0.179×10^{9}	2.8	0.168×10^{9}
2.9	0.157×10^{9}	3.0	0.147×10^{9}	3.1	0.138×10^{9}	3.2	0.129×10^{9}
3.3	0.121×10^{9}	3.4	0.113×10^{9}	3.5	0.106×10^{9}	3.6	0.992×10^{8}
3.7	0.929×10^{8}	3.8	0.870×10^{8}	3.9	0.814×10^{8}	4.0	0.762×10^{8}
4.1	0.713×10^{8}	4.2	0.667×10^{8}	4.3	0.624×10^{8}	4.4	0.584×10^{8}
4.5	0.546×10^{8}	4.6	0.511×10^{8}	4.7	0.478×10^{8}	4.8	0.447×10^{8}
4.9	0.418×10^{8}	5.0	0.391×10^{8}	5.1	0.365×10^{8}	5.2	0.341×10^{8}
5.3	0.319×10^{8}	5.4	0.298×10^{8}	5.5	0.279×10^{8}	5.6	0.260×10^{8}
5.7	0.243×10^{8}	5.8	0.227×10^{8}	5.9	0.212×10^{8}	6.0	0.198×10^{8}
6.1	0.185×10^{8}	6.2	0.173×10^{8}	6.3	0.161×10^{8}	6.4	0.151×10^{8}
6.5	0.140×10^{8}	6.6	0.131×10^{8}	6.7	0.122×10^{8}	6.8	0.114×10^{8}
6.9	0.107×10^{8}	7.0	0.994×10^{7}	7.1	0.928×10^{7}	7.2	0.866×10^{7}
7.3	0.807×10^{7}	7.4	0.753×10^{7}	7.5	0.702×10^{7}	7.6	0.655×10^{7}
7.7	0.611×10^{7}	7.8	0.570×10^{7}	7.9	0.531×10^{7}	8.0	0.495×10^{7}
8.1	0.462×10^{7}	8.2	0.430×10^{7}	8.3	0.401×10^{7}	8.4	0.374×10^{7}
8.5	0.349×10^{7}	8.6	0.325×10^{7}	8.7	0.303×10^{7}	8.8	0.282×10^{7}
8.9	0.263×10^{7}	9.0	0.245×10^{7}	9.1	0.229×10^{7}	9.2	0.213×10^{7}
9.3	0.198×10^{7}	9.4	0.185×10^{7}	9.5	0.172×10^{7}	9.6	0.160×10^{7}
9.7	0.149×10^{7}	9.8	0.139×10^{7}	9.9	0.129×10^{7}	10.0	0.120×10^{7}

Table E.3 (continued)

Tabulated Results for Differential Flux at D.7

10.1	0.112×10^7	10.2	0.104×10^7	10.3	0.972×10^6	10.4	0.905×10^6
10.5	0.843×10^6	10.6	0.785×10^6	10.7	0.731×10^6	10.8	0.680×10^6
10.9	0.633×10^6	11.0	0.589×10^6	11.1	0.548×10^6	11.2	0.510×10^6
11.3	0.475×10^6	11.4	0.442×10^6	11.5	0.411×10^6	11.6	0.383×10^6
11.7	0.356×10^6	11.8	0.332×10^6	11.9	0.309×10^6	12.0	0.287×10^6
12.1	0.267×10^6	12.2	0.248×10^6	12.3	0.231×10^6	12.4	0.215×10^6
12.5	0.200×10^6	12.6	0.186×10^6	12.7	0.173×10^6	12.8	0.161×10^6
12.9	0.150×10^6	13.0	0.139×10^6	13.1	0.130×10^6	13.2	0.121×10^6
13.3	0.112×10^6	13.4	0.104×10^6	13.5	0.969×10^5	13.6	0.902×10^5
13.7	0.838×10^5	13.8	0.780×10^5	13.9	0.725×10^5	14.0	0.674×10^5
14.1	0.627×10^5	14.2	0.583×10^5	14.3	0.542×10^5	14.4	0.504×10^5
14.5	0.468×10^5	14.6	0.435×10^5	14.7	0.405×10^5	14.8	0.376×10^5
14.9	0.350×10^5	15.0	0.325×10^5	15.1	0.302×10^5	15.2	0.281×10^5
15.3	0.261×10^5	15.4	0.243×10^5	15.5	0.226×10^5	15.6	0.210×10^5
15.7	0.195×10^5	15.8	0.181×10^5	15.9	0.168×10^5	16.0	0.156×10^5
16.1	0.145×10^5	16.2	0.135×10^5	16.3	0.126×10^5	16.4	0.117×10^5
16.5	0.108×10^5	16.6	0.101×10^5	16.7	0.936×10^4	16.8	0.870×10^4
16.9	0.808×10^4	17.0	0.751×10^4	17.1	0.698×10^4	17.2	0.648×10^4
17.3	0.603×10^4	17.4	0.560×10^4	17.5	0.520×10^4	17.6	0.483×10^4
17.7	0.446×10^4	17.8	0.415×10^4	17.9	0.385×10^4	18.0	0.358×10^4
18.1	0.332×10^4	18.2	0.309×10^4	18.3	0.287×10^4	18.4	0.266×10^4
18.5	0.247×10^4	18.6	0.230×10^4	18.7	0.213×10^4	18.8	0.198×10^4
18.9	0.184×10^4	19.0	0.171×10^4	19.1	0.159×10^4	19.2	0.148×10^4
19.3	0.137×10^4	19.4	0.127×10^4	19.5	0.118×10^4	19.6	0.110×10^4
19.7	0.102×10^4	19.8	0.947×10^3	19.9	0.880×10^3	20.0	0.816×10^3

Table E.4

Exponent Parameter Variation of Position D.7 Results

Kmin = 0.1 , Kmax = 0.2

E	Flux	E	Flux	E	Flux	E	Flux
0.5	0.399×10^9	1.0	0.342×10^9	1.5	0.292×10^9	2.0	0.244×10^9
2.5	0.198×10^9	3.0	0.158×10^9	3.5	0.124×10^9	4.0	0.961×10^8
4.5	0.735×10^8	5.0	0.557×10^8	5.5	0.418×10^8	6.0	0.312×10^8
6.5	0.231×10^8	7.0	0.171×10^8	7.5	0.125×10^8	8.0	0.914×10^7
8.5	0.665×10^7	9.0	0.482×10^7	9.5	0.349×10^7	10.0	0.251×10^7
10.5	0.181×10^7	11.0	0.130×10^7	11.5	0.927×10^6	12.0	0.662×10^6
12.5	0.472×10^6	13.0	0.336×10^6	13.5	0.239×10^6	14.0	0.169×10^6
14.5	0.120×10^6	15.0	0.848×10^5	15.5	0.599×10^5	16.0	0.423×10^5
16.5	0.298×10^5	17.0	0.210×10^5	17.5	0.148×10^5	18.0	0.103×10^5
18.5	0.724×10^4	19.0	0.508×10^4	19.5	0.356×10^4	20.0	0.249×10^4

Table E.5

Exponent Parameter Variation of Position D.7 Results

Kmin = 0.2 , Kmax = 0.4

E	Flux	E	Flux	E	Flux	E	Flux
0.5	0.563×10^9	1.0	0.420×10^9	1.5	0.331×10^9	2.0	0.261×10^9
2.5	0.203×10^9	3.0	0.156×10^9	3.5	0.119×10^9	4.0	0.894×10^8
4.5	0.668×10^8	5.0	0.496×10^8	5.5	0.365×10^8	6.0	0.268×10^8
6.5	0.195×10^8	7.0	0.142×10^8	7.5	0.103×10^8	8.0	0.741×10^7
8.5	0.532×10^7	9.0	0.382×10^7	9.5	0.273×10^7	10.0	0.195×10^7
10.5	0.139×10^7	11.0	0.985×10^7	11.5	0.699×10^6	12.0	0.495×10^6
12.5	0.350×10^6	13.0	0.247×10^6	13.5	0.174×10^6	14.0	0.123×10^6
14.5	0.862×10^5	15.0	0.606×10^5	15.5	0.425×10^5	16.0	0.298×10^5
16.5	0.209×10^5	17.0	0.146×10^5	17.5	0.102×10^5	18.0	0.711×10^4
18.5	0.496×10^4	19.0	0.346×10^4	19.5	0.241×10^4	20.0	0.168×10^4

Table E.6

Exponent Parameter Variation of Position D.7 Results

Kmin = 0.4 , Kmax = 0.6

E	Flux	E	Flux	E	Flux	E	Flux
0.5	$0.782x10^9$	1.0	$0.509x10^9$	1.5	$0.370x10^9$	2.0	$0.275x10^9$
2.5	$0.204x10^9$	3.0	$0.152x10^9$	3.5	$0.112x10^9$	4.0	$0.820x10^8$
4.5	$0.599x10^8$	5.0	$0.435x10^8$	5.5	$0.314x10^8$	6.0	$0.227x10^8$
6.5	$0.163x10^8$	7.0	$0.116x10^8$	7.5	$0.831x10^7$	8.0	$0.591x10^7$
8.5	$0.420x10^7$	9.0	$0.298x10^7$	9.5	$0.211x10^7$	10.0	$0.149x10^7$
10.5	$0.105x10^7$	11.0	$0.738x10^6$	11.5	$0.519x10^6$	12.0	$0.364x10^6$
12.5	$0.255x10^6$	13.0	$0.179x10^6$	13.5	$0.125x10^6$	14.0	$0.875x10^5$
14.5	$0.611x10^5$	15.0	$0.427x10^5$	15.5	$0.297x10^5$	16.0	$0.207x10^5$
16.5	$0.144x10^5$	17.0	$0.100x10^5$	17.5	$0.699x10^4$	18.0	$0.482x10^4$
18.5	$0.335x10^4$	19.0	$0.233x10^4$	19.5	$0.161x10^4$	20.0	$0.112x10^4$

Table E.7

Exponent Parameter Variation of Position D.7 Results

Kmin = 0.8 , Kmax = 0.9

E	Flux	E	Flux	E	Flux	E	Flux
0.5	$0.125x10^{10}$	1.0	$0.662x10^9$	1.5	$0.426x10^9$	2.0	$0.290x10^9$
2.5	$0.202x10^9$	3.0	$0.142x10^9$	3.5	$0.998x10^8$	4.0	$0.703x10^8$
4.5	$0.496x10^8$	5.0	$0.349x10^8$	5.5	$0.245x10^8$	6.0	$0.172x10^8$
6.5	$0.121x10^8$	7.0	$0.844x10^7$	7.5	$0.590x10^7$	8.0	$0.412x10^7$
8.5	$0.287x10^7$	9.0	$0.200x10^7$	9.5	$0.139x10^7$	10.0	$0.969x10^6$
10.5	$0.673x10^6$	11.0	$0.467x10^6$	11.5	$0.324x10^6$	12.0	$0.225x10^6$
12.5	$0.156x10^6$	13.0	$0.108x10^6$	13.5	$0.746x10^5$	14.0	$0.516x10^5$
14.5	$0.356x10^5$	15.0	$0.246x10^5$	15.5	$0.170x10^5$	16.0	$0.117x10^5$
16.5	$0.809x10^4$	17.0	$0.558x10^4$	17.5	$0.385x10^4$	18.0	$0.264x10^4$
18.5	$0.182x10^4$	19.0	$0.125x10^4$	19.5	$0.860x10^3$	20.0	$0.592x10^3$

BIBLIOGRAPHY

1. CLARE, D. M., MARTIN, W. H., KELLY, B. T., (1963), Intercomparison of Fast Neutron Flux Monitors in a Hollow Fuel Element in Pluto, NS&E, 18, 448-458.

2. EDWARDS, D. R., Unpublished paper.

3. BONNER, T. et al., (1952), A Study of the Spectrum of the Neutrons of Low Energy from the Fission, Phy Rev, 87, 1034.

4. HILL, D. L., (1952), The Neutron Energy Spectrum from U-235 Thermal Fission, Phy Rev, 87, 1034.

5. WATT, B. E., (1952), Energy Spectrum of Neutrons from Thermal Fission of U-235, Phy Rev, 87, 1037.

6. NERESON, N., (1951), Fission Neutron Spectrum of U-235, Phy Rev, 85, 600.

7. CRANBERG, L. et al., (1956), Fission Neutron Spectrum of U-235, Phy Rev, 103, 662.

8. HUGHES, D. J., (1953), Pile Neutron Research, Addison Wesley, p.93.

9. BECKURTS, K. H., and WIRTZ, K., (1964), Neutron Physics, Springer-Verlag, New York, Chapter 13.

10. GERKAN, W., (1963), Measurements of Neutron Energy Effects Using Multiple Threshold Detectors, Thesis, University of Maryland.

11. TRICE, J. B., WECHSLER, M. S., (1964), Tentative Procedures for Measuring Neutron Flux by Radioactivation Techniques, R 64 SDIO.

12. GRUNDL, I., and USNER, A., (1960), Nuclear Science and Engineering, 8, 598.

√13. MARTIN, W. H., CLARE, D. M., (1963), Determination of Fast Neutron Spectrum by Nickel Activation NS&E, 18, 468-473.

√14. HOGG, C. H., WEBER, D. L., and YEATS, E. C., (1962), IDO 16744 or/also Trans. Am. Nuc. Soc. 4, 271.

15. PASSELL, T. O., and HEATH, R. L., (1961), Cross-Sections of Threshold Reactions for Fission Neutrons; Nickel as a Fast Flux Monitor, NS&E10, 308-315.

16. RYDIN, R. A. et al., (1964), Fast Neutron Spectroscopy and Dosimetry of the MIT Reactor Medical Therapy Facility Beam, AFCRL-64-404.

17. BROWNELL, G. D., SWEET, W. H., (1959), Studies in Neutron Capture Therapy, Prog. Nucl, Ener. 2, p. 114.

18. GAGE, K. L., (1966), Fast Flux Measurement by a Single Multi-Threshold Foil, Masters Thesis, UMR.

19. UTHE, P. M., (1957), Attainment of Neutron Flux Spectra from Foil Activations, WADC-TR-57-3, GNE-9.

20. BRESESTI, M. et al., (1963), Fast Neutron Measurements by Threshold Detectors in ISPRA-1 (CP5-Type) and Avogadro RS-1 (Swimming Pool) Reactors, Neutron Dosimetry, Vol.1, IAEA Vienna, p. 27.

21. PRICE, W. J., (1958), Nuclear Radiation Detection, McGraw-Hill, New York.

22. DIERCKX, R., (1963), In-Pile Fast-Neutron Spectrum Measurements by Threshold Detectors, Neutron Dosimetry, Vol. 1, IAEA Vienna, p. 325.

23. ATEN, A. H., BRINKMAN, G. A., HEERTJE, I., and NAGEL, W., (1963), Remarks on the Use of Threshold Detectors, Neutron Dosimetry, Vol. I, IAEA, Vienna, p. 400.

24. STEIN, J. R., GOLDBERG, M. D., MARGURNO, B. A., RENATE, W. C., (1964), Neutron Cross-Sections, Vol.1, Z 1 to 20, BNL 325.

25. GOLDBERG, M. D., MUGHABGHAB, S. F., MARGURNO, B. A., and MAY, V. M., (1966), Neutron Cross-Sections, Vol. II A, Z 21 to 40, BNL 325.

26. GOLDBERG, M. D. MUGHABGHAB, S. F., SURENDRA, N. P., MARGURNO, B. A., MAY, V. M., (1966), Vol. II B, Z 41 to 60, BNL 325.

27. MURPHY, H. M., (1966), PPA, A Computer Program for Photo-Peak Analysis, AFWL-TR-65-111.

28. CROUTHAMEL, C. E., (1960), Applied Gamma-Ray Spectrometry, Pergamon Press, New York

29. HOLLANDER, J. M., PERLMAN, I., SEABORG, G. T., (1953), Table of Isotopes, Review of Modern Physics 25, No. 2.

30. HOWERTON, R. J., (1959), Tabulated Neutron Cross Sections, UCRL (Rev) Part 1, Vol. 1 and 2.

31. GOLDBERG, M. D., MUGHABGHAB, S. F., PUROHIT, S. N., MARGURNO, B. A., and MAY, V. M., (1966), BNL 325, Vol. II B.

32. STROMINGER, D., HOLLANDER, J. M., and SEABORG, G. T., (1958), Table of Isotopes, Reviews of Modern Physics, 30, No. 2, Part II.

33. U.M.R.R., Hazards Report

VITA

The author was born on August 7, 1933 in Chicago, Illinois. He received his primary and secondary education in Maywood, Illinois.

He has received his college education from Bradley University, in Peoria, Illinois and Illinois Institute of Technology, Chicago, Illinois where he received a Bachelor of Science Degree in Physics in January, 1964.

Prior to enrolling in the Graduate School of the University of Missouri at Rolla in September 1966, he was employed at Argonne National Laboratory, Argonne, Illinois where he worked in Health Physics, and at present is employed by UMR as Health Physicist.